EFFECTIVENESS EVALUATION OF FLUORESCENT TRACER IN SHALY-SANDSTONE
RESERVOIR

Mr. Harid Pataveepaisit

A Thesis Submitted in Partial Fulfillment of the Requirements

for the Degree of Master of Engineering in Georesources and Petroleum Engineering

Department of Mining and Petroleum Engineering

FACULTY OF ENGINEERING

Chulalongkorn University

Academic Year 2019

การประเมินประสิทธิภาพของสารติดตาม ชนิดฟลูออเรสเซนต์ ในแหล่งกักเก็บปิโตรเลียม
ชนิดหินทรายผสมหินดินดาน

นายหฤษฎ์ ปฐวีไพสิฐ

วิทยานิพนธ์นี้เป็นส่วนหนึ่งของการศึกษาตามหลักสูตรปริญญาวิศวกรรมศาสตรมหาบัณฑิต
สาขาวิชาวิศวกรรมทรัพยากรธรณีและปิโตรเลียม ภาควิชาวิศวกรรมเหมืองแร่และปิโตรเลียม
คณะวิศวกรรมศาสตร์ จุฬาลงกรณ์มหาวิทยาลัย
ปีการศึกษา 2562

Thesis Title	EFFECTIVENESS EVALUATION OF FLUORESCENT TRACER IN SHALY-SANDSTONE RESERVOIR
By	Mr. Harid Pataveepaisit
Field of Study	Georesources and Petroleum Engineering
Thesis Advisor	Assistant Professor FALAN SRISURIYACHAI, Ph.D.

Accepted by the FACULTY OF ENGINEERING, Chulalongkorn University in Partial Fulfillment of the Requirement for the Master of Engineering

-- Dean of the FACULTY OF ENGINEERING

(Professor SUPOT TEACHAVORASINSKUN, D.Eng.)

THESIS COMMITTEE

-- Chairman

(Assistant Professor JIRAWAT CHEWAROUNGROAJ, Ph.D.)

-- Thesis Advisor

(Assistant Professor FALAN SRISURIYACHAI, Ph.D.)

-- Examiner

(Associate Professor DAWAN WIWATTANADATE, Ph.D.)

-- External Examiner

(Monrawee Pancharoen, Ph.D.)

หฤษฎ์ ปฐวีไพสิฐ : การประเมินประสิทธิภาพของสารติดตาม ชนิดฟลูออเรสเซนต์ ในแหล่งกักเก็บปิโตรเลียม ชนิดหินทรายผสมหินดินดาน. (EFFECTIVENESS EVALUATION OF FLUORESCENT TRACER IN SHALY-SANDSTONE RESERVOIR) อ.ที่ปรึกษาหลัก : ผศ. ดร.ฟ้าลั่น ศรีสุริยชัย

ในอุตสาหกรรมการสำรวจและผลิตปิโตรเลียม สารติดตามคือสารใด ๆ ที่ผสมกับของเหลวที่ใช้ในการฉีดอัดลงแหล่งการกักเก็บปิโตรเลียม และสามารถตรวจจับได้ในปริมาณที่น้อยมาก ๆ ฟลูออเรสซีนโซเดียมคือสารติดตามชนิดฟลูออเรสเซนต์ที่เป็นที่นิยมอย่างกว้างขวางในงานวิชาการต่าง ๆ เพราะเป็นสารที่สามารถเปล่งแสงฟลูออเรสเซนต์ได้แม้ในความเข้มข้นต่ำ ตลอดจนเป็นสารที่ไม่มีพิษและไม่โดนย่อยสลายตามธรรมชาติ ในการศึกษานี้ ได้ทำการประเมินประสิทธิภาพของฟลูออเรสซีนโซเดียม ในรูปแบบของสารละลาย เมื่อใช้ในแหล่งกักเก็บปิโตรเลียมแบบหินทรายผสมหินดินดาน

ในส่วนแรกของการศึกษานี้ได้มุ่งเน้นไปที่การศึกษาคุณลักษณะทางเคมีของสารละลายฟลูออเรสซีนโซเดียม ความเข้มข้นต่ำที่สุด ที่การเปล่งแสงฟลูออเรสเซนต์ของสารละลายฟลูออเรสซีน โดยใช้น้ำกลั่นเป็นตัวทำละลายสามารถตรวจจับได้เมื่อใช้เครื่อง ฟลูออเรสเซนต์สเปคโตรโฟโตมิเตอร์ในการตรวจจับคือความเข้มข้นระดับ 500 ส่วนใน 1 ล้านล้านส่วน ความเข้มข้นของสารละลายฟลูออเรสซีนที่ระดับ 10 ส่วนใน 1 ล้านส่วนเป็นความเข้มข้นที่เปลี่ยนความสัมพันธ์ระหว่างความเข้มข้นแสงฟลูออเรสเซนต์กับความเข้มข้นของสารละลายฟลูออเรสซีน ความยาวคลื่นของแสงฟลูออเรสเซนต์ที่ความเข้มข้นแสงสูงสุดเป็นสัดส่วนโดยตรงกับความเข้มข้นของสารละลายฟลูออเรสซีนและหยุดเป็นสัดส่วน โดยตรงเมื่อความยาวคลื่นลดลงถึง 512 นาโนเมตร ที่ความเข้มข้นระดับ 1 ส่วนใน 1 ล้านส่วน การเก็บรักษาสารละลายฟลูออเรสซีนควรเก็บอยู่ ภายในขวดสีชาเพื่อป้องกันผลกระทบจากแสง และในสภาพเป็นกลางถึงด่าง ทั้งนี้อุณหภูมิของแหล่งกักเก็บปิโตรเลียมตั้งแต่ 30-70 องศาเซลเซียสนั้น ไม่มีผลใด ๆ กับสารละลายฟลูออเรสซีน

ต่อมาในส่วนครึ่งหลังของการศึกษาได้เน้นไปในการประเมินปฏิสัมพันธ์ระหว่างสารละลายฟลูออเรสซีนและหินทรายผสมหินดินดาน ในการตรวจสอบแบบสถิต ผลกระทบของหินทรายผสมหินดินดานที่มีต่อการตรวจจับแสงฟลูออเรสเซนต์ มีมากกว่าผลกระทบจากไฮโดรคาร์บอน และ/หรือ น้ำโคลนสำหรับการขุดเจาะ อย่างไรก็ดี ผลกระทบของหินทรายผสมหินดินดานลดลง เมื่อความเข้มข้นของสารละลาย ฟลูออเรสซีนเพิ่มขึ้นและ หายไปเมื่อความเข้มข้นเพิ่มขึ้นถึงระดับ 100 ส่วนใน 1 ล้านส่วน เมื่อความเข้มข้นเพิ่มขึ้นมากกว่าระดับนี้ การดูดซับของโมเลกุลฟลูออเรสซีนบนพื้นผิวของหินทรายผสมหินดินดานได้เกิดขึ้น ต่อมาในการตรวจสอบแบบพลวัต เวลาในการไหลผ่าน ของโมเลกุลฟลูออเรสซีนที่ความเข้มข้นระดับ 1 ส่วนใน 1 พันล้านส่วน มีความใกล้เคียงกับเวลาในอุดมคติของของเหลวใด ๆ ที่ไหลผ่านช่อง ว่างที่ไหลได้ในหินทรายผสมหินดินดาน เมื่อสารละลายฟลูออเรสซีนมีความเข้มข้นเพิ่มขึ้นเป็นระดับ 100 ส่วนใน 1 ล้านส่วน และ 1 ส่วนใน 1 ล้านส่วน เวลาในการไหลผ่านของโมเลกุลฟลูออเรสซีนยาวนานขึ้น เนื่องจากการแพร่ของโมเลกุลฟลูออเรสซีนเข้าสู่น้ำส่วนที่ผลิตไม่ได้ภายในหินและ การดูดซับของฟลูออเรสซีนบนพื้นผิวหินทรายผสมหินดินดาน ในท้ายสุดไอออนประจุบวกถูกพบว่าสามารถเพิ่มความเข้มข้นแสง ฟลูออเรสเซนต์ของสารละลายฟลูออเรสซีนได้ ดังนั้นการตรวจจับการเปล่งแสงฟลูออเรสเซนต์ของความเข้มข้นระดับ 500 ส่วนใน 1 ล้านล้านส่วน เมื่อสารอยู่ในหินทรายผสมหินดินดานจึงเป็นไปได้ ดังนั้นความเข้มข้นของสารละลายฟลูออเรสซีนที่เหมาะสมสำหรับใช้ในแหล่งกักเก็บปิโตรเลียม ชนิดหินทรายผสมหินดินดาน คือในช่วงระดับ 500 ส่วนใน 1 ล้านล้านส่วน ถึง 1 ส่วนใน 1 พันล้านส่วนโดยขึ้นอยู่กับชนิดของของเหลวที่ใช้ในการฉีดอัด

สาขาวิชา	วิศวกรรมทรัพยากรธรณีและปิโตรเลียม	ลายมือชื่อนิสิต ....
ปีการศึกษา	2562	ลายมือชื่อ อ.ที่ปรึกษาหลัก ....

Harid Pataveepaisit : EFFECTIVENESS EVALUATION OF FLUORESCENT TRACER IN SHALY-SANDSTONE RESERVOIR. Advisor: Asst. Prof. FALAN SRISURIYACHAI, Ph.D.

In petroleum exploration and production industry, tracer is a compound added to injected fluids, and can be easily detected even in a trace amount. Fluorescein sodium, a chemical tracer that can illuminate upon receiving a specific wavelength of light, was mentioned by several literatures due to its strong fluorescence at low concentration, non-toxicity, and non-biodegradability. In this study, fluorescein sodium in the form of fluorescein solution was evaluated with shaly-sandstone to observe their interactions.

The first half of this study focused on the evaluation of the chemical characteristics of fluorescein. First, the detection limit of fluorescein solution in deionized water characterized by fluorescence spectrophotometer was at 500 ppt. Fluorescein concentration at 10 ppm was a critical concentration to reverse the relationship between fluorescence intensity and fluorescein concentration. Fluorescence emission wavelength at maximum fluorescence intensity was a function of fluorescein concentration and stopped to decline as emission wavelength reached the wavelength of 512 nm at the concentration of 1 ppm. Appropriate storage for fluorescein solution was recommended to be inside an amber-colored glass bottle to prevent photodegradation at neutral to basic pH values. Fluorescein solution could be used in a petroleum reservoir with a temperature range of 30-70 degrees Celsius for 12 days without substantial thermal degradation.

The second half of this study focused on the interactions between fluorescein solution and shaly-sandstone. In the static investigation of fluorescein solution, it was found that the effects of shaly-sandstone on fluorescence dominated the presence of hydrocarbon and/or drilling fluids. Nevertheless, the effects of shaly-sandstone diminished as fluorescein concentration increased and this effect disappeared at the concentration of 100 ppm. As the concentration increased above 100 ppm, fluorescein adsorption onto shaly-sandstone occurred. In the dynamic investigation, the fluorescein breakthrough time of 1-ppb fluorescein solution was similar to the ideal breakthrough time for any liquid flowing through the movable pore volume of shaly-sandstone core sample. At higher concentrations of 100 ppb and 1 ppm, the breakthrough times were delayed possibly due to diffusion of fluorescein molecules into irreducible water portions of the core sample and fluorescein adsorption onto shaly-sandstone. Lastly, positively charged ions were found that they could amplify fluorescence intensity of fluorescein solution. Hence, at very low fluorescein concentrations in the presence of shaly-sandstone, such as at the concentration of 500 ppt, fluorescence detection would be possible. Therefore, appropriate fluorescein concentrations used in the pilot project could be in a range of 500 ppt to 1 ppb depending on the type of injected water.

| Field of Study: | Georesources and Petroleum Engineering | Student's Signature .... |
| Academic Year: | 2019 | Advisor's Signature .... |

ACKNOWLEDGEMENTS

TABLE OF CONTENTS

จุฬาลงกรณ์มหาวิทยาลัย
CHULALONGKORN UNIVERSITY

List of Tables

List of Figures

List of Abbreviation

ASP	Alkaline-Surfactant-Polymer
CEC	Cation Exchange Capacity
CFS	Core Flooding System
GSG	Glass-Silicon-Glass
IUPAC	International Union of Pure and Applied Chemistry
IWTA	Inter-Well Tracer Analysis
pH	Potential of Hydrogen
PMT	Photomultipliers
USA	United States of America
XRF	X-Ray Fluorescence
Å	Ångström
atm	Standard Atmosphere
cm	Centimeter
cm^{-1}	Inverse Centimeter
cm^2	Square Centimeter
cm^3	Cubic Centimeter
cm^3/min	Cubic Centimeter Per Minute
cm^3/s	Cubic Centimeter Per Second
cP	Centipoise
ft	Foot
ft/d	Foot Per Day
g	Gram
g/cm^3	Gram Per Cubic Centimeter
g/mL	Gram Per Milliliter
lb/ft^3	Pound Per Cubic Foot
m	Meter

mD	Millidarcy
min	Minute
mL	Milliliter
mM	Millimolar
mm	Millimeter
nM	Nanomolar
nm	Nanometer
ppb	Part Per Billion
ppm	Part Per Million
ppt	Part Per Trillion
psi	Pound Per Square Inch
rpm	Round Per Minute
s	Second
s^{-1}	Inverse Second
V	Volt
°C	Degree Celsius
°F	Degree Fahrenheit

List of Nomenclature

A	Cross-Sectional Area
A_c	Arrhenius Constant, Frequency Factor, or Pre-Exponential Factor
C	Final Fluorochrome Concentration
C^0	Initial Fluorochrome Concentration
C_B	Final Benzoic Acid Concentration
C_B^0	Initial Benzoic Acid Concentration
C_F	Final Fluorescein Concentration
C_F^0	Initial Fluorescein Concentration
D	Diameter
E_A	Activation Energy
K	First-Order Rate Constant
K_B	First-Order Rate Constant of Benzoic Acid
K_F	First-Order Rate Constant of Fluorescein
k	Absolute Permeability
q	Liquid Flow Rate
L	Length
M_{dry}	Dried Weight
M_{sat}	Saturated Weight
ΔP	Pressure Difference
R	Universal Gas Constant
S_0	Electronic Ground State
S_1	Lower-Energy Electronic Excited Singlet State
S_2	Higher-Energy Electronic Excited Singlet State
T	Temperature
T_1	Electronic Excited Triplet State
t	Time
V_b	Bulk Volume

V_p	Pore Volume
X	Time Interval from 30 Minutes to Fluorescein Breakthrough Time for 1-ppb Fluorescein Solution Flowing Through Shaly-Sandstone Core Sample
x	Fluorescein Concentration in Equivalent Fluorescein Concentration Determination
Y	Time Interval from 30 Minutes to Fluorescein Breakthrough Time for 100-ppb Fluorescein Solution Flowing Through Shaly-Sandstone Core Sample
y	Maximum Fluorescence Intensity in Equivalent Fluorescein Concentration Determination
Z	Time Interval from 30 Minutes to Fluorescein Breakthrough Time for 1-ppm Fluorescein Solution Flowing Through Shaly-Sandstone Core Sample
ρ_L	Liquid Density
μ_L	Liquid Viscosity
ϕ	Porosity

CHAPTER 1: INTRODUCTION

Nowadays, the world's crude oil consumption is significantly increased due to the rises of global oil demand and world population. Various production techniques, such as waterflooding, gasflooding, and enhanced oil recovery methods, have a major role to improve oil production around the world. However, the first task that must be achieved before any technique is executed in order to guarantee an accomplishment of the project is determination of reservoir connectivity between injection wells and production wells which can be evaluated by performing an inter-well tracer test [1].

Fluorescein in the form of fluorescein sodium salt, which is classified as one subtype of chemical tracers so-called fluorescent tracer [2], is an organic xanthene-derivative fluorescent compound appearing as crimson powder. In the form of fluorescein solution, it can emit fluorescence in green spectrum. Advantages of the use of fluorescein in a tracer test over other types of chemical tracers are having easy and simple detection method, having no concentration background in the reservoir, having very low detection limit, having high thermal stability, and having no toxicity and biodegradability. However, it has three main drawbacks including being photodegraded, being highly pH-dependent on alkaline, and being adsorbed by rock formation.

Shaly sandstone, a sandstone with greater than 10% clay content, is a detrital sedimentary rock formed by an alternate sedimentation between clay-sized and sand-sized particles during transgressive-regressive cycles. Clay in shaly-sandstone is the major problem that causes wrong geological interpretations and formation damages. Physical characteristics of clay are having large negatively charged surface that can adsorb positively charged ions in reservoir fluid, and having high cation exchange capacity that can release a lot of adsorbed positively charged ions back to reservoir

fluid and those released positively charged ions can further affect negatively charged ions suspended in the fluid.

Therefore, the objectives of this study are to evaluate the effectiveness of fluorescein sodium salt in the form of fluorescein solution with shaly-sandstone, and to identify appropriate conditions for implementation of tracer tests using fluorescein solution in shaly-sandstone reservoir. In addition, the results of this study can be further applied to both petroleum and geothermal reservoirs.

Scope of this study can be divided into two parts. The first part focuses on characteristics evalution of fluorescein solution using deionized water as solvent at laboratory scale. Detection limit and thermal stability at petroleum reservoir temperatures of fluorescein solution would be determined. Drawbacks of fluorescein solution including photosensitivity and pH-sensitivity would also be investigated. Next, the second part focuses on effectiveness evaluation of fluorescein solution with shaly-sandstone. Fluorescein solution was evaluated with shaly-sandstone cutting powders in static investigation or stirring tests in order to observe full interactions between fluorescein and shaly-sandstone and to determine fluorescein adsorption on shaly-sandstone surface. Subsequently, fluorescein solution was further evaluated with shaly-sandstone core sample in dynamic investigation or coreflooding tests to observe actual interactions between fluorescein and shaly-sandstone, and to determine appropriate fluorescein concentrations for a tracer test in shaly-sandstone reservoir. Moreover, salt effect on fluorescein solution was also evaluated to support the results from two previous tests.

Besides, fluorescein solution from all experiments was characterized by using fluorescence spectrophotometer with photomultiplier (PMT) voltage of 400 - 800 V and slit size of 5 and 10 nm. The higher values of PMT voltage and slit size are used to characterize the samples with lower fluorescence intensity. Importantly, only limitation of this study is that the results in the form of fluorescence intensity with

different values of PMT voltage and slit size could not be compared. In order to compare the results, fluorescence intensity must be converted into equivalent fluorescein concentration using calibration curves for each range of concentrations with specific PMT voltage and slit size.

จุฬาลงกรณ์มหาวิทยาลัย
CHULALONGKORN UNIVERSITY

CHAPTER 2: LITERATURE REVIEW

2.1. Fluorescein in Petroleum Industry

Födisch *et al.* [3] conducted an investigation on connate water displacement during EOR chemical processes in glass-silicon-glass (GSG) micromodel. Fluorescein-brine solution with fluorescein concentrations of 10 ppm to 300 ppm were prepared by mixing the solutions using magnetic stirring bar at speed of 500 rpm for 1 hour. After the micromodel was fully saturated with the solution followed by paraffin oil injection to achieve an initial oil saturation, waterflooding and polymer flooding were performed through the micromodel. The results showed that fluorescein clearly demonstrated visual access on connate water displacement. It also showed clear differentiation between viscous fingering caused by waterflooding and stable displacement flood caused by polymer flooding at which fluorescein concentration decreased rapid when viscous fingering occurred. This phenomenon of viscous fingering was also observed experimentally using fluorescein by Peters and Flock [4] during wettability number estimation.

Bryant *et al.* [5] conducted microbial-enhanced waterflooding tests in Mink Unit located in Delaware-Childers field in Nowata County, Oklahoma, USA in which this field was used to produce oil from Bartlesville sandstone formation. They found that fluorescein was compatible with reservoir fluids as well as with their microbial cultures. Thus, fluorescein was chosen as fluorescent tracer to determine flow patterns of injected fluids in the unit. Samples from producing wells were collected daily for the first five days after tracer injection and then on weekly basis onward for two months. The samples were protected from sunlight before being transported to the laboratory where fluorescein concentration was analyzed by using spectrophotometric method. Fluorescein concentration curve was plotted as a function of time for each producing well. The results showed that all producing wells showed signal responses from injected fluorescein that indicated reservoir connectivity among the wells.

Olsen *et al.* [6] conducted coreflooding tests using core samples from the oil-wet Cretaceous Upper Edwards carbonate reservoir located in Central Texas, USA in order to describe an application of alkaline-surfactant-polymer (ASP) technology with wettability alteration in carbonate reservoir. Fluorescein solution with concentration of 10 ppm was injected with pre-waterflooding slug, ASP slug, and post-waterflooding slug through the core samples. The results showed that fluorescein could be used to determine both degree of dispersion and effects from heterogeneity of the cores which could cause poor sweep efficiency during an oil displacement, and to correlate breakthrough times of injected chemicals.

Aparecida de Melo, de Holleben, and Almeida [7] used three tracers including fluorescein in order to characterize Carmopolis field in Brazil as a candidate area for polymer pilot project for mobility control in which Muribeca-Carmopolis formation mainly consisted of sandstones and conglomerates. The result showed that fluorescein indicated 17% fluorescein adsorption of the injected slug. The authors suggested that required fluorescein slug size should be large whereas distance between wells and residence time in the reservoir should be short so that adsorption could be neglected.

Greenkorn [8] performed an experiment using 13 tracers including fluorescein to select five tracers that can be used together to locate flow paths in a pilot flood. The satisfied tracers of this literature should (1) be easy to be analyzed and (2) show similar breakthrough-elution curves as the curves of chloride ions which tracers were believed to have almost the same velocity as flood front. Naturally, tracers could not travel at the same speed as the flood front because of adsorption-desorption effect and diffusion-dispersion effect which caused tracers to lag behind and spread more than the flood front [9]. For the experiment, it consisted of two tests. The first test was static tests which the remaining concentration of each tracer after mixed with sand was compared with its initial concentration. The results showed that fluorescein still remained 88.7% after it had been mixed with sand for 29 days. The literature suggested that fluorescein solution should be kept inside colored bottles in order to prevent

exposure from light and pH of the solution should be within alkaline range. The second test was dynamic tests in which tracers were injected along with brine at injection rate of 1 ft/d through a sandstone model and breakthrough-elution curves were observed. The results showed that the curve of fluorescein lagged all the other tracers and it tended to be adsorbed in greater amount than the others. Fortunately, a degree of fluorescein adsorption was only 6% higher than that of chloride. Finally, Greenkorn concluded that fluorescein might be satisfactory; however, it seemed not to follow the flow well compared to other tracers.

Khalil and Oliveira [10] evaluated a performance of oleophilic fluorescein in assessment of volume in subsea flowline. Oleophilic fluorescein was a derivative of fluorescein that was non-polar and only soluble in non-polar solvents. It could be synthesized in the reaction so-called Fischer esterification using hydrophilic fluorescein and higher alcohol as reactants and mineral acid as catalyst. The reaction focused on esterification of carboxyl group (RCOOH) in hydrophilic fluorescein into ester (RCOOR^1) using higher alcohol. Mechanisms of the esterification reaction and chemical structure of oleophilic fluorescein were shown in figure 1 and figure 2, respectively. It was noted that the alphabet R referred to other parts of fluorescein, whereas R^1 referred to other parts of higher alcohol. Next, oleophilic fluorescein was found to be fully soluble in non-polar solvents including crude oil, diesel oil, xylene, benzene, kerosene, and toluene. Since fluorescence of oleophilic fluorescein could not be observed when being dissolved in crude oil, for better fluorescence visualization, the reaction so-called saponification was used to convert oleophilic fluorescein back to hydrophilic fluorescein by adding water followed by strong alkaline solution into non-polar solvent containing oleophilic fluorescein.
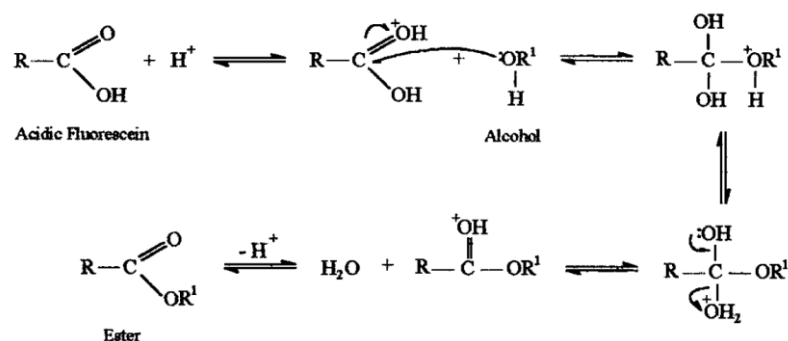
Figure 1. *Mechanisms of Fischer esterification reaction.*
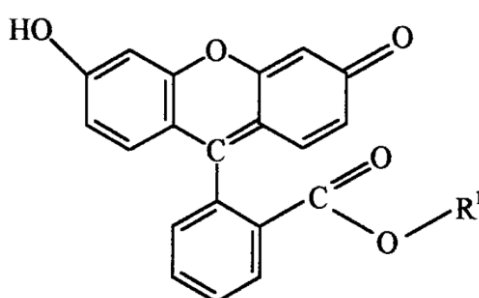
Figure 2. *Chemical structure of oleophilic fluorescein.*

Doty [11] performed a drilling experiment on Berea sandstone and Pierre shale using four types of drilling fluid including (1) $CaCl_2$/$CaBr_2$/polymer drilling fluid used to epitomize nearly solids-free drilling fluid, (2) $CaCl_2$/$CaBr_2$/polymer/Rev Dust A drilling fluid used to epitomize highly solids-contaminated brine drilling fluid, (3) conventional lignosulfonate water-based drilling fluid, and (4) relaxed filtrate oil-invert-emulsion-based drilling fluid. Both drilling fluids (3) and (4) contained Rev Dust A which were used to epitomize drilling fluids that had been used for certain period of time. Fluorescein concentration of 90 ppm was added into drilling fluids (1) to (3) in order to trace and demonstrate the drilling fluid invasion pattern through Berea sandstone by both sectioning the sandstone and using ultraviolet light. The results showed that fluorescein was detected in all parts after sectioning the sandstone sample into ¼-in-thick segments.

Metidji *et al.* [12] described that in the field test, produced water samples contained high concentration of water-soluble hydrocarbons that could interfere

fluorescence detection. Aromatic hydrocarbons in crude oil were an epitome of the major hindrance for using fluorescein as fluorescent tracer since they contained organic fluorescence which could cause wrong detection results. Luckily, organic fluorescence from aromatic hydrocarbon had short lifetime which could affect the results only after being produced from the reservoir.

2.2. Fluorescein in Geothermal Industry

Kennedy *et al.* [13] started Geothermal Technologies Program since 1976 to overcome challenges in reservoir engineering and make geothermal electricity more cost-competitive. Four fields including (1) Geysers steam-dominated geothermal system in California, USA, (2) Cerro Prieto water-dominated geothermal power system in Baja California, Mexico, (3) Larderello geothermal power system in southern Tuscany, Italy and (4) Dixie Valley non-magmatic basin and range geothermal system in Nevada, USA were selected to be studied in this program. Many types of tracers were added and injected with lower-temperature augmentation fluid in order to ensure that injection wells provided the longest time for the fluid to absorb heat before it appeared at a production well. Fluorescein was also one of selected tracers in the program as the first geothermal tracer to gain widespread application in the geothermal industry. Fluorescein was thermally stable which could be used in reservoir temperature up to 260 °C (500 °F) and would decay rapidly in temperature beyond this value. Furthermore, Kennedy *et al.* and Morris *et al.* [14] also mentioned that fluorescein was classified as conservative tracer which was non-reactive with rock formation in the reservoir. However, it could behave different ways in different reservoir conditions at which fluorescein would exhibit adsorptive and non-adsorptive behaviors under different conditions.

Nielson *et al.* [15] investigated the uses of tracers at Dixie Valley geothermal system in Nevada, USA to evaluate rock-water interactions of geothermal tracers. Fluorescein was also used in this investigation as geothermal tracer. The authors described that fluorescein normally showed significant adsorption during underground

water tests which retarded an arrival time of the peak and interfered with interpretation of breakthrough time analysis. Simultaneous injection of fluorescein with non-adsorbing tracer (i.e. benzoic acid) would show two distinct peaks resulting in time separation of the arrival of the peaks of each tracer. However, after both tracers were injected, the results showed that there was no peak separation. Since reservoir temperature was about 232 °C (450 °F), they concluded that fluorescein did not adsorb at this temperature and was chosen to be an appropriate tracer for this reservoir conditions.

Tester, Bivins, and Potter [16] conducted a characterization of a hot, low-matrix-permeability, hydraulically fractured granitic reservoir in Los Alamos National Laboratory at Fenton Hill site near Valles Caldera in Jemez Mountains of north-central New Mexico using tracers including fluorescein in order to estimate sweep efficiency and fracture volumes inside the reservoir. Fluorescein solution with concentrations of 200 to 1,000 ppm was injected into the reservoir. Recovered amount of fluorescein from the production well was analyzed by spectrophotometric equipment as functions of volume and time to determine residence time distribution. The authors also performed additional experiments of fluorescein in fluorescein-granite-water system. Fluorescein detection limit used in this experiment was about 50 ppb which was lower than normal limit used in field operation of about 4,000 to 20,000 times. The results showed that there was neither adsorption nor decomposition of fluorescein at temperature of 200°C (392°F) for 24 hours.

Adams and Davis [17] evaluated kinetics of fluorescein decay when used as geothermal tracer with different temperatures, fluid compositions, pH, and oxygen content. First, decay rate of fluorescein at constant pH could be described by using first-order rate law as shown in equation (1):

$$C = C^0 e^{-Kt} \qquad\qquad (1)$$

where C is final fluorochrome concentration, C^0 is initial fluorochrome concentration, K is first-order rate constant (s^{-1}), and t is time (s). For better demonstration, equation (1) was converted to linear relationship of $ln(C)$ and t as shown in equation (2):

$$ln(C) = -C^0Kt \qquad (2)$$

First-order rate constant was calculated with Arrhenius equation as shown in equation (3):

$$K = A_c e^{-\frac{E_A}{RT}} \qquad (3)$$

where A_c is Arrhenius constant, frequency factor, or pre-exponential factor, E_A is activation energy, R is universal gas constant, and T is temperature. Second, stability test of fluorescein was performed with a presence of altered quartz diorite consisted of quartz, illite, chlorite, and epidote. The results showed that decay rates of the solution with and without diorite were identical which could imply that no adsorption occurred. Third, thermal stability of fluorescein was evaluated inside hydrothermal autoclaves at temperatures ranging from 210-270 °C (410-518 °F). The results showed that at reservoir temperature between 210-260 °C (410-500 °F), fluorescein was considered as relatively conservative tracer inside the reservoir, and at temperature above 260 °C (500 °F), fluorescein could be used only when residence time was very short inside the reservoir. Half-lives and 10% decay time of fluorescein at different temperatures are listed in table 1. Fourth, an effect from salinity on decay rate was evaluated using geothermal fluid from Heber geothermal system as solvent. Sodium-saturated cation-exchange resin was used to replace calcium and magnesium ions in geothermal fluid with sodium ions in order that calcium and magnesium phosphate would not precipitate when phosphate-buffered saline consisting of potassium phosphate monobasic (KH$_2$PO$_4$) and sodium phosphate dibasic (Na$_2$HPO$_4$ • 7H$_2$O) was added to the fluid to maintain pH 6.5. Total dissolved solids of unbuffered and buffered geothermal fluid was differed by approximately 8%. The results showed that decay rate was not significantly affected by salinity change at room temperature. However, significant effect could be observed at high temperature in which an increase

in salinity resulted in a decrease in decay rate. Fifth, an effect from oxygen content in the fluid resulted in rapid fluorescein degradation; however, the effect was diminished when pH of the fluid was higher than 8. It was recommended to flash injected fluid prior to the injection which resulted in higher pH and lower oxygen content. Moreover, fluorescein was used in Dixie Valley geothermal system, which was mainly composed of altered basalts and gabbro, simultaneously with other tracers that their first-order rate constants were recognized. Fluorescein was injected together with benzoic acid and 4-ethylbenzenesulfonic acid in different wells, whereas benzenesulfonic acid was solely injected in another well. Two months after injection, only fluorescein and benzoic acid were detected in one production well. Effective temperature of injection-production flow path, which was average temperature of the flow path, but accounted towards high temperature due to temperature-dependence of Arrhenius equation, was determined by using a ratio of equation (1) for fluorescein to equation (1) for benzoic acid as shown in equation (4):

$$\frac{C_F}{C_B} = \frac{C_F^0}{C_B^0} e^{(K_B - K_F)T} \tag{4}$$

where subscriptions F and B refer to fluorescein and benzoic acid, respectively. Since only first-order rate constant of benzoic acid was already known, by measuring changes in tracer concentrations, the effective temperature was calculated by using Arrhenius equation. The results showed that effective temperature was determined to be about 225-230 °C (437-446 °F) which was temperatures between pre-exploitation temperature of 221 °C (429.8 °F) and reservoir temperature of 240 °C (464 °F). Furthermore, tracer breakthrough time curves showed that there was no distinct peak between fluorescein and benzoic acid, meaning that fluorescein behaved as non-adsorptive behavior at this reservoir conditions.

Table 1. *Half-lives and 10% decay time of fluorescein at different temperatures.*

Temperature (°C)	Temperature (°F)	Half-life (days)	10% decay time (days)
200	392	643	98
210	410	303	46
220	428	146	22
230	446	73	11
240	464	37	6
250	482	20	3
260	500	11	2
270	518	6	1

Sugita *et al*. [18] evaluated effects of pH and dissolved ions on fluorescence intensity of fluorescein being used as geothermal tracer. The results showed that when pH was lower than 9, fluorescence intensity was a function of pH, whereas when pH was higher than 9, the intensity became stable. Next, fluorescein in clear and brown glass bottles could be degraded by fluorescent light, but fluorescein in bottles warped with aluminum foil was not degraded within one month. Later, various of chemicals including sodium chloride (NaCl), potassium chloride (KCl), magnesium chloride hexahydrate (MgCl$_2 \cdot$ 6H$_2$O), calcium chloride hexahydrate (CaCl$_2 \cdot$ 6H$_2$O), aluminium chloride (AlCl$_3$), iron(III) chloride hexahydrate (FeCl$_3 \cdot$ 6H$_2$O), sodium sulfate (Na$_2$SO$_4$), and sodium carbonate (Na$_2$CO$_3$) were used to evaluate effects of dissolved ions on fluorescein. The results showed that the effects of K$^+$, Ca^{2+}, Cl$^-$, SO$_4^{2-}$, and CO$_3^{2-}$ ions were difficult to be observed. Subsequently, fluorescence intensity showed to be unaffected by Al^{3+} ions which was the same Al^{3+} content as in geothermal fluid of about 1 mg/L. The intensity was then affected by Mg^{2+} ions, but increasing pH to 12 could solve this problem. Finally, the intensity seemed to be affected when Fe^{3+} concentration increased. This was due to precipitation of iron(III) oxide (FeOH$_3$) which acted as adsorbent and resulted in fluorescein adsorption in the form of colloidal.

2.3. Fluorescein in Medical and Pharmaceutical Study

Hiramoto *et al.* [19] investigated effects of change in hydrogen ion concentration to fluorescent antibody-labelling agents including amino fluorescein (green fluorescence) and 3-aminotetramethylrhodamine (orange fluorescence) used in a conjugation of horse antirabbit gamma globulin for a detection of rabbit antibodies to rat kidney glomeruli in order to control fluorescence of either fluorescein or tetramethylrhodamine when both were used concurrently on a single tissue section. From the results, fluorescence of fluorescein was quenched at pH 3, perceptibly quenched at pH 4 to 5, and fluoresced well at pH 7 to 11. Tetramethylrhodamine was also perceptibly quenched at pH 3 and fluoresced well at pH 4 to 11. When fluorescein and tetramethylrhodamine were employed simultaneously, yellow fluorescence which was a fluorescence between green and orange could be observed. By shifting pH value to 4, green fluorescence of fluorescein was solely quenched and orange fluorescence of tetramethylrhodamine finally revealed.

Doughty [20] examined a change in fluorescence spectra of fluorescein solution in unbuffered 1% NaCl solution. For concentrated fluorescein solution of 3.32 mM or 0.125% (equivalent to 1,250 ppm), fluorescence emission wavelength at maximum fluorescence intensity was at 560 nm. As the solution was diluted, emission wavelength at maximum intensity had shifted to shorter wavelength (higher energy) and eventually at extremely diluted solution of 51 nM or 0.000002% (equivalent to 20 ppb), the wavelength was at 513 nm. Moreover, pH of this extremely diluted solution was varied from 4.5 to 8.5. Fluorescence spectra of the solution with different pH values showed that the higher the pH, the higher the maximum fluorescence intensity.

Conversion of molar to parts per million:

$$ppm = molar \times molecular\ weight \times 1{,}000$$

Conversion of percentage to parts per million:

$$ppm = percentage \times 10{,}000$$

Conversion of gram per milliliter to parts per million:

$$ppm = g/mL \times 1,000,000$$

2.4. Fluorescein in Advanced Chemistry Study

Panchompoo *et al.* [21] performed modification of carbon black nanoparticles with fluorescein in order to use as fluorescent probe for a detection of palladium in presence of iron in wastewater steam. They explained that fluorescein was highly pH-dependent and could exist in seven prototropic structures depending on pH values of solution as shown in figure 3. First, at pH below 2, cationic fluorescein existed that had one positive charge. Second, at pH 2-4, neutral fluorescein existed in structures of para-quinoid, zwitterion, and lactone. For para-quinoid and lactone, they had no charge, whereas zwitterion had one positive charge and one negative charge. Third, at pH 4.3-6.4, monoanionic fluorescein existed in structures of carboxylate and phenolate which had one negative charged. Finally, at pH above 6.4, dianionic fluorescein existed which had two negative charges and showed strong fluorescence.
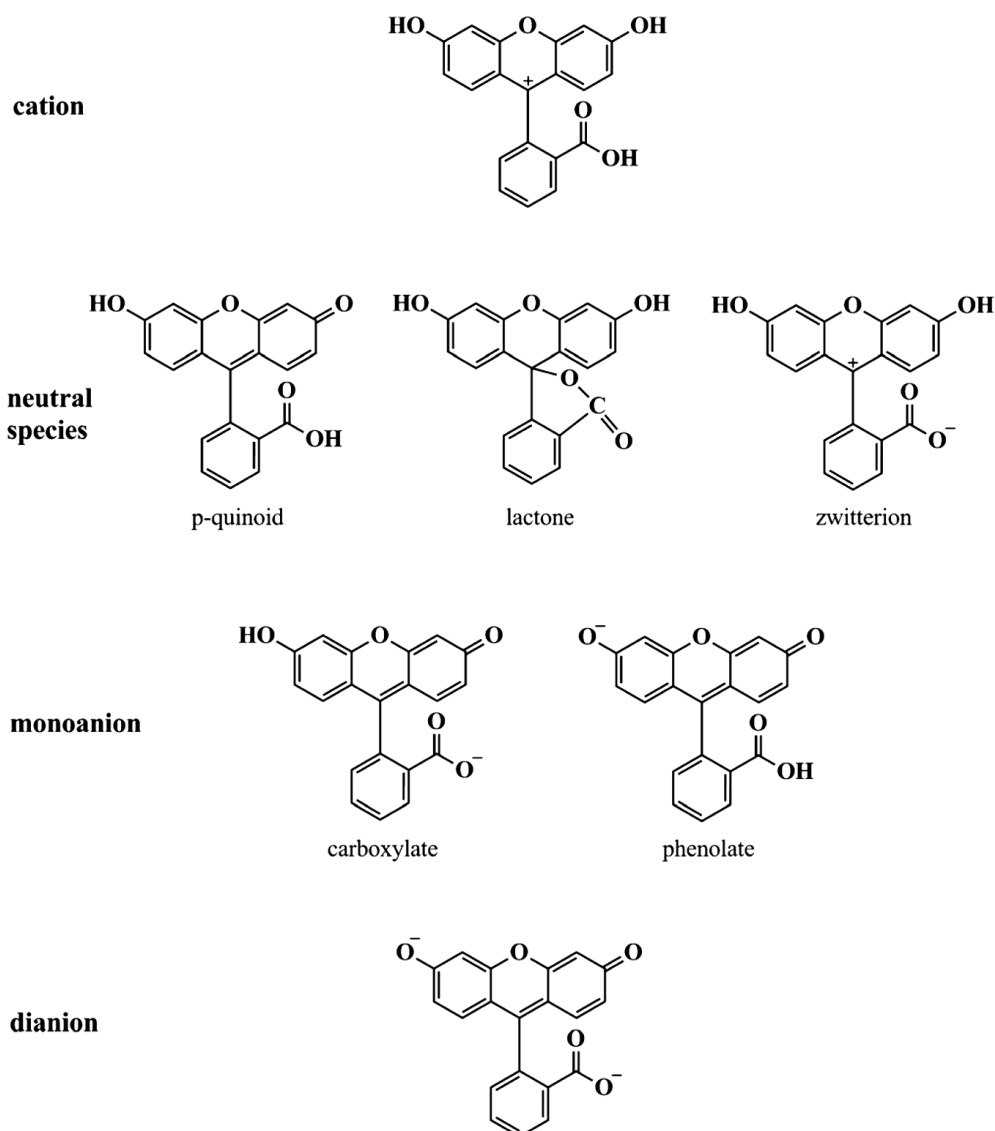
Figure 3. *Prototropic structures of fluorescein at different pH values of solution.*

Markuszewski and Diehl [22] investigated three neutral solid structures of fluorescein including para-quinoid, zwitterion, and lactone. First, para-quinoid – assigned as red solid fluorescein – contained highly conjugated structure in several resonance structures, which was the source of red color, and also had the same color as fluorescein sodium salt. Second, zwitterion – assigned as yellow solid fluorescein – had amphoteric nature with high melting point and low solubility. The source of yellow color was from the presence of positive charge in central heterocyclic ring containing oxygen atom. The positive charge could be either on oxygen atom which made the

ring similar to pyrylium cation ($C_5H_5O^+$) or on central carbon atom so-called carbonium ion. Yellow color could still be observed in strongly acidic solution containing cationic structure of fluorescein due to the presence of positively charged ring. Lastly, lactone – assigned as colorless solid fluorescein – had low stability due to a repulsive strain between xanthene ring, which was composed of two benzene rings and heterocyclic ring containing oxygen atom, and lactone ring, which was a ring with an ester as functional group. The source of colorless was from the presence of the central carbon atom that bonded with other atoms using four single bonds. This behavior was also observed in phenolphthalein and 3,6-dihydroxy-9,9-dimethylxanthene. In addition, lactone could only be observed in anhydrous solvents and it could change from colorless to yellow in the presence of water. Next, in the production phase, commercial fluorescein was purified in many steps and finally converted into diacetylfluorescein in order to avoid an effect from metal and heavy metal ions present in commercial fluorescein on physico-chemical properties of fluorescein. After that, yellow zwitterion and red para-quinoid solids were formed using ethanolic sodium hydroxide with many steps, followed by glacial acetic acid for yellow zwitterion solids, and dilute hydrochloric acid for red para-quinoid solids. Red para-quinoid solids were also formed by heating yellow zwitterion solids at temperature above 250 ℃ (482 ℉) in sublimation apparatus. Finally, colorless lactone solids were formed by dissolving red para-quinoid solids in dioxan, followed by freeze-drying. Furthermore, they continued to study the nature of fluorescein in structures of zwitterion and para-quinoid in water solution [23]. Using descriptions of both solubility and acid dissociation constant, they found that zwitterion was only structure that could exist in water solution because only yellow fluorescence from zwitterion could be observed in all pH values.

CHAPTER 3: RELEVANT THEORIES

In this chapter, the concepts of tracer including definition, characterisitics, and classification were provided. Characteristics and production of fluorescein sodium salt was also emphasized. Furthermore, the concepts of fluorescence was described including definition, effects of parameters on fluorescence intensity, and fluorescence spectrophotometry. As clay in shaly-sandstone was crucial part of this study, characteristics of clay was also summarized in this section.

3.1. Tracer

3.1.1. Definition and Characteristics of Tracer

Inter-well tracer analysis (IWTA) is one of common methods used to determine reservoir connectivity between wells [1]. The word "tracer" is described as any compound that either can be found naturally in the reservoir with known concentration or is added to injected fluids, and can be easily detected even in a trace amount. Tracer selection should be on a basis of tracer characteristics including (1) being non-existent or having well-known background concentration in the reservoir, (2) having low detection limit level with simple and easy analysis to reduce injection volume, cost, and environmental impact, (3) being thermally, chemically, biologically, and physically stable and inert in both atmospheric and reservoir conditions for a long period of time, (4) following the phase being injected with the same flood front velocity and having minimal influence into other phases, (5) having no adsorption and reaction to rock formation, surface and subsurface equipment, (6) having toxic-free or very low toxicity and minimal environmental consequence, and (7) being commercially available in large amounts at an acceptable price [2, 7, 24, 25].

3.1.2. Classification of Tracer [2]

Tracer can be classified into two main groups – natural and artificial. Natural tracer is any compound that can be found naturally in the reservoir and is used to gain reservoir information about production time distribution, origin of produced water, and

contribution of injected fluid to production wells. Natural tracer can be used in the oilfield only if the following conditions are met. Firstly, reservoir fluids must be characterized before, during, and after water breakthrough. Secondly, injected fluids must have significantly higher salinity than reservoir fluids. Lastly, natural tracer must be inert to rock formation and reservoir fluids. Opposingly, artificial tracer is any compound that is not naturally existent in the reservoir and is added into injected fluids. It can be used to gain information in terms of both qualitative such as inter-well connectivity, fluid flow direction, and reservoir heterogeneity, and quantitative such as sweep volume, fluid flow velocity, rock permeability, and residual oil saturation.

Tracer can also be classified into two groups depending on its physico-chemical properties in the reservoir – passive and active. Passive tracer, which can be called non-partitioning, aqueous, or conservative tracer, has the same properties as injected fluid and travel in a reservoir at the same flood front velocity as injected fluid without having interactions with rock formation or reservoir fluids. In contrast, active tracer, which can be called partitioning tracer, can be soluble in both water and oil phases, and can interact with rock formation or reservoir fluids. These interactions result in delay of response of active passer compared to that of passive tracer. The major mechanism of the interaction is partitioning effect of active tracer with reservoir fluids. Other mechanisms are tracer adsorption on rock formation, size exclusion effect, and ion exchange effect. Usually, active tracer is injected simultaneously with passive tracer being used as reference in order to estimate residual oil saturation.

3.1.2.1. Natural Tracer

Natural tracer includes all compounds that can be found naturally in the reservoir such as reservoir fluids. Advantages of natural tracer in comparison to artificial tracer are lower cost and more environmentally friendly since foreign compounds are not bought and injected into the reservoir. Some ions can be used as natural tracer including sodium ion (Na^+), potassium ion (K^+), magnesium ion (Mg^{2+}), calcium ions (Ca^{2+}), strontium ion (Sr^{2+}), barium ion (Ba^{2+}), chloride ion (Cl^-), bromide ion (Br^-), sulfate

ion (SO_4^{2-}), and bicarbonate ion (HCO_3^-), but only K^+, Mg^{2+}, Cl^-, and SO_4^{2-} ions are considered as passive natural tracer. Some isotropic elements such as deuterium (^2H), carbon-13 (^{13}C), and oxygen-18 (^{18}O) can also be used as natural tracer. However, the main drawback of natural tracer is that it is difficult and complex for interpretation and differentiation between reservoir fluids and injected fluids, and requires sophisticated equipment that have high accuracy and sensitivity for analysis. Therefore, the use of natural tracer is less preferable and substituted with the use of artificial tracer.

3.1.2.2. <u>Artificial Tracer</u>

Artificial tracer can be divided into two main categories – radioactive and chemical based on the ability of substances to emit radioactivity.

3.1.2.2.1. *Radioactive Tracer*

Radioactive tracer became widespread in oilfield applications during 1960s to 1990s. Tritium (^3H) is one of the most popular neutral radioactive tracer and generally used in the form of tritiated water (T_2O) due to its similar physico-chemical properties as water molecules. It has low reactivity with rock formation and reservoir fluids, low radioactive emission, and relatively low cost, but the results may be affected by the presence of natural tritium. Tritium and carbon-14 (^{14}C) can be used as a label on some compounds such as alcohols, ketones, aldehydes, and benzoic acids to be used as neutral radioactive tracer. Since both ^3H and ^{14}C have long half-lives of about 12.5 and 5,730 years, respectively, they can be applied in long-term tracer tests. Heavy water or deuterated water which consists of deuterium oxide (D_2O) rather than oxidane (H_2O) was also used as passive neutral radioactive tracer during 1990s. Some isotopic elements in the form of ions can also be used as anionic radioactive tracers such as chloride-36 ($^{36}Cl^-$), bromide-82 ($^{82}Br^-$), iodide-125 ($^{125}I^-$), iodide-129 ($^{129}I^-$), iodide-131 ($^{131}I^-$), thiocyanates with sulfur-35 ($^{35}SCN^-$), thiocyanates with carbon-14 ($S^{14}CN^-$), sulfates with sulfur-35 ($^{35}SO_4^{2-}$), bicarbonates with carbon-14 ($H^{14}CO_3^-$), and some can be used as cationic radioactive tracers such as sodium-22 ($^{22}Na^+$), cobalt(II)-60 ($^{60}Co^{2+}$), cobalt(III)-60 ($^{60}Co^{3+}$), nickel(II)-63 ($^{63}Ni^{2+}$), zinc-65 compounded with yttrium ($[^{65}ZnY]^{2-}$),

strontium-90 ($^{90}Sr^{2+}$), strontium-90 compounded with yttrium ($[^{90}SrY]^{2-}$), caesium-134 ($^{134}Cs^+$), and caesium-137 ($^{137}Cs^+$). These radioactive tracers have high thermal stability which can be used in elevated temperature applications up to 200 °C (392 °F); however, they are expensive and some can be affected by and adsorbed onto rock formation. Only $^{22}Na^+$, $^{63}Ni^{2+}$, $[^{65}ZnY]^{2-}$, $^{134}Cs^+$, and $^{137}Cs^+$ ions can be applied in long-term tracer tests due to their long half-lives. In spite of being measurable easily, being detectable at very low concentration, being injectable at very small injected volume, having low natural existent in the reservoir, and being inert with rock formation and reservoir fluids, radioactive emission was the major concern that made the use of radioactive tracers became less popular and was substituted by the use of chemical tracers.

3.1.2.2.2. *Chemical Tracer*

Chemical tracer became more popular than radioactive tracer during 1990s owing to an absence of radioactive emission and ease of detection with simple analytical methods. Nonetheless, some problems were found related to the use of chemical tracer such as chemical adsorption by rock formation, thermal and bacterial deterioration [26], detection hindrance by a presence of natural compounds, and large-required injection volume. Moreover, chemical tracer can be divided into three groups depending on chemical characteristics.

3.1.2.2.2.1. <u>*Inorganic Salts*</u>

Inorganic salts are mainly used as chemical tracer because of being inexpensive and being analyzed easily. The most ubiquitous inorganic salt is halides including chloride ions (Cl^-), bromide ions (Br^-), and iodide ions (I^-). Cl^- and Br^- ions are considered to be passive chemical tracer that has low adsorption and low reactivity with rock formation and reservoir fluids at low temperature; however, they can be used only when aquifer has lower salinity than injected fluids in order to avoid large injection volume. I^- ion is less preferable in oil reservoirs because of a presence of natural iodide and being less passive than Cl^- and Br^- ions. Other inorganic tracers are nitrite ion

(NO_2^-), nitrate ion (NO_3^-), thiocyanate ion (SCN^-), hexacyanocobaltate(III) ion ($[Co(CN)_6]^{3-}$), sulfate ion (SO_4^{2-}), borate ion (BO_3^{3-}), hydrogenborate ion (HBO_3^{2-}), and tetraborates ion ($B_4O_7^{2-}$).

3.1.2.2.2.2. *Alcohols and Ketone*

Only alcohols and ketone with partitioning coefficient near zero can be used as chemical tracer including methanol (CH_3OH), ethanol (CH_3COOH), n-propanol ($CH_3(CH_2)_2OH$), isopropanol (($CH_3)_2CHOH$), and acetone (C_3H_6O). Even though these chemicals can be used in elevated temperature applications, they can be affected by chemical adsorption by rock formation, bacterial degradation, and detection hindrance by natural compounds.

3.1.2.2.2.3. *Fluorescent Molecules*

Fluorescent molecules or fluorochromes being used as fluorescent tracer show a unique effect to illuminate itself upon receiving specific wavelength of light. They are considered to be inexpensive, safe, simple to be analyzed and have well-fined kinetics, and can also be detected visually without conducting laboratory analysis [7]. Major fluorochromes used in oilfield applications as fluorescent tracers are fluorescein ($C_{20}H_{12}O_5$), eosin Y ($C_{20}H_6Br_4Na_2O_5$), and rhodamine B ($C_{28}H_{31}ClN_2O_3$). Fluorescein is considered as passive fluorescent tracer with high thermal stability when being used in geothermal applications. However, the use of fluorochromes have drawbacks including fluorochrome adsorption by rock formation, partitioning with oil phase, being bacterially degraded, being affected by a presence of oxygen, and being interfered by a presence of natural fluorochromes. The recommendation is to use fluorescent tracers only in fracture-dominant reservoirs with breakthrough time at most 5 days. Other fluorochromes are substituted polycyclic aromatic sulfonic acids such as naphthalene sulfonic acid ($C_{10}H_8O_3S$), naphthalene disulfonic acid ($C_{10}H_8O_6S_2$), naphthalene trisulfonic acid ($C_{10}H_8O_9S_3$), 4,4'-biphenyl-disulfonic acid ($C_{12}H_{10}O_6S_2$), and fluorene sulfonic acids ($C_{13}H_{10}O_3S$), which are mainly used in geothermal applications with reservoir temperature up to 330 °C (626 °F), and substituted benzoic acid such as

sodium benzoate ($C_7H_5NaO_2$), p-toluic acid ($C_8H_8O_2$), fluorinated benzoic acid ($C_7H_5FO_2$), and tetra benzenic carboxylic acid ($C_{10}H_6O_8$), which are considered to be passive fluorescent tracers that are not adsorbed by rock formation due to high electrostatic repulsive force.

3.2. Fluorescein Sodium Salt

3.2.1. Characteristics of Fluorescein Sodium Salt

Fluorescein sodium salt with IUPAC name of disodium;3-oxospiro[2-benzo furan-1,9'-xanthene]-3',6'-diolate, one of the most referenced fluorescent tracers in several pieces of literature due to its strong fluorescence at low concentration, and the absences of both toxicity and biodegradability, is an organic xanthene-derivative fluorochrome appearing as crimson powder. In the form of fluorescein solution, it absorbs most light from blue spectrum and emits fluorescence in green spectrums. It is considered to be highly pH-dependent on alkaline and loses its fluorescent property if pH of the solution changes to acidic [10, 27]. Molecular structure of fluorescein sodium salt is shown in figure 4, and physico-chemical properties of fluorescein sodium salt are listed in table 2.
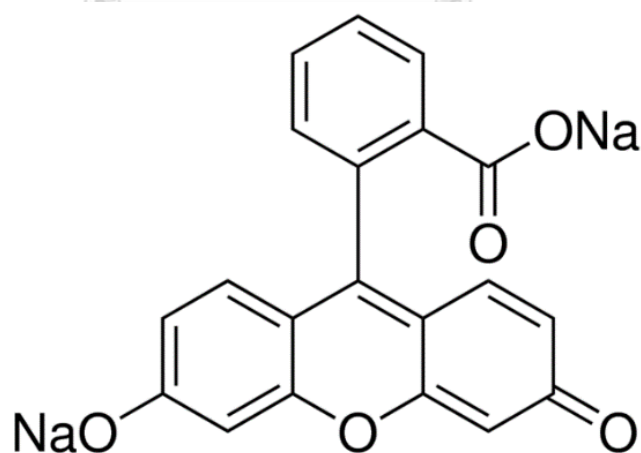
Figure 4. *Molecular structure of fluorescein sodium salt.*

Table 2. *Physico-chemical properties of fluorescein sodium salt.*

Properties	Value
Molecular formula	$C_{20}H_{10}Na_2O_5$
Molecular weight	376.3
Melting point	315 °C (599 °F)
Decomposition temperature	395 °C (743 °F)
Density	1.60 g/cm^3 (99.88 lb/ft^3)
Excitation wavelengths	490 nm
Emission wavelengths	512 nm

3.2.2. Production of Fluorescein Sodium Salt

Fluorescein sodium salt can be synthesized by using two petroleum products which are resorcinol and phthalic anhydride in a ratio of 7:5 at temperature of 195 °C (383 °F) in an anhydrous medium. The processes are done in several steps including boiling, filtering, purifying, dissolving, and precipitating with many solutions, especially sodium hydroxide (NaOH) solution [10, 27]. The final product becomes pure substance in the form of crimson powder. Chemical structures of resorcinol and phthalic anhydride are shown in figure 5, and physico-chemical properties of resorcinol and phthalic anhydride are listed in table 3.

(a)   (b)
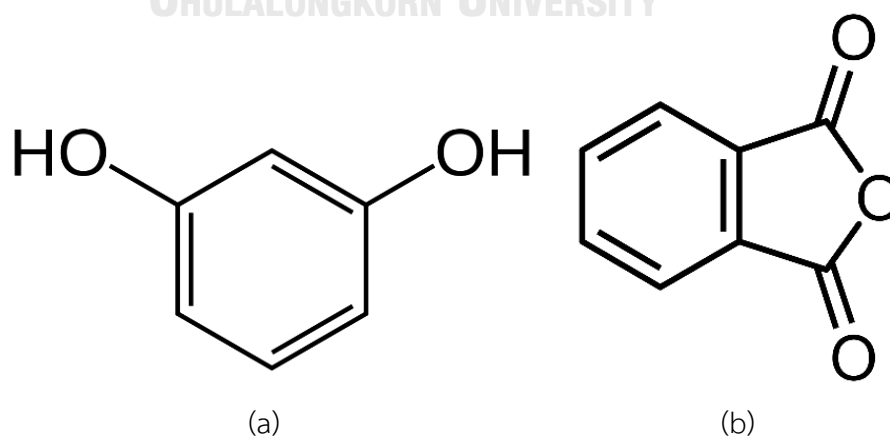
Figure 5. *Chemical structures of (a) resorcinol, and (b) phthalic anhydride.*

Table 3. *Physico-chemical properties of resorcinol and phthalic anhydride.*

Characteristics and Properties	Resorcinol	Phthalic Anhydride
IUPAC name	benzene-1,3-diol	2-benzofuran-1,3-dione
Molecular formula	$C_6H_6O_2$	$C_8H_4O_3$
Molecular weight	110.1	148.1
Appearance	white solid, turns pink on exposure to air, light, and iron	white flakes
Density	1.28 g/cm^3 (79.91 lb/ft^3)	1.53 g/cm^3 (95.51 lb/ft^3)
Melting point	110 °C (230 °F)	131.6 °C (268.9 °F)
Boiling point	277 °C (531 °F)	295 °C (563 °F)

3.2.3. Applications of Fluorescein Sodium Salt

Fluorescein sodium salt can be used in many applications such as medical, agricultural, automotive, industrial, pharmaceutical, food, manufacturing, personal care, pesticide, geology, and petroleum. Since it is widely used in many medical and pharmaceutical applications such as ophthalmic armamentarium [27], labeling agents for antibody and immunoglobulin [28], breast cancer brain-metastasis surgery [29], and vascular neurosurgery [30], it can be obviously verified that it is absolutely harmless to environment and human being. Furthermore, in petroleum-related literatures and pilot tests, fluorescein sodium salt was usually used as fluorescent tracer to determine inter-well hydraulic connectivity, preferential flow channels [31], dispersive characteristics, fracture volume [13], and fluid residence time distribution within the reservoir [32]. It was also used for other purposes in petroleum field; for instance, subsea flowline assessment under wax deposition [10], and sensors for corrosion detection on aluminum alloy surfaces [33].

3.3. Fluorescence and Phosphorescence [34-38]

Fluorescence is one of photoluminescence which is related to a photonic emission process by fluorochromes during a molecular relaxation from electronic excited states to electronic ground state after being excited by electromagnetic radiations. The transition of excited electrons involves with two states: electronic and vibrational states. Electronic states are separated by energies of the order of 10,000 cm^{-1}. Each electronic state is divided into multiple sublevels so-called vibrational states which are separated by energies of the order of 100 cm^{-1}. Electromagnetic radiations in the range of ultraviolet to blue light are required to trigger the transition.

Originally, electrons remain as electron pairs on the lowest vibrational state of the electronic ground state and rotate on their own orbitals around the nucleus. Each electron pair stays in the form of antisymmetric electronic wave function so-called singlet state or single electronic state in which each electron has opposite electron spin. After electron pairs are impacted by electromagnetic radiations, photon absorption occurs on the time scale of femtoseconds (10^{-15}) which excite electrons. After that, one electron from each electron pair leaves its own orbital on the lowest vibrational state of the electronic ground state and goes to the higher orbital on the accessible vibrational state of the accessible electronic excited state. This makes singlet state of electron pair to be excited singlet state in which one electron on the electronic excited state still has the opposite electron spin from its own pair electron that still remains on the electronic ground state. The higher energy impact of electromagnetic radiation on electrons is, the higher accessible vibrational state of the higher accessible electronic excited state of excited electrons will be reached.

Subsequently, unstable excited electrons are quickly relaxed to the lowest vibrational state of the electronic ground state. During relaxation, excited electrons lose their energies through four processes: vibrational relaxation, collisional quenching, internal conversion, and photochemical reaction. Vibrational relaxation is a process that makes excited electrons lose their energies in the form of vibrational energy,

whereas collisional quenching is a process that excited electrons lose their energy by colliding with quenchers which are substances that can absorb fluorescence such as oxygen, chloride ions, iodide ions and acrylamide [39-41]. These two processes make excited electrons to relax from higher vibrational state to lower vibrational state of the same excited electronic state. Internal conversion is a process that makes excited electrons on the lowest vibrational state of the higher excited electronic state to lose their energies and goes to the highest vibrational state of the lower excited electronic state. Photochemical reactions require energy to form photoproducts and these reactions normally are monomolecular reactions with first-order rate constant, but sometimes bimolecular reactions with second-order rate constant can occur. These four processes occur on the time scale of femtoseconds (10^{-15}) to picoseconds (10^{-12}) and continue until excited electrons reach the lowest vibrational state of the lowest electronic excited state.

Next, excited electrons stay on the lowest vibrational state of the lowest electronic excited state for a period of time on the order of nanoseconds (10^{-9}) and the last interval conversion from this state to the allowable vibrational state of the electronic ground state occurs in two ways: non-radiative and radiative processes. Non-radiative process is a process that excited electrons lose their energies in the form of thermal energy, whereas radiative process is a process that excited electrons lose their energies by emitting photon in the form of fluorescence occurring on the time scale of nanoseconds (10^{-9}) to decimicroseconds (10^{-7}) which refers to fluorescence lifetime. This lifetime is the time that detected fluorescence intensity reaches 1/e of its maximum fluorescence intensity. This type of fluorescence is named as direct-line fluorescence in which fluorescence emission wavelength is longer than absorption wavelength of electromagnetic radiation due to the loss of energy though vibrational relaxation, collisional quenching, internal conversion, and photochemical reactions and the difference between these two wavelengths at maximum fluorescence intensity is called stroke shift. Eventually, vibrational relaxation and collisional

quenching occurs until excited electrons reach the lowest vibrational state of the electronic ground state.

Moreover, during the relaxation of excited electrons on excited singlet state, intersystem crossing can occur instead of internal conversion which is caused by spin orbit coupling that reverses electron spin of electron pairs from antisymmetric (opposite electron spin; singlet) to symmetric (same electron spin; triplet) electronic wave function; that is, the relaxation of excited elections from higher energy of excited singlet state to lower energy of excited triplet state occurs. The following processes occur in the same manners as described in the previous paragraph. When excited triplet electrons reach the lowest vibrational state of the lowest electronic excited state, intersystem crossing occurs again which makes excited triplet electrons to lose energies and change back to grounded singlet electrons upon reaching the electronic ground state. The energies are also lost in two ways: non-radiative and radiative processes. Non-radiative process also causes the energy lost in the form of thermal energy, whereas radiative process causes excited triplet electrons to lose energies by emitting photon in the form of another type of photoluminescence so-called phosphorescence occurring on the time scale of milliseconds (10^{-3}) to seconds which refers to phosphorescence lifetime. Since phosphorescence lifetime is much longer than fluorescence lifetime, phosphorescence is still emitted for a period of time even through electromagnetic radiation is already stopped. In contrarily, fluorescence is stopped as electromagnetic radiation is stopped. During relaxation of excited triplet electrons, photochemical reactions also occur in bimolecular reactions with second-order rate constant. Phosphorescence has larger stroke shift than fluorescence because triplet excited state has lower energy than singlet excited state. Unfortunately, phosphorescence can occur only at low temperature and is rarely detected in aqueous systems at average temperature; however, it can still be detected at cryogenic temperatures using phosphorescence spectrophotometry.

The electronic transition can be clearly illustrated by using Jablonski diagram shown in figure 6 where S_0, S_1, S_2, and T_1 represent electronic ground state, lower-energy electronic excited singlet state, higher-energy electronic excited singlet state, and electronic excited triplet state, respectively. Singlet and triplet states of electron spin are also illustrated in figure 7.
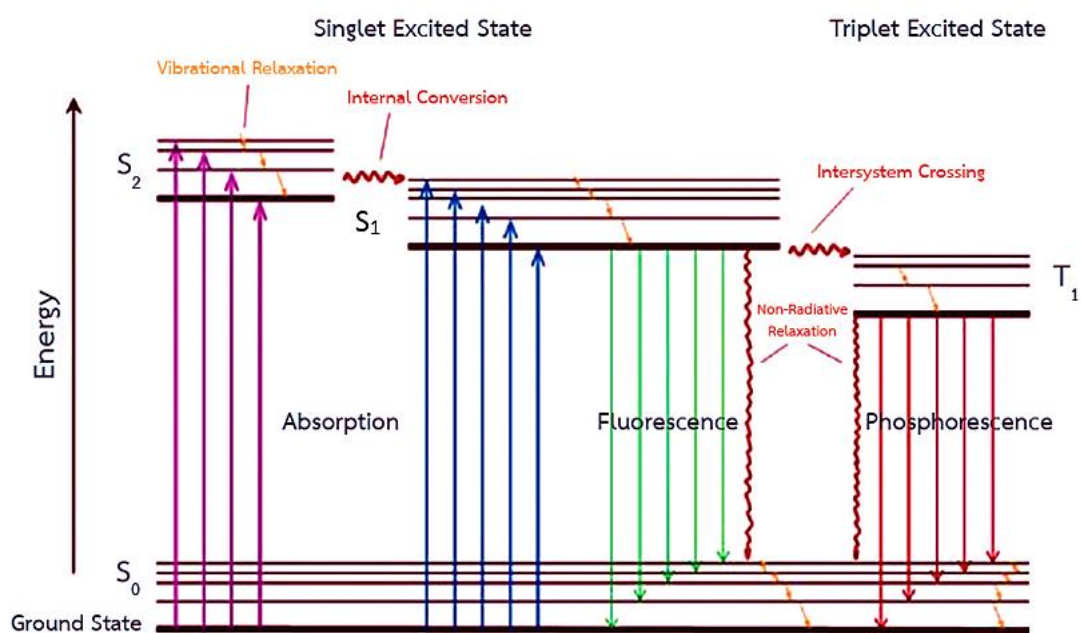
Figure 6. *Jablonski diagram.* [37]
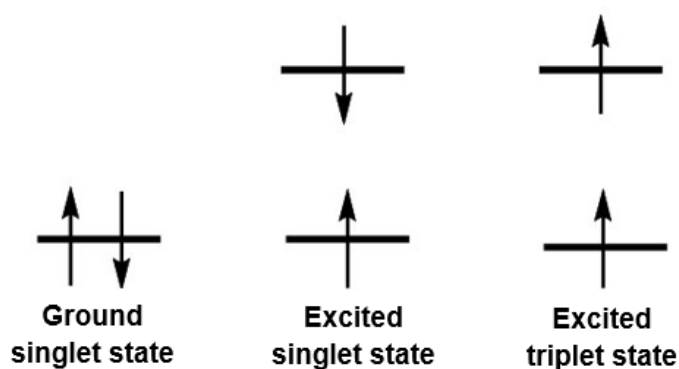
Figure 7. *Schematic representation of electron spin.* [42]

3.4. Effects of Various Factors on Fluorescence Intensity [34, 36]

3.4.1. Fluorochrome Concentration

If fluorochrome concentration is high, self-quenching and self-absorption will greatly reduce fluorescence intensity. Self-quenching is a process that excited electrons collide with other excited electrons themselves without radiating fluorescence, whereas self-absorption is a process that fluorochromes absorb fluorescence emitted by other fluorochromes. On the other way, if the concentration is low in which both self-quenching and self-absorption are already stopped, the intensity will also be low due to low amount of fluorochromes to emit fluorescence. Therefore, it can be concluded that in low fluorochrome concentration, fluorescence intensity is directly proportional to fluorochrome concentration, whereas in high fluorochrome concentration, fluorescence intensity is inversely proportional to fluorochrome concentration.

3.4.2. Temperature

High temperature causes excited electrons to be more excited and lose more energy through vibrational relaxation, collisional quenching and internal conversion, resulting in more attenuation of fluorescence intensity. It was found that the intensity was attenuated about 1-2% per 1.8°F increase in temperature.

3.4.3. Dissolved Oxygen

Dissolved oxygen in fluorochrome solution can cause an oxidation reaction with fluorochromes, resulting in more attenuation of fluorescence intensity. In a low temperature condition, dissolved oxygen also promotes intersystem crossing which causes a transition of excited singlet electrons to excited triplet electron, resulting in more phosphorescence and less fluorescence.

3.4.4. Potential of Hydrogen (pH)

For organic compounds having acidic or basic functional groups, changes in pH strongly affect fluorescence in terms of fluorescence emission wavelength and

fluorescence intensity, especially aromatic compounds having resonance ability which can stabilize excited electrons.

3.4.5. Molecular Structures

Fluorochromes normally are aromatic hydrocarbons that have electrons being easily excited by using less excitation energy. Aromatic hydrocarbons that have no substituent yield more fluorescence emission. An increase in numbers of rings in aromatic hydrocarbons results in higher fluorescence intensity. The compounds that are aliphatic and alicyclic with multiple conjugated double bonds can also emit fluorescence, but having weaker intensity than fluorescence emitted by aromatic hydrocarbons. Heterocyclic compounds with only one ring such as pyridine, furan, thiophene, and pyrrole cannot emit fluorescence because excited singlet electrons rapidly change to excited triplet electrons; however, heterocyclic compounds with fused rings such as quinoline, isoquinoline, and indole can emit fluorescence. If fluorochromes have functional groups being as electron withdrawing group such as halogens, nitrile, carbonyl, and nitro groups, they can emit fluorescence with low fluorescence intensity, whereas if they have functional groups being as electron donating group such as alkyl, alcohol, and amino groups, they can emit fluorescence with high fluorescence intensity.

3.4.6. Solvent Viscosity

Solvents that have high viscosity can reduce an energy loss of excited electrons by lowering a chance of collisional quenching and self-quenching, resulting in higher fluorescence intensity. In addition, there is a chance that fluorescence can be emitted during collisional quenching and self-quenching so-called sensitized fluorescence.

3.4.7. Hydrogen Bonding

Hydrogen bonding between fluorochromes and solvents causes a reduction of fluorescence intensity. Fluorochromes dissolving in strong acidic solution that can make hydrogen bonding results in shorter fluorescence emission wavelength than that

in strong basic solution. In some cases, hydrogen bonding reduces fluorescence by promoting intersystem crossing.

3.4.8. Impurities

Impurities can affect fluorescence intensity by either absorb or emit light that has the same wavelength as electromagnetic radiation or fluorochromes. The effect that impurities absorb light from electromagnetic radiation or fluorochromes which results in lower fluorescence intensity is called inner filter effect.

3.4.9. Light Scattering

Light scattering can disturb fluorescence detection in many ways. Five major light scatterings that can affect fluorescence intensity consist of:

- Rayleigh-Tyndall scattering which is caused by scattering of electromagnetic radiation when it is not absorbed by fluorochromes in form of molecules (Rayleigh scattering) or colloids (Tyndall scattering) and is detected along with fluorescence, resulting in inaccurate outcome [43],

- Raman scattering which is caused by scattering of electromagnetic radiation when its photon energy is converted into vibrational and rotational energy and then has lower energy and longer wavelength than electromagnetic radiation; however, this type of light scattering has no or less effect on fluorescence detection [43],

- secondary order ray which is light that is emitted from electromagnetic radiation having two times longer wavelength than usual wavelength, and can affect fluorescence that has small different gap of wavelength from secondary order ray,

- light scattering due to the presence of large biological molecules such as proteins or protein-related compounds that can also emit fluorescence and disturb the actual fluorescence detection, and

- light scattering due to turbidity which is caused by suspended solids that can reflect the light, resulting in higher fluorescence intensity.

3.4.10. Electromagnetic Radiation [40]

Fluorochromes are very light-sensitive which can be easily photodegraded by light emitted from electromagnetic radiation. This effect can be solved by attenuating the light source with filters or screens.

3.5. Fluorescence Spectrophotometry

3.5.1. Definition of Fluorescence Spectrophotometry

Fluorescence spectrophotometry is a quantitative measurement technique for fluorescence emission. General purpose of this technique is to quantify intensity of fluorescence emitted by fluorochromes when being exposed to ultra-violet light, visible light, or other electromagnetic radiations.

3.5.2. Fluorescence Spectrophotometer

Fluorescence spectrophotometer is the main instrument used in this technique and can be called interchangeably as fluorometer, fluorimeter, or spectrofluorometer depending on their designs and instrument complexity. It is a combination of two devices: spectrometer and photometer. Spectrometer is responsible on generation of electromagnetic radiation and selection of desired wavelength, whereas photometer is responsible on fluorescence detection and fluorescence intensity measurement [44].

3.5.3. Instrumentation of Fluorescence Spectrophotometer

Fluorescence spectrophotometer consists of six main components including light source, excitation filter, cuvette, emission filter, fluorescence detector, and signal processors and data readout.

3.5.3.1. Light Source [34]

Light source is used to generate electromagnetic radiation that triggers the excitation of fluorochromes. There are two common light sources used in this technique: mercury-arc and xenon-arc lamps. Mercury-arc lamp can emit uniform light with high intensity in the range of wavelengths of 254 to 1,014 nm, while xenon-arc lamp is more popular because it can emit high energy continuum of light in the wide

range of wavelengths of 190 to 1,200 nm. However, in past decades, laser becomes more popular due to its specific wavelength generation, small size, and ease of applications in many designs. Examples of laser are argon laser used in flow cytometer and helium-neon laser used in atomic detection techniques. Other light sources include light-emitting diode, deuterium lamp, hydrogen lamp, tungsten filament lamp, tungsten/halogen lamp, etc.

3.5.3.2. Excitation Filter [34, 40]

Excitation or primary filter is used to eliminate undesirable wavelength radiation capable of triggering the excitation of fluorochromes and allows only short wavelength radiation to pass through. It can be classified into two types: normal light filter and monochromator. Monochromator is an optical device that allows only one monochromatic light to pass through and can be either prism or grating. It can be also equipped with slits when a narrow slit provides high resolution and spectral purity, while a large slit provides high intensity.

3.5.3.3. Cuvette [34, 40]

Cuvette is sample cell used to hold fluorochrome solution during the analysis. It is usually made in rectangular shape that is polished on all four vertical sides and on the bottom, which can reduce the effect from light scattering rather than using round tubes with flat polished bottoms. The cuvette made from quartz can be used with range of wavelength of 190 to 2,700 nm, whereas the cuvette made from borosilicate glass can be used with range of wavelength of 320 to 2,500 nm. The cuvette made from plastic can be also used, but it may have contaminated fluorochromes which disturb actual fluorescence detection. An appropriate size of cuvette is about 1 to 3 mL, but can be as small as 0.1 to 0.3 mL depending on the applications.

3.5.3.4. Emission Filter [34, 40]

Emission or secondary filter is used to eliminate undesirable wavelength radiation and light scatterings before reaching the detectors and allows only long wavelength radiation to pass through. It is also classified into two types: normal light filter and monochromator equipped with slits.

3.5.3.5. Fluorescence Detector [34, 45]

Fluorescence detector is used to detect, measure, and amplify fluorescence intensity. There are two common detectors used in this technique: photomultiplier tube and photodiode array detectors. Photomultiplier tube detector is a detector that is sensitive to light in the regions of ultraviolet and visible lights and can be used to detect very trace amount of fluorescence with range of wavelength of 190 to 1,000 nm, while photodiode array detector is portable multichannel detector that can simultaneously detect various wavelength radiation and can be used with range of wavelength of 190 to 1,100 nm.

3.5.3.6. Signal Processors and Data Readout [34, 36, 43]

Signal processors and data readout are used to process and show the results on meter or digital display equipped with computer, printer, or microprocessor in terms of fluorescence intensity or transmittance in a function of fluorescence emission wavelength.

3.5.4. Classification of Fluorescence Spectrophotometer [34, 45]

Fluorescence spectrophotometer can be classified into two types depending on radiation pathways:

3.5.4.1. Single-Beam Fluorescence Spectrophotometer

Single-beam fluorescence spectrophotometer, as shown in figure 8, consists of a detector that must be placed perpendicularly to the light source which allows electromagnetic radiation to pass through fluorochrome solution without disturbing emitted fluorescence. It is easy to handle and inexpensive; however, only one

wavelength can be measured per time and blank solution must be changed every time as wavelength is changed.
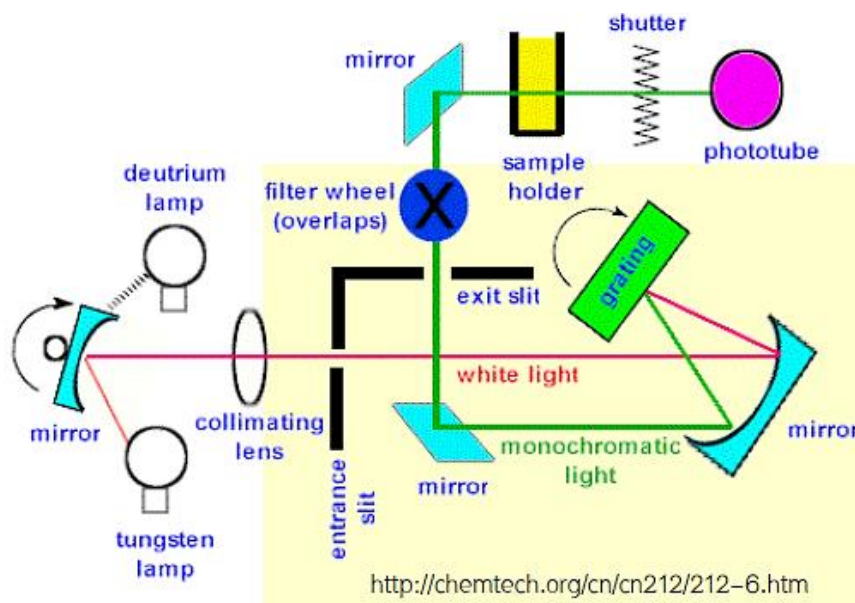
Figure 8. *Schematic diagram of single-beam fluorescence spectrophotometer.* [45]

3.5.4.2. Double-Beam Fluorescence Spectrophotometer

Double-beam fluorescence spectrophotometer can be classified into two subtypes which are double beam with one detector and two detectors. The device with one detector, as shown in figure 9, measures fluorescence emitted from both sample and reference cuvettes, whereas another device with two detectors, as shown in figure 10, measures fluorescence from both cuvettes independently. This type of fluorescence spectrophotometer can be used to measure different wavelengths simultaneously but it is considered to be expensive.
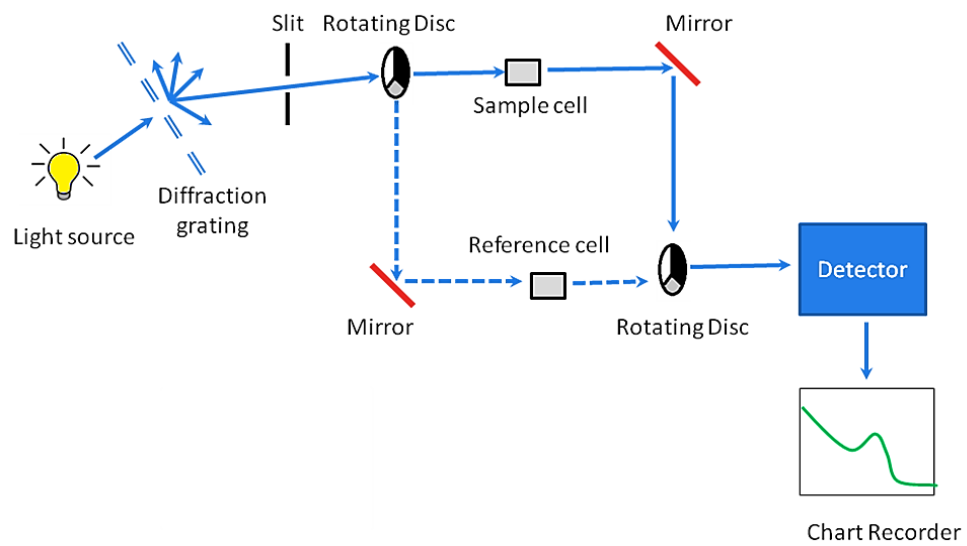
Figure 9. *Schematic diagram of double-beam fluorescence spectrophotometer with one detector.* [45]
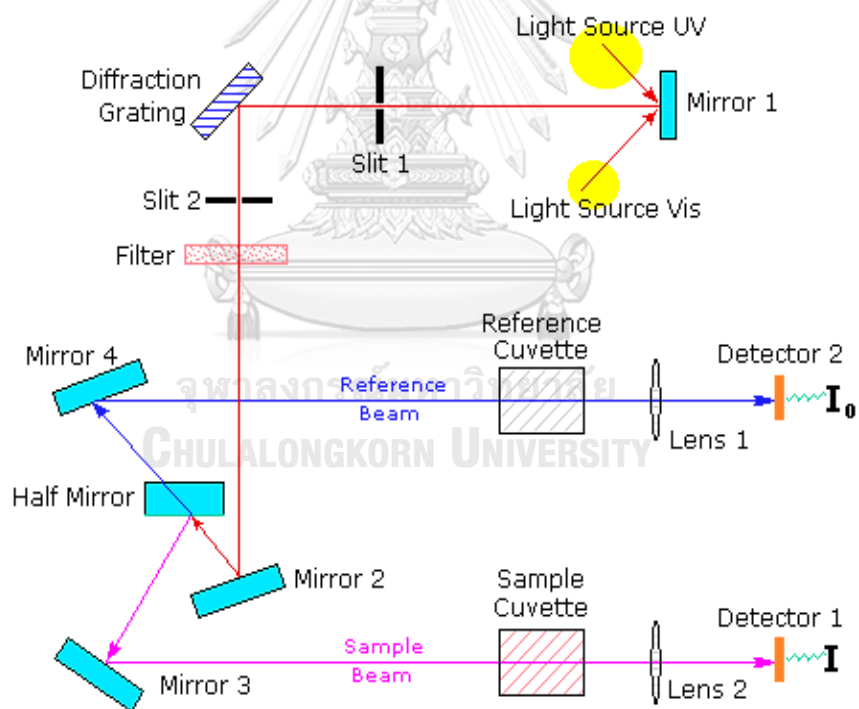
Figure 10. *Schematic diagram of double-beam fluorescence spectrophotometer with two detectors.* [45]

3.6. Phosphorescence Spectrophotometry [36]

Phosphorescence spectrophotometry is a quantitative measurement technique for phosphorescence emission. Phosphorescence spectrophotometer, which is a device used to measure phosphorescence, has almost the same components and design as fluorescence spectrophotometer except for two parts. The first part is phosphorescence solution preparation in which the solution must be prepared in temperature of liquid nitrogen (-321 °F) as shown in figure 11. Phosphorochrome compounds and solvent are mixed and frozen in a liquid nitrogen tube until the solution becomes like a glass. Appropriate solution is a combination of ether, propane, and ethanol which are mixed in the ratio of 5:5:2. The second part is an electrical gate used to block electromagnetic radiation and then leaves for a period of time, so-called delay time, before measuring phosphorescence. This electrical gate is an auxiliary component that can be installed with fluorescence spectrophotometer so that it can be used to measure both fluorescence and phosphorescence. Another method rather than electrical gate is the use of pulsed excitation light source which emits electromagnetic radiation periodically.
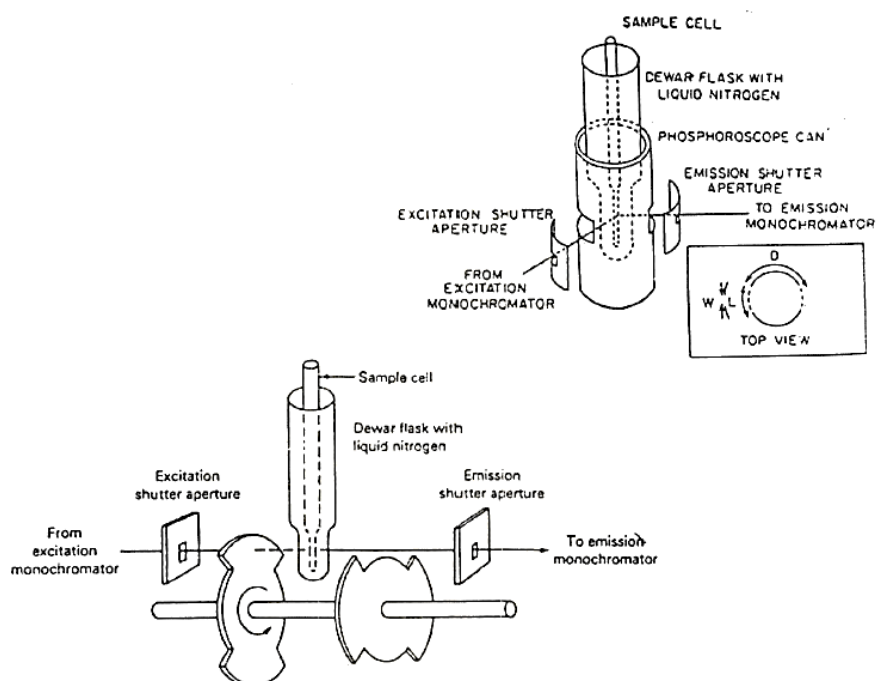
Figure 11. *Schematic diagram of phosphorescence measurement.* [36]

3.7. Shaly-Sandstone

3.7.1. Definition and Formation of Shaly-Sandstone

Shaly-sandstone, a sandstone with greater than 10% clay content, is a detrital sedimentary rock formed by a transgressive-regressive cycle which is a mechanism of sea level change due to alternate melting and freezing of polar continental ice. During transgressive fining-upward part of the cycle, clay-sized particles were moved towards land and deposited in the basin, whereas during regressive coursing-upward part of the cycle, sand-sized particles were moved towards sea and deposited on top of clay layer. Over million rounds of the cycle, clay-sand layers were compacted and finally formed rocks having alternate layers between clay and sand [46].

3.7.2. Characteristics of Shaly-Sandstone

In petroleum industry, clay in shaly-sandstone is the major problem that causes wrong interpretations of water saturation and porosity using well loggings [47] and productivity loss from clay swelling and fine migration [48]. Additionally, from previous study, it was found that clays had large negatively charged surface that tended to adsorb positively charged ions suspended in reservoir fluid [49]. Clays also had high cation exchange capacity (CMC) and could release considerable amounts of divalent ions which affected some chemicals being susceptible to divalent ions such as surfactants in surfactant-based enhanced oil recovery [50]. These behaviors can greatly reduce abilities of chemicals containing both positively and negatively charged ions being used through shaly-sandstone reservoir.

3.7.3. Shaly-Sandstone in Thailand

Shaly-sandstone can be typically found in the northern part of Thailand. Clays in shaly-sandstone predominantly composes of illite, kaolinite, montmorillonite, and chlorite. Characteristics of these four clays are listed in table 4.

Table 4. *Characteristics of illite, kaolinite, montmorillonite, and chlorite.*

Characteristics	Illite	Kaolinite	Montmorillonite	Chlorite
Type of clay	migrating clay	migrating clay	swelling clay	migrating clay
Formula	(K,H_3O) $(Al,Mg,Fe)_2$ $(Si,Al)_4O_{10}$ $[(OH)_2,(H_2O)]$	$Al_2(OH)_4$ Si_2O_5	$(Na,Ca)_{0.33}$ $(Al,Mg)_2$ (Si_4O_{10}) $(OH)_2 \cdot nH_2O$	$(Mg,Fe)_3$ $(Si,Al)_4O_{10}$ $(OH)_2 \cdot$ $(Mg,Fe)_3$ $(OH)_6$
Mohs scale	1-2	2-2.5	1-2	2-2.5
Specific gravity	2.6-2.9	2.16-2.68	1.7-2.0	2.6-3.3

3.8. Clay Minerals [51]

3.8.1. Clay Origin

Clay is a member of phyllosilicates that composes of sheet-like structures of silica tetrahedra (SiO_4^{4-}) with other elements presented in the earth's crust as fundamental structural units. It was primarily formed by congruent and incongruent weathering reactions of less-resistant primary minerals such as pyroxenes and amphiboles, which were originated from igneous or metamorphic rocks. Congruent weathering reaction results in secondary minerals with the same chemical composition as primary minerals, whereas incongruent weathering reactions results in secondary minerals with different chemical composition to primary minerals. After that, clays deposited during sedimentation and encapsulated in rock matrix formed detrital clay, whereas clays precipitating from subsurface fluids and adsorbing on rock matrix formed authigenic clay [52].

3.8.2. Clay Structure

Clay is a group of hydrous aluminosilicates which is a combination of silica tetrahedra with cations in a presence of water as constituent. A silica tetrahedron consists of one silicon ion (Si^{4+}) at the center bonded with four oxygen anions (O^{2-}) at each apex of tetrahedron as shown in figure 12. Silica tetrahedral, sharing their oxygen ions in the same plane, forms interconnected hexagonal linkage so-called silica tetrahedral sheet with repeating unit of $Si_2O_5^{2-}$ and remains negatively charged. Some cations such as magnesium ions (Mg^{2+}), ferrous ions (Fe^{2+} and Fe^{3+}), and aluminum ions (Al^{3+}) can act as coordinating cations that bond with oxygen ions or hydroxyl groups (R-OH) of silica tetrahedral sheet and form octahedron structure as illustrated in figure 13, and a group of octahedra in interconnected horizontal linkage by sharing oxygen ions is called octahedral sheet. If coordinating cations are divalent cations (Mg^{2+} or Fe^{2+}), all octahedra are occupied by divalent cations to maintain charge neutral which is so-called trioctahedral sheet. If coordinating cations are trivalent cations (Al^{3+} or Fe^{3+}), one of every three octahedra are left empty which is so-called dioctahedral sheet. The combination of silica tetrahedral sheets and trioctahedral or dioctahedral sheets bonded by sharing oxygen ions form aluminosilicate layers which have many arrangements, resulting in different types of clay.
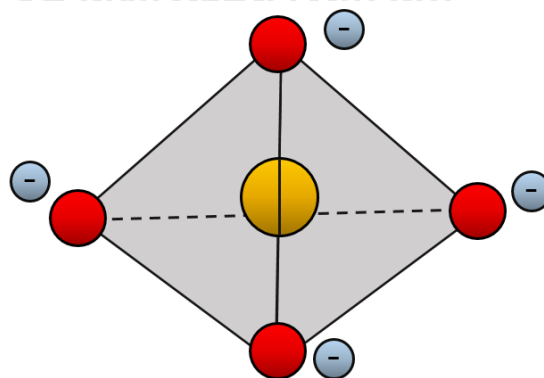
Figure 12. *Silica tetrahedral structure; red circles represent oxygen ions, whereas yellow circle represents silicon.*
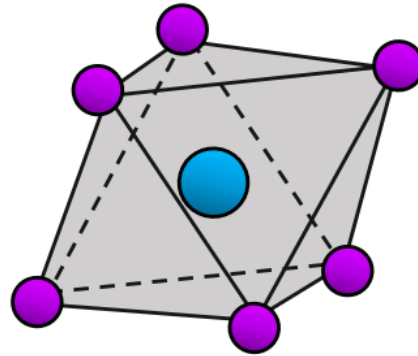
Figure 13. *Octahedral structure; purple circles represent oxygen ions or hydroxyl groups, whereas blue circle represent coordinating cation.*

3.8.3. Isomorphous Substitution

Isomorphous substitution is process promoted by weathering that replaces cations with other exchangeable cations with similar crystal ionic radii, which are listed in table 5. Si^{4+} ions at the center of silica tetrahedron can be replaced by Al^{3+} ions , and Al^{3+} or Mg^{2+} ions in octahedron can be replayed by Fe^{2+} or Fe^{3+} ions without interfering the crystal structures. The replacement of cations with higher valence by cations with lower valence results in negatively charged, whereas the replacement of cations with lower valence by cations with higher valence results in positively charged. Typically, negatively charged replacement exceeds positively charged replacement, resulting in net negatively charged surface of clay. Since clays have cation exchange capacity (CMC), which is capacity of clay to adsorb, retain, and release cations, negatively charged surface is then stabilized by adsorption of cations presented in the liquid at the interlayer space.

Table 5. *Crystal ionic radii of cations related to clay structure.*

Ion	Ionic Diameter (Å)
Si^{4+}	1.08
Li^+	1.20
Mg^{2+}	1.30
Al^{3+}	1.35
Fe^{3+}	1.38
Fe^{2+}	1.50
Na^+	1.90
Ca^{2+}	1.98
NH_4^+	2.42
K^+	2.66

จุฬาลงกรณ์มหาวิทยาลัย

CHULALONGKORN UNIVERSITY

CHAPTER 4: METHODOLOGY

The experiments of this study to investigate and evaluate fluorescein sodium salt in the form of fluorescein solution as fluorescent tracer with shaly-sandstone were divided into five sections. All steps of each section were clearly explained below.

4.1. Fluorescein Characteristics

4.1.1. Determination of Detection Limit of Fluorescein Solution

Fluorescence spectrophotometer is the main equipment used to characterize fluorescence emission. It can be used to generate fluorescence spectra which is a plot of fluorescence intensity as a function of fluorescence emission wavelength. There are two adjustable parameters that can affect the shape of the spectra including photomultipliers (PMT) voltage and slit sizes for both excitation and emission filters. PMT voltage ranges from 400 to 800 V, whereas slit sizes are 5 and 10 nm. The higher values of PMT voltage and slit size were used for characterizing the solution containing lower fluorescence intensity and the results with different PMT voltage or slit size could not be compared. In all experiments of this study, Cary Eclipse fluorescence spectrophotometer available at Supramolecular Chemistry Research Unit, Department of Chemistry, Faculty of Science, Chulalongkorn University was utilized.

First, fluorescein sodium salt was prepared as 1,000-ppm fluorescein solution by using deionized water as a solvent. After that, the solution was diluted down to 500 ppm, 200 ppm, 100 ppm, 50 ppm, 10 ppm, 1 ppm, 500 ppb, 200 ppb, 100 ppb, 50 ppb, 10 ppb, 1 ppb, 500 ppt, 100 ppt, and 10 ppt sequentially. Suitable PMT voltages and slit sizes were selected to match with detectable limit of each sample. Glass dropper was used to drop the sample into a standard rectangular fluorimeter quartz cuvette with dimensions of 12.5 mm length x 12.5 mm width x 45 mm height, path length and internal width of 10 mm, and nominal volume of 3.5 mL. The cuvette has four windows and base-polished, and a polyethylene-vaned lid is used to provide

a liquid-tight seal. The cuvette containing the solution was then placed inside fluorescence spectrophotometer for the characterization.

Also, pure deionized water, pure formation water, and pure tap water were characterized and the results were compared to those of fluorescein solution at very low concentrations. Formation water used in this study was artificially prepared based on the formulation of formation water taken from Sirikit (S1) Oilfield operated by PTT Exploration and Production Public Company Limited, and chemical composition of the formation water based on 1 liter of deionized water consisting of total dissolved solid content of 14,098 ppm was listed in table 6. Finally, detection limit of fluorescein solution using deionized water as solvent was determined. Figure 14 illustrated the flowchart for determination of detection limit of fluorescein solution.

It is noted that all laboratory equipment used with fluorescein must be cleaned properly using water followed by acetone before, during, and after the tests; otherwise for characterization of the solution with very low concentrations, trace amount of the solution at high concentration could totally alter the results.

Table 6. *Chemical Composition of formation water based on 1 liter of deionized water.*

Chemical	Weight (g)	Percent by composition (%)
Sodium Chloride (NaCl)	12.403	87.98
Sodium Bicarbonate (NaHCO$_3$)	0.719	5.10
Calcium Chloride (CaCl$_2$)	0.706	5.01
Potassium Chloride (KCl)	0.160	1.13
Magnesium Chloride (MgCl$_2$)	0.110	0.78
Total	14.098	100.00

```
┌─────────────────────────────────────────────────────────┐
│              1,000-ppm fluorescein solution              │
└─────────────────────────────────────────────────────────┘
                            │ Dilution
                            ▼
┌─────────────────────────────────────────────────────────┐
│  Fluorescein concentrations of 500, 200, 100, 50, 10, and 1  │
│  ppm, 500, 200, 100, 50, 10, and 1 ppb, 500, 100 and 10 ppt  │
└─────────────────────────────────────────────────────────┘
                            │
                            │        ┌──────────────────────────┐
                            │        │      Result comparison       │
                            │        │  using pure deionized water, │
                            ◄────────│  pure formation water, and   │
                            │        │       pure tap water         │
                            │        └──────────────────────────┘
                            ▼
┌─────────────────────────────────────────────────────────┐
│  Sample characterization using fluorescence             │
│  spectrophotometer                                       │
└─────────────────────────────────────────────────────────┘
                            │
                            ▼
┌─────────────────────────────────────────────────────────┐
│  Determination of detection limit of fluorescein solution │
└─────────────────────────────────────────────────────────┘
```
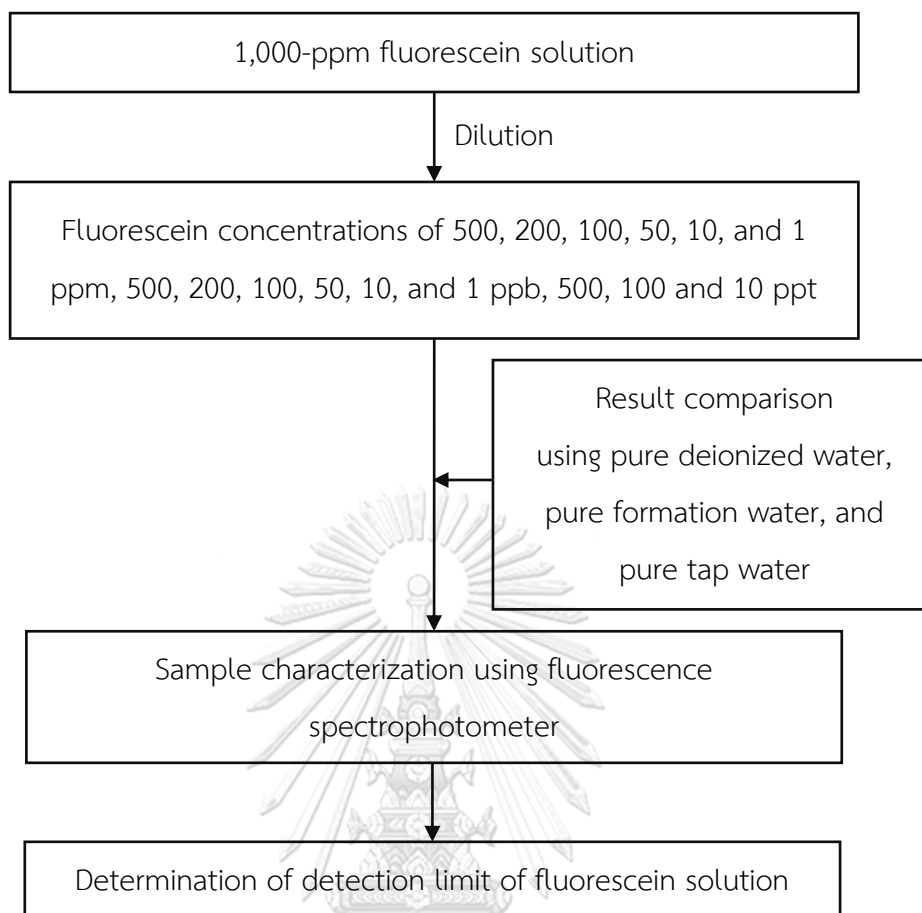
Figure 14. *Flowchart for determination of detection limit of fluorescein solution.*

4.1.2. Investigation of Photosensitivity of Fluorescein Solution

From the literatures, there are two main concerns regarding storage conditions for fluorescein solution which are light and pH value. In this section, photosensitivity or an effect of light exposure on fluorescein solution was investigated. Fluorescein solution at concentration of 100 ppm was selected to represent all quantitative and qualitative comparisons in the first part of this study. There are two reasons for choosing this concentration. First, this concentration was an average value of fluorescein concentration widely used in the literatures. Second, this concentration contains neither excessive nor diminutive amount of fluorescein which can illustrate better quantitative and qualitative comparison results.

First, 100-ppm fluorescein solution was prepared by using deionized water as solvent. Next, 30 mL of the solution was placed into transparent and amber-colored

glass bottles. Three sets of this experiment were designed including (1) all-time exposure to light using transparent glass bottles, (2) all-time concealment inside closed storage using amber-colored glass bottles, and (3) normal exposure to light using amber-colored glass bottles. Three samples were placed in each experimental set as shown in figure 15. Each sample in each set was collected every 1, 2, and 7 days. Then all samples were characterized by using fluorescence spectrophotometer and an appropriate storage for fluorescein solution was determined. Figure 16 summarized the flowchart for investigation of photosensitivity of fluorescein solution.

(a)

(b)

(c)

Figure 15. *Experimental sets for investigation of photosensitivity of fluorescein solution including (a) all-time exposure to light, (b) all-time concealment, and (c) normal exposure to light.*
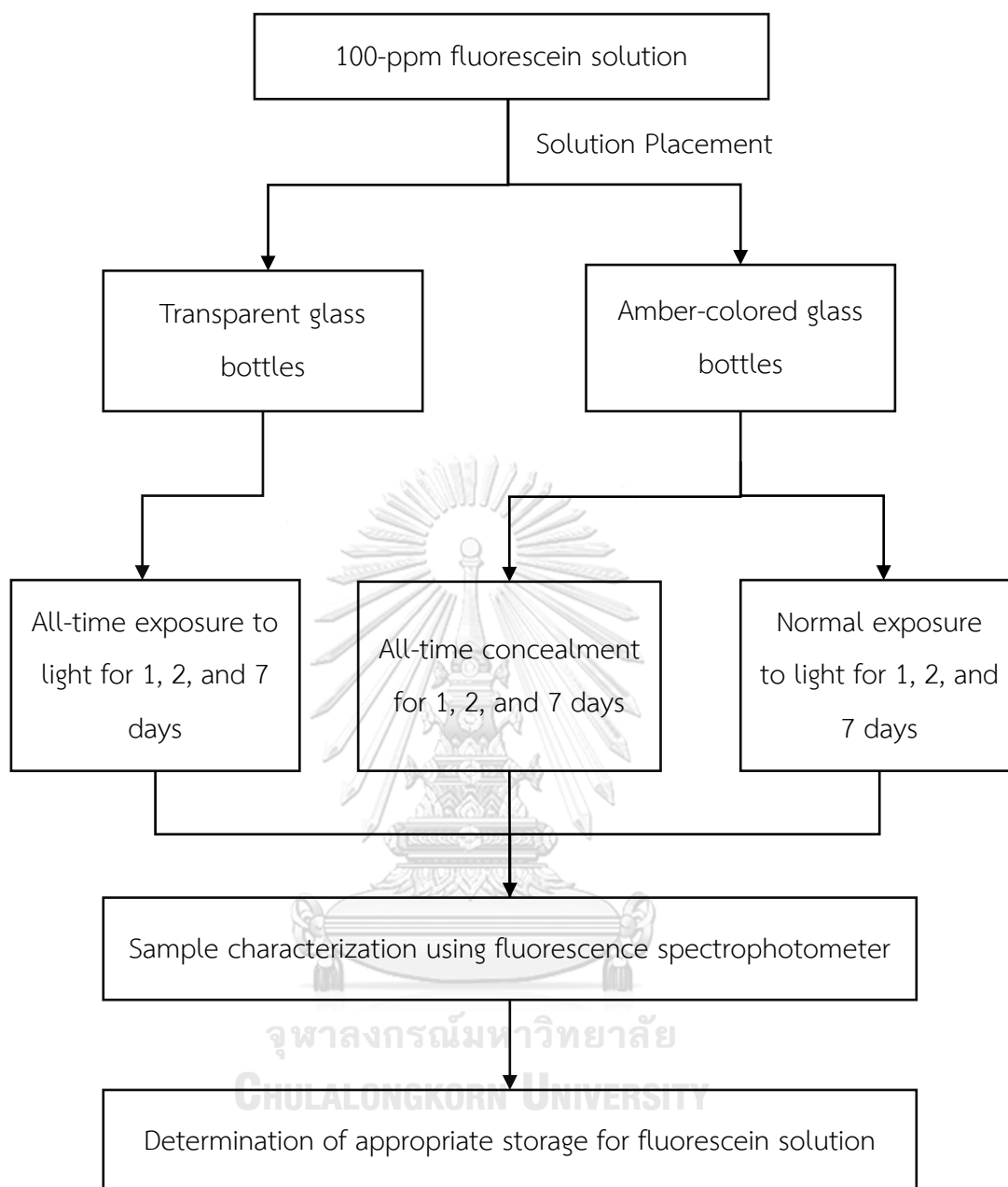
Figure 16. *Flowchart for investigation of photosensitivity of fluorescein solution.*

4.1.3. Investigation of pH-Sensitivity of Fluorescein Solution

Next, pH-sensitivity of fluorescein solution was investigated by preparing 100-ppm fluorescein solution using deionized water as solvent. After that, the solution was equally divided into three beakers. Next, 5 mL of acetic acid (CH_3COOH) and 0.5 grams of sodium carbonate (Na_2CO_3) were added into first two beakers to make the solution acidic and basic, respectively. The last beaker was left without adding anything to

represent neutral pH. The pH universal indicator papers were used to measure pH of each solution. The solution in each breaker was poured into 10-mL borosilicate glass measuring cylinders for better comparative observation. Finally, the samples were characterized by using fluorescence spectrophotometer and an appropriate pH value of storage for fluorescein solution was determined. Figure 17 depicted the flowchart of investigation of pH-sensitivity of fluorescein solution.
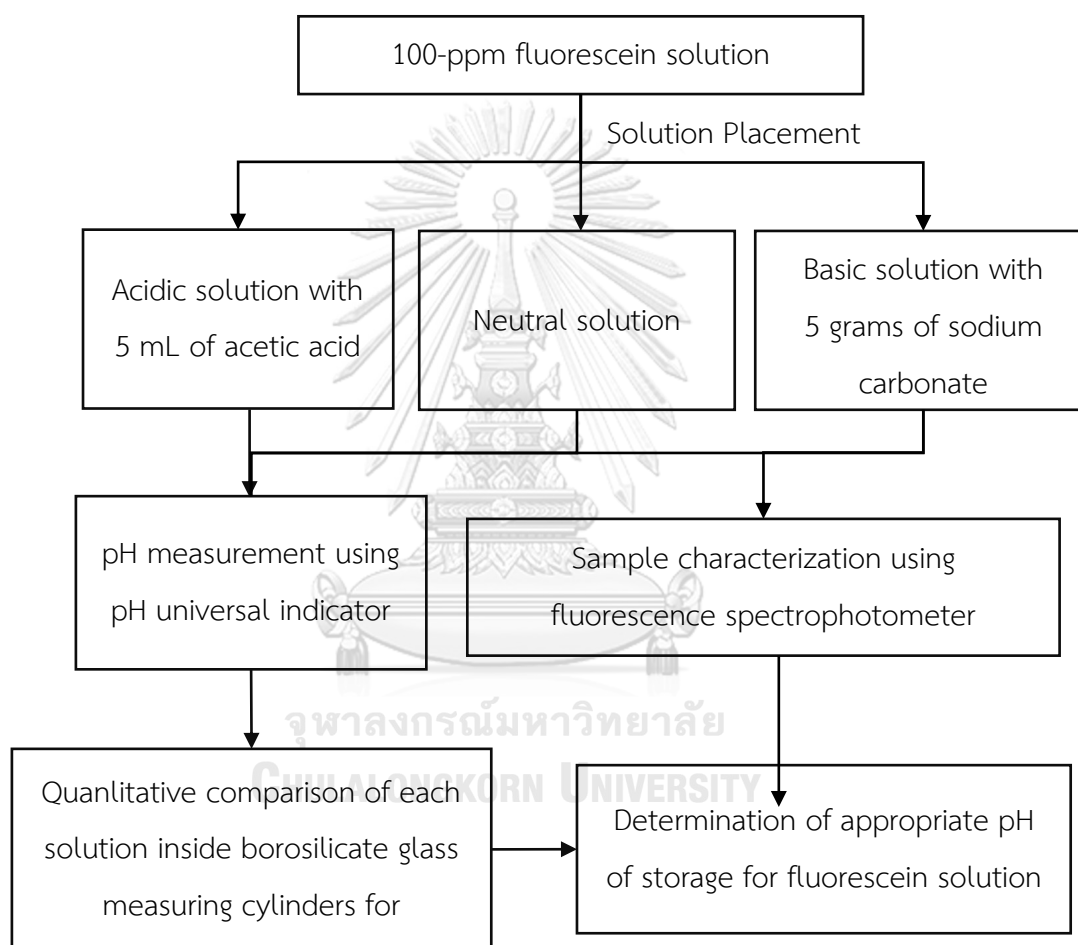
Figure 17. *Flowchart for investigation of pH-sensitivity of fluorescein solution.*

4.1.4. Determination of Thermal Stability of Fluorescein Solution

Next, themal stability of fluorescein solution at petroleum reservoir temperatures was determined. First, 100-ppm fluorescein solution was prepared using deionized water as solvent and then placed inside amber-colored glass bottles. Four bottles were soaked in a plastic jar filled with water at temperature of 30 °C (86 °F)

and each four bottles in BWS-20 water bath (illustrated in figure 18) filled with water at temperatures of 50 °C (122 °F) and 70 °C (158 °F). Each sample at each temperature was collected within time period of 1, 2, 5, and 12 days. Finally, all samples were characterized by using fluorescence spectrophotometer and thermal stability of fluorescein solution was determined. The flowchart of determination of thermal stability of fluorescein solution was shown in figure 19.

Figure 18. *BWS-20 water bath used in determination of thermal stability of fluorescein solution.*
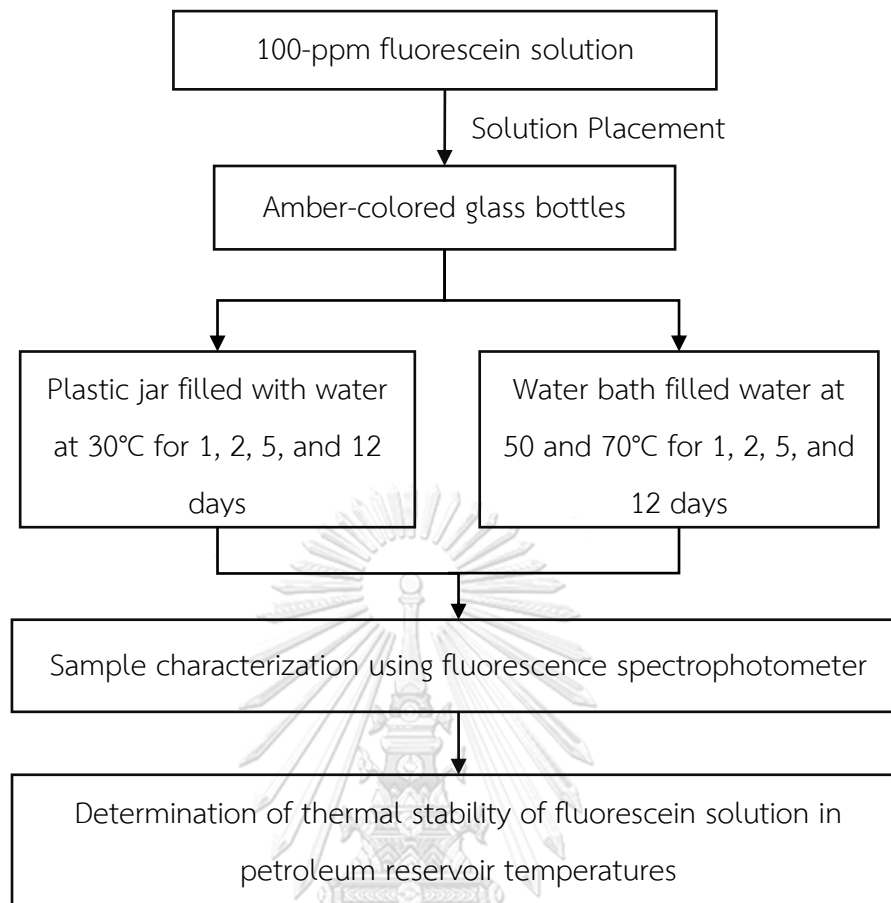
Figure 19. *Flowchart for determination of thermal stability of fluorescein solution.*

4.2. Rock Samples

4.2.1. Background of Shaly-Sandstone Core Samples

Shaly-sandstone core samples provided by PTT Exploration and Production Public Company Limited were used in this study. The core samples were taken from well LKU-CB12 at average depth of 1,967.84 m (6,456.17 ft) which is located at Lan Krabue District, Kamphaeng Phet, Thailand. Shaly-sandstone cuttings from nearby depth were also collected and ground into powder and were used in static investigation of fluorescein solution with shaly-sandstone. Clay content in the core sample, provided by PTTEP, consists of 46% illite, 26% mixed layer between illite and montmorillonite, 16% kaolinite, and 12% chlorite.

4.2.2. Determination of Physical Properties of Shaly-Sandstone Core Samples

Shaly-sandstone core sample was cleaned by using toluene followed by methanol inside Soxhlet apparatus for approximately 24 hours. After the methanol refluxed, the sample was dried in an oven and stored in a desiccator. Dried weight of the sample was detected by electronic balance prior to the saturation process. After that, the sample was saturated by using coreflooding system until the sample was fully saturated. Formation water was also utilized in this step. Pore volume, bulk volume and effective porosity of shaly-sandstone core sample were calculated by using equation (5), equation (6), and equation (7), respectively:

$$V_p = \frac{M_{sat} - M_{dry}}{\rho_L} \tag{5}$$

$$V_b = \frac{\pi D^2 L}{4} \tag{6}$$

$$\phi = \frac{V_p}{V_b} \tag{7}$$

where V_p is pore volume (cm^3), M_{sat} is saturated weight (g), M_{dry} is dried weight (g), ρ_L is liquid density (g/cm^3), ϕ is porosity (fraction), V_b is bulk volume (cm^3), D is diameter (cm), and L is length (cm).

Absolute permeability of shaly-sandstone core sample was determined by measuring liquid flow rates flowing through the core sample with pressure difference between two ends of the core sample and was calculated by using Darcy's equation as shown in equation (8):

$$k = \frac{q\mu_L L}{A\Delta p} \tag{8}$$

where k is absolute permeability (Darcy), q is liquid flow rate (cm^3/s), μ_L is liquid viscosity (cP), A is cross-sectional area (cm^2), and ΔP is pressure difference (atm).

Shaly-sandstone powder was prepared in two different ways: untreated and treated. Untreated powder was directly obtained from grinding of the cuttings which

was still contaminant with hydrocarbon and drilling fluids, whereas treated powder was untreated power that was cleaned by toluene followed by methanol inside Soxhlet apparatus.

4.2.3. Characterization of Elemental Composition of Shaly-Sandstone Samples

Elemental composition of shaly-sandstone sample was characterized by using X-ray fluorescence (XRF) analyzer (shown in figure 20) available at Chevron Petroleum Engineering Laboratory, Department of Mining and Petroleum Engineering, Faculty of Engineering, Chulalongkorn University. Mortar and pestle were used to grind shaly-sandstone powder into very fine powder and was transferred into a small plastic cup before put inside the XRF analyzer. Analyzed time was 15 min and minimum helium flow rate of 1.58 L/min was used to maintain vacuum inside the analyzer.

Figure 20. *X-ray fluorescence (XRF) analyzer used in characterization of elemental composition of shaly-sandstone samples.*

4.3. Static Investigation of Fluorescein Solution with Shaly-Sandstone

Static investigations of fluorescein solution with untreated and treated shaly-sandstone powders were performed in order to observe full interactions between shaly-sandstone and fluorescein. Determination of fluorescein adsorption on shaly-sandstone surface was expected to obtain in this step in order to identify appropriate fluorescein concentrations for dynamic investigation of fluorescein solution with shaly-sandstone. First, 1,000-ppm fluorescein solution was prepared by using deionized water as solvent. Then, the solution was diluted down to 100 ppm, 1 ppm, 100 ppb,

and 1 ppb sequentially. The solutions of 30 mL at different concentrations were placed into amber-colored glass bottles. Pure deionized water of 30 mL was also used to assess baseline of the results. Next, untreated and treated powders were weighed 2 grams and added into each bottle separately. Mixtures of shaly-sandstone powders and the solutions were mixed together by using magnetic stirring bars incooperted with magnetic stirrer at room temperature for 6 hours which was observed to be an optimal time of shaly-sandstone to reach an equilibrium with added chemical substances [53]. After stirring process, the powder was filtered out from the solution using 125-mm filter papers. Finally, filtrates were characterized by using fluorescence spectrophotometer. Summary of the experiment in this section was depiced in figure 21.

1,000-ppm fluorescein solution

Dilution

Fluorescein concentrations of 100, and 1 ppm, 100, and 1 ppb

Stirring of 2 grams of each shaly-sandstone powders with fluorescein solution at different concentration and with pure deionized water

Flitering of shaly-sanstone powders from mixtures using 125-mm filter papers

Filtrate characterization using fluorescence spectrophotometer

Determination of fluorescein adsorption on shaly-sandstone surface, and appropriate fluorescein concentrations for dynamic investigation

Figure 21. *Flowchart for static investigation of fluorescein solution with shaly-sandstone.*

4.4. Dynamic Investigation of Fluorescein Solution with Shaly-Sandstone

Dynamic investigation of fluorescein solution with shaly-sandstone core sample was performed in order to observe actual interactions between shaly-sandstone and fluorescein, and appropriate fluorescein concentration for a tracer test in shaly-sandstone reservoir. CFS-700 coreflooding system (shown in figure 22) available at Chevron Petroleum Engineering Laboratory, Department of Mining and Petroleum Engineering, Faculty of Engineering, Chulalongkorn University was used to perform a flow test of fluorescein solution through shaly-sandstone core sample. Appropriate fluorescein concentrations obtained from section 4.3 were prepared and filled into accumulator C. The core sample, after being saturated with formation water, was then set into the coreholder inside the system. Formation water, filled inside accumulator A, was used to fill in the flowline and the core sample prior to the test. Confining pressure of 1,500 psi was used to confine an area around the core sample to prevent bypass of the flow. The solution at different concentrations was injected with an injection rate of 0.5 cm^3/min at 26°C through the core sample. Effluent of 5 mL was collected every 10 minutes starting from the beginning until reaching 110 minutes (total of 11 samples). Contaminant in effluent was filtered out from the solution using 125-mm filter papers. Finally, the filtrates were characterized by using fluorescence spectrophotometer. Figure 23 showed the flowchat for dynamic investigation of fluorescein solution with shaly-sandstone.

Figure 22. *CFS-700 coreflooding system used in dynamic investigation of fluorescein solution with shaly-sandstone.*

```
┌─────────────────────────────────────────────────────────────────────┐
│                                                                       │
│  Preparation of fluorescein solution at appropriate concentrations    │
│  obtained from previous section                                       │
│                                                                       │
└─────────────────────────────────────────────────────────────────────┘
                                    │
                                    ▼
┌─────────────────────────────────────────────────────────────────────┐
│  Preparation of coreflooding system by setting shaly-sandstone core   │
│  sample at the core holder, filling the flowline with formation       │
│  water, and setting confining pressure at 1,500 psi to prevent bypass │
└─────────────────────────────────────────────────────────────────────┘
                                    │
                                    ▼
┌─────────────────────────────────────────────────────────────────────┐
│  Injection of each fluorescein solution through shaly-sandstone core  │
│  sample with an injection rate of 0.5 cm³/min at 26°C                 │
└─────────────────────────────────────────────────────────────────────┘
                                    │
                                    ▼
┌─────────────────────────────────────────────────────────────────────┐
│  Collection of 5 mL of effluent from 0 to 110 min (total of 11        │
│  samples)                                                             │
└─────────────────────────────────────────────────────────────────────┘
                                    │
                                    ▼
┌─────────────────────────────────────────────────────────────────────┐
│  Filtering of contaminant from effluent using 125-mm filter paper     │
└─────────────────────────────────────────────────────────────────────┘
                                    │
                                    ▼
┌─────────────────────────────────────────────────────────────────────┐
│  Filtrate characterization using fluorescence spectrophotometer       │
└─────────────────────────────────────────────────────────────────────┘
                                    │
                                    ▼
┌─────────────────────────────────────────────────────────────────────┐
│  Determination of appropriate fluorescein concentrations for a        │
│  tracer test in shaly-sandstone reservoir                            │
└─────────────────────────────────────────────────────────────────────┘
```

Figure 23. *Flowchart for dynamic investigation of fluorescein solution with shaly-sandstone.*

4.5. Evaluation of Salt Effect on Fluorescein Solution

Salt effect on fluorescein solution was evaluated to observe a change of fluorescence intensity of fluorescein solution in a presence of salts. First, prepare 1-ppm fluorescein solution using deionized water as solvent. Then, prepare formation water based on formulation of formation water according to table 6 and individual salt solution with the same quantity in formation water were prepared using 1-ppm fluorescein solution as solvent. Next, 1-ppm fluorescein solution without salt was diluted down to 1 ppb, 500 ppt, 100 ppt, and 10 ppt, sequentially. Formation water prepared by using deionized water as solvent was added equally into each fluorescein solution during the solution dilution. Finally, all solutions with salts were characterized by using fluorescence spectrophotometer and the results were compared to the solutions at the same concentrations without salt. Figure 24 summarized the flowchart for evaluation of salt effect on fluorescein solution.

Figure 24. *Flowchart for evaluation of salt effect on fluorescein solution.*

CHAPTER 5: RESULTS AND DISCUSSION

This section revealed the results obtained according to the methodology in chapter 4 and in each subsection, discussion was added prior to the conclusions.
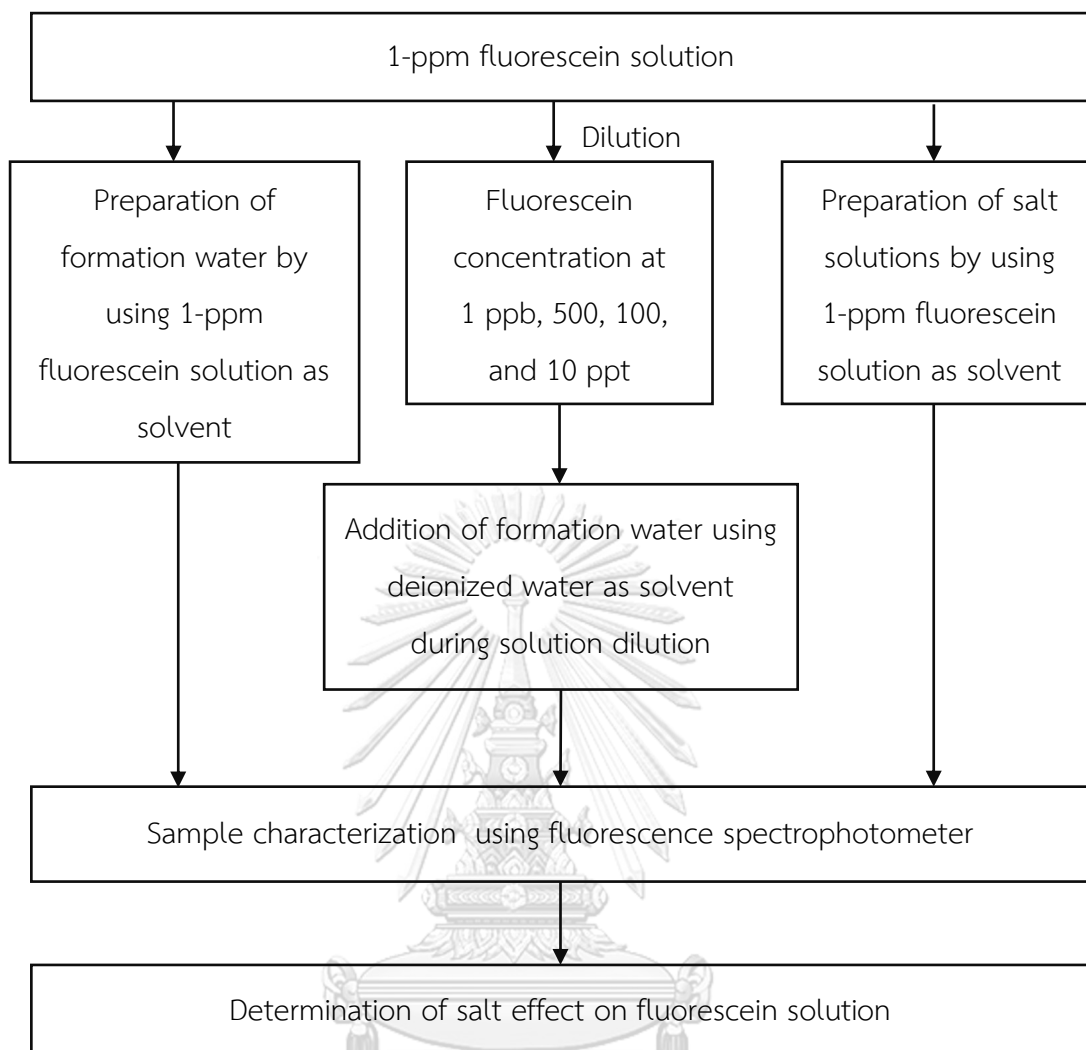
5.1. Fluorescein Characteristics

5.1.1. Determination of Detection Limit of Fluorescein Solution

In this subsection, detection limit of fluorescein solution would be determined. Fluorescein solution using deionized water as solvent at concentration of 1,000 ppm was prepared and diluted down to 10 ppt and each concentration was characterized by using fluorescence spectrophotometer. Pure deionized water, pure formation water, and pure tap water was also characterized and the results were compared to the solution with very low concentration.

The results and discussion started with the highest fluorescein concentration used in this study which was 1,000 ppm. Comparison of fluorescence spectra of fluorescein solution at 1,000 and 500 ppm were depicted in figure 25. The reason why only two solutions were compared was due to the same values of PMT voltage and slit size for these two concentrations. For lower concentration than this, the setting of PMT voltage and slit size must be modified and hence, they could be directly compared to results from lower concentration. From the figure, results showed that when fluorescein concentration was high (1,000 ppm), maximum fluorescence intensity was lower than that of fluorescein solution prepared at lower concentration (500 ppm) which might be due to self-quenching effect. In addition, 1,000-ppm solution had fluorescence emission wavelength at maximum fluorescence intensity of 545 nm, whereas 500-ppm solution had slightly shorter emission wavelength of 541 nm. It was also observed that the solution with higher concentration took more time to emit fluorescence compared to the solution with lower concentration. Physical appearances of both concentrations were shown in figure 26 where 1,000-ppm solution was slightly darker than 500-ppm solution.

Figure 25. *Fluorescence spectra of fluorescein solutions of 1,000 and 500 ppm in determination of detection limit of fluorescein solution with PMT voltage of 600 V and slit size of 5 nm.*

(a)   (b)

Figure 26. *Physical appearances of fluorescein solution with concentrations of (a) 1,000 ppm and (b) 500 ppm.*

As fluorescein concentrations were lower to 200 and 100 ppm, PMT voltage was adjusted to 500 V to refine the detection of fluorescence intensity. Likewise, fluorescein solution with the concentrations of 100 and 200 ppm still followed the similar trend in which the spectrum of 200-ppm solution had lower maximum intensity

than that of 100-ppm solution as shown in figure 27. Moreover, 200-ppm solution had slightly longer emission wavelength at maximum intensity of 532 nm than 100-ppm solution which had emission wavelength of 527 nm. In comparison, 100-ppm solution emitted brighter fluorescence than 200-ppm solution as shown in figure 28.
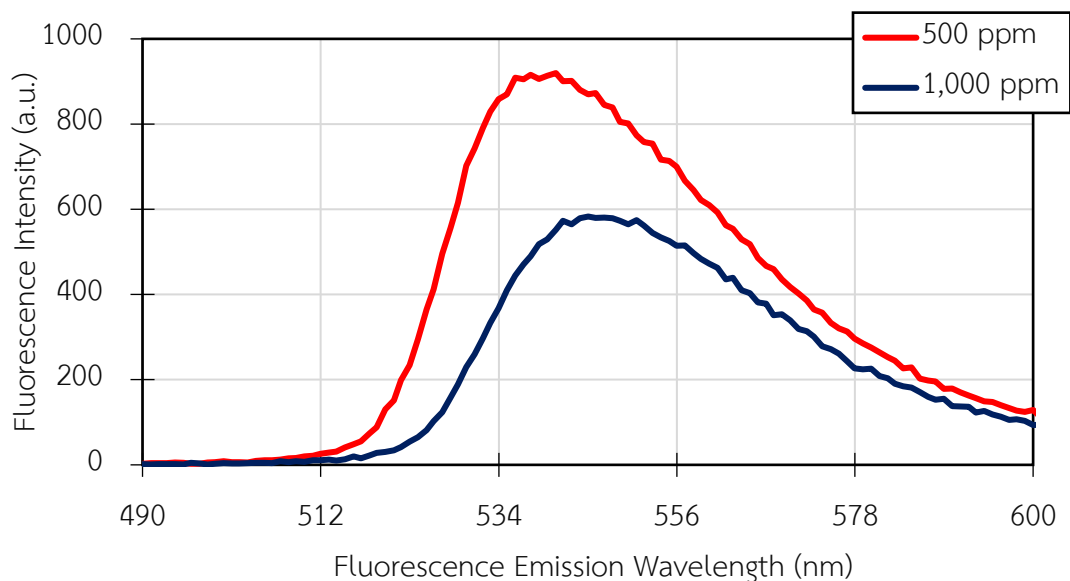

Figure 27. *Fluorescence spectra of fluorescein solutions of 500 and 1,000 ppm in determination of detection limit of fluorescein solution with PMT voltage of 500 V and slit size of 5 nm.*
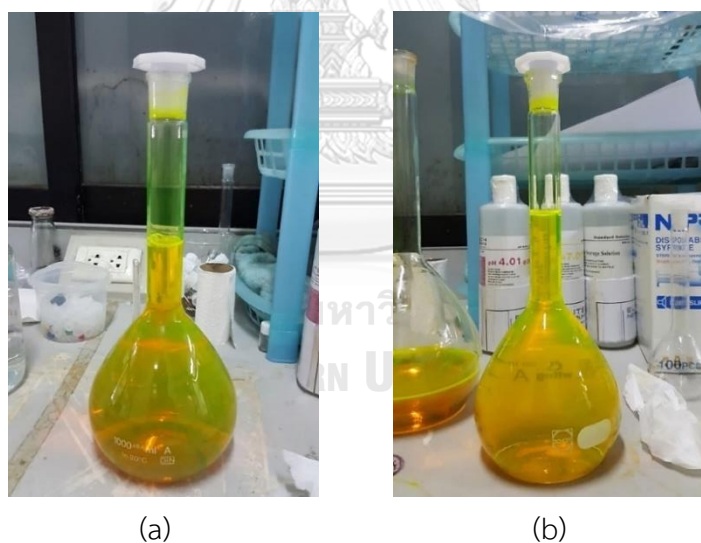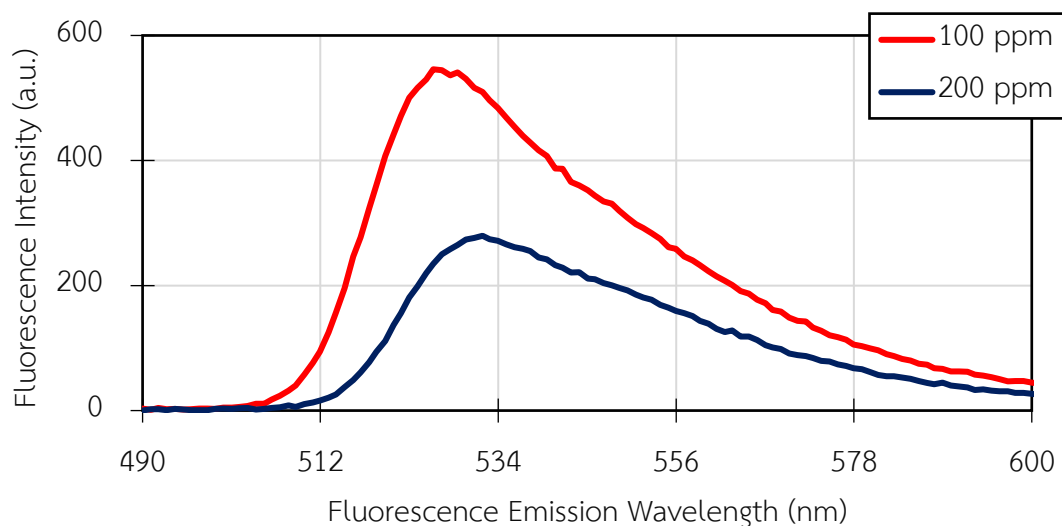

(a)   (b)

Figure 28. *Physical appearances of fluorescein solution with concentrations of (a) 200 ppm and (b) 100 ppm.*

As fluorescein concentration was lowering down, PMT voltage was lowered down to 400 V for an appropriate detection. Within this setting, fluorescein concentration of 500 ppb (0.5 ppm) was still detectable. Interestingly, when fluorescein concentration was lowering down from 100 ppm to 500 ppb, reversed point existed where fluorescence intensity was directly proportional to fluorescein concentration once the concentration fell below 10 ppm as shown in figure 29. Semi-log plot of maximum fluorescein intensity as a function of fluorescein concentration shown in figure 30 revealed reversed-point concentration appeared to be at 10 ppm, meaning that both self-quenching and self-absorption had stopped at this concentration. Furthermore, higher fluorescein concentrations still had slightly longer emisison wavelength at maximum intensity than the lower ones where emission wavelengths were 529, 523, 516, 512, and 512 nm for the concentrations of 100, 50, 10, 1, and 0.5 ppm, respectively. In addition, 50-ppm solution were brighter than 100-ppm solution and below 10 ppm, fluorescence became fader as shown in figures 31 and 32.

Figure 29. *Fluorescence spectra of fluorescein solutions of 100, 50, 10, 1 and 0.5 ppm in determination of detection limit of fluorescein solution with PMT voltage of 400 V and slit size of 5 nm.*

Figure 30. *Semi-log plot of maximum fluorescence intensity as a function of fluorescein concentration of fluorescein solution in determination of detection limit of fluorescein solution with PMT voltage of 400 V and slit size of 5 nm.*

(a)   (b)

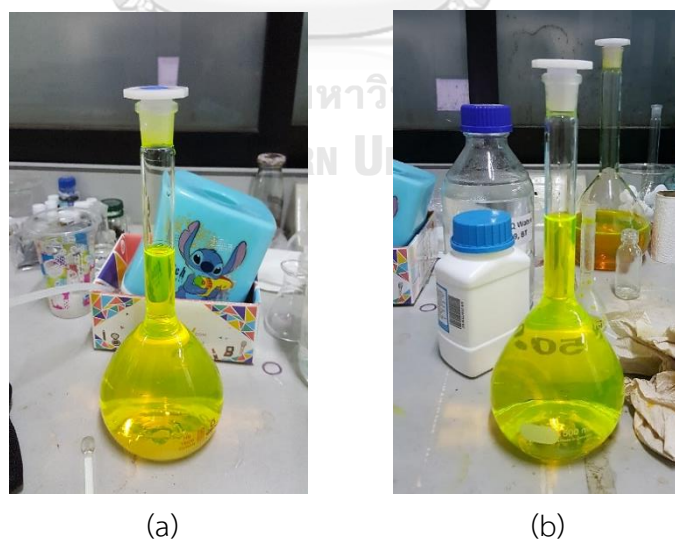**Figure 31.** *Physical appearances of fluorescein solutions with concentrations of (a) 50 ppm, (b) 10 ppm.*

(a)   (b)

Figure 32. *Physical appearances of fluorescein solutions with concentrations of (a) 1 ppm and (b) 500 ppb (0.5 ppm).*

Subsequently, as fluorescein concentration was lowered below 500 ppb, PMT voltage was lowering down to 800 V as shown in figures 33, 34, 35, and 36 for the concentrations of 100-500 ppb, 50-100 ppb, 10-50 ppb, and 1-10 ppb, respectively. Emission wavelength at maximum intensity of each concentration stopped declining at emission wavelength of about 512 nm when the concentration falls below 1 ppm. As shown in figure 37, fluorescence of fluorescein solutions became fader as the concentration decreased and eventually could not be observed by naked eyes when the concentration fells below approximately 50 ppb. It was noted that when the concentration decreased, there was a lot of noise created in the spectra, meaning that for very small concentration, slit size should be increased to 10 nm so that the spectra became smoother and clearer.
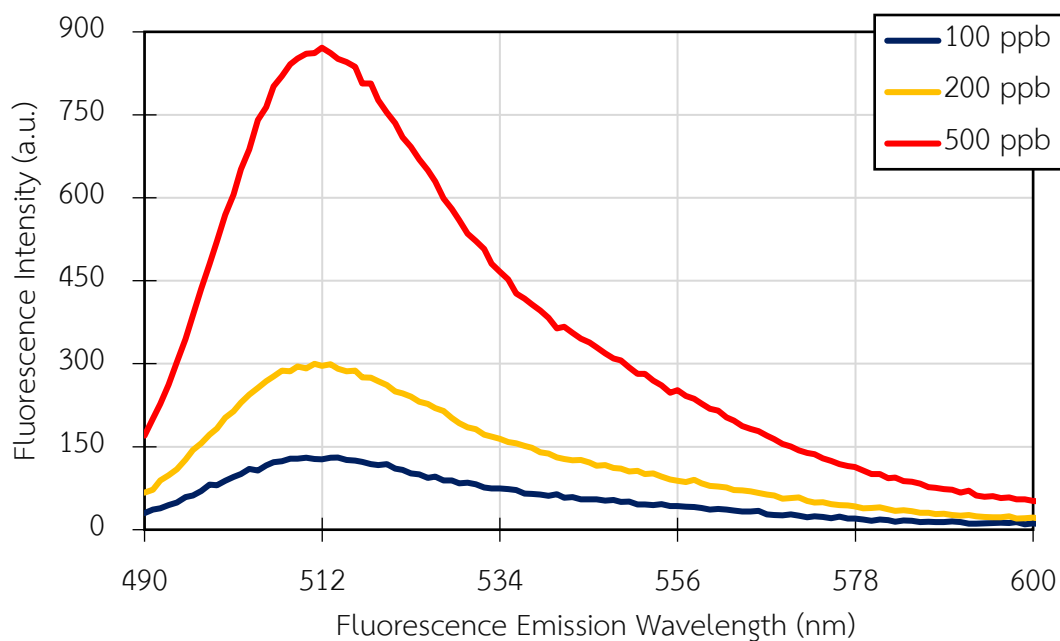
Figure 33. *Fluorescence spectra of fluorescein solutions of 500 ppb, 200 ppb, and 100 ppb in determination of detection limit of fluorescein solution with PMT voltage of 550 V and slit size of 5 nm.*
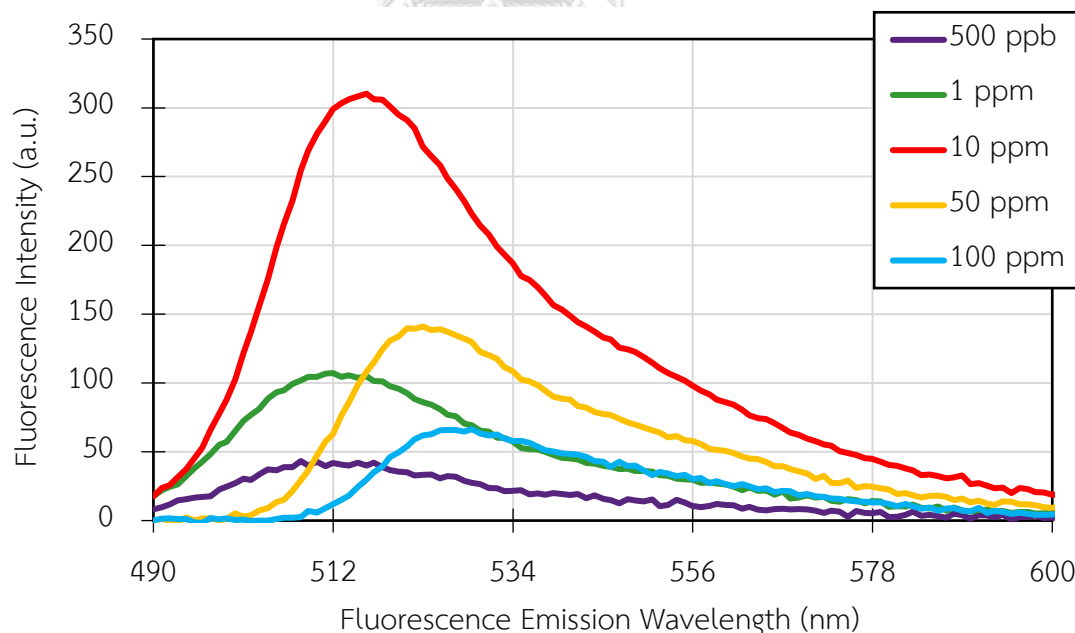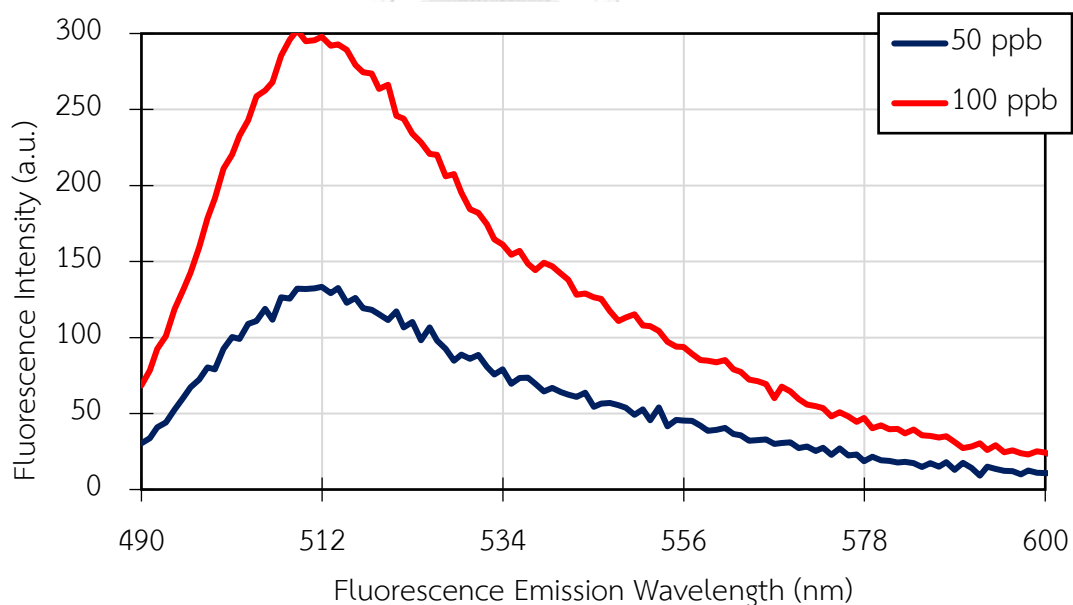

Figure 34. *Fluorescence spectra of fluorescein solutions of 100 ppb and 50 ppb in determination of detection limit of fluorescein solution with PMT voltage of 600 V and slit size of 5 nm.*
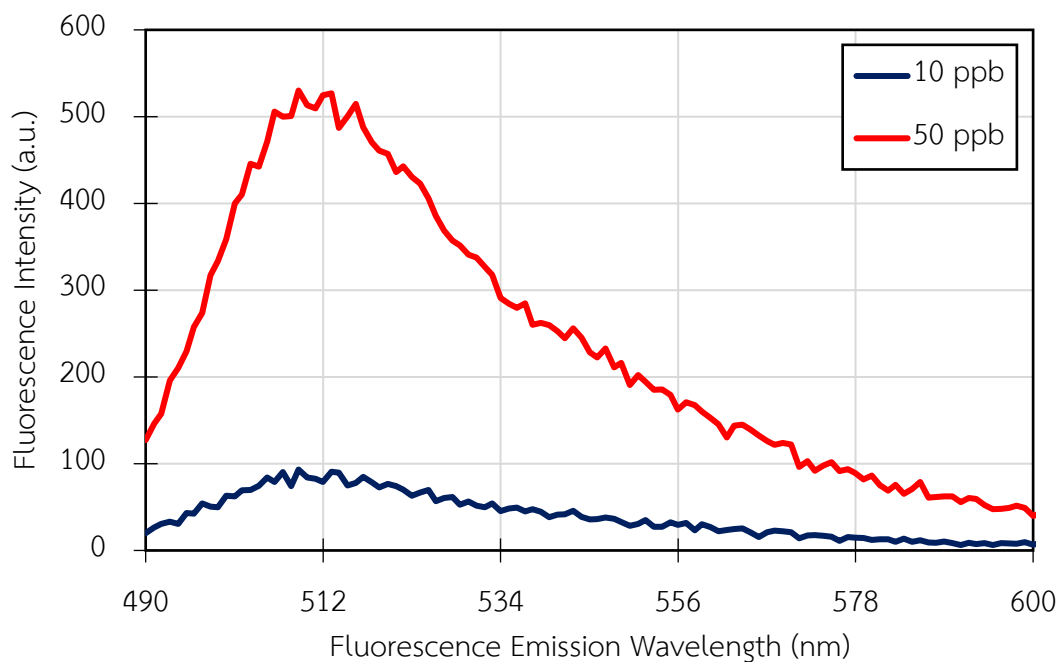
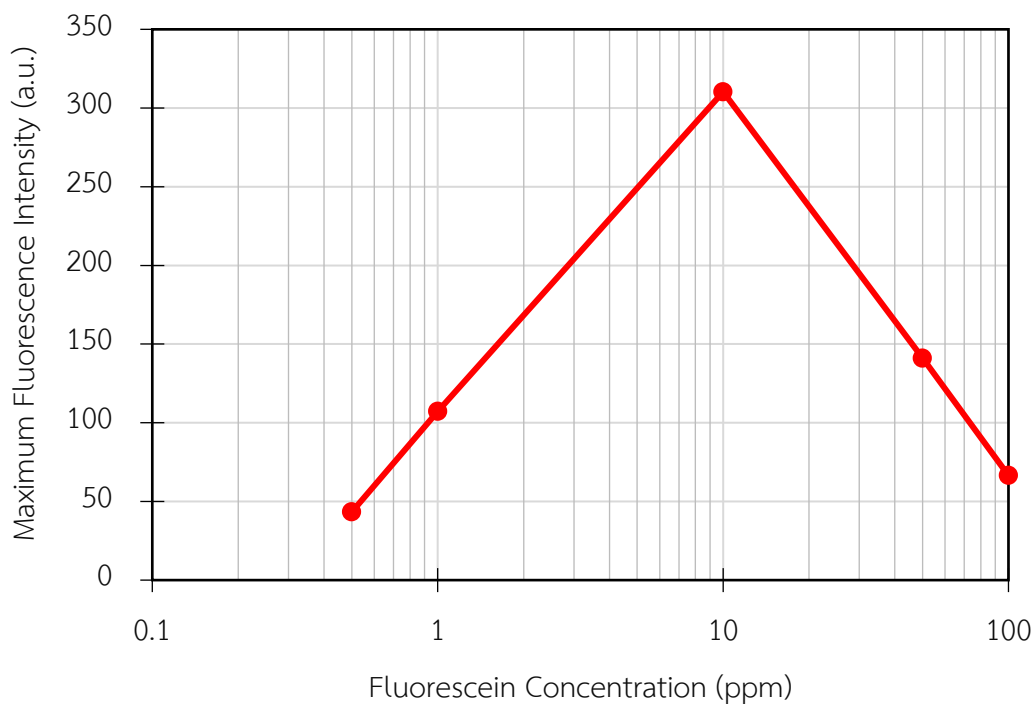**Figure 35.** *Fluorescence spectra of fluorescein solutions of 50 ppb and 10 ppb in determination of detection limit of fluorescein solution with PMT voltage of 700 V and slit size of 5 nm.*
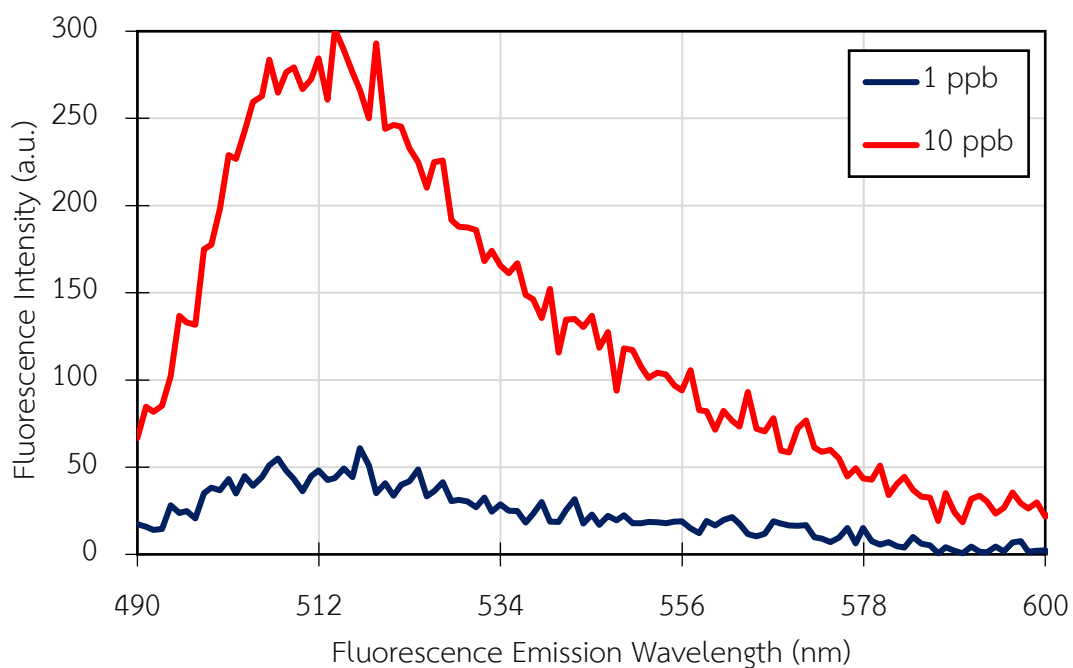
Figure 36. *Fluorescence spectra of fluorescein solutions of 10 and 1 ppb in determination of detection limit of fluorescein solution with PMT voltage of 800 V and slit size of 5 nm.*
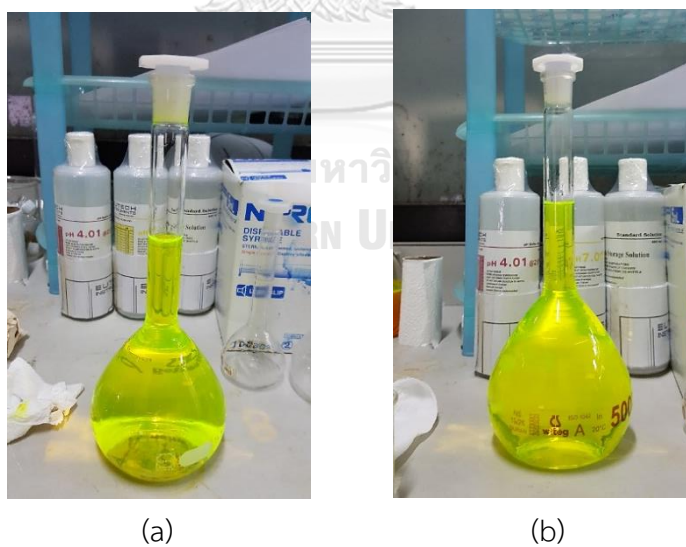
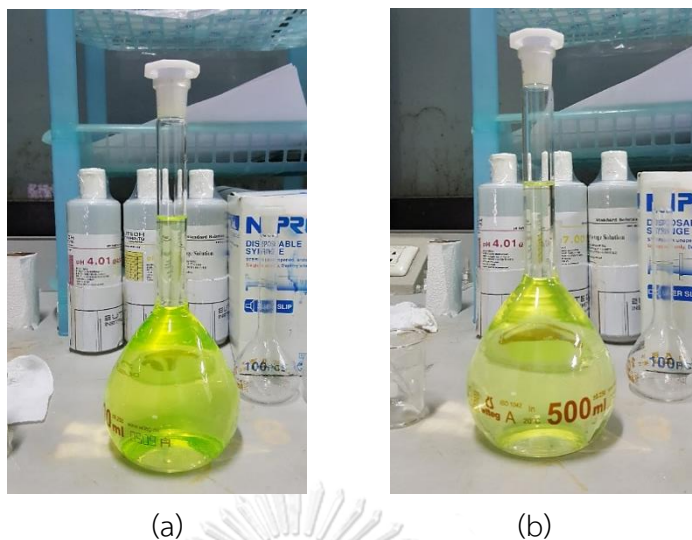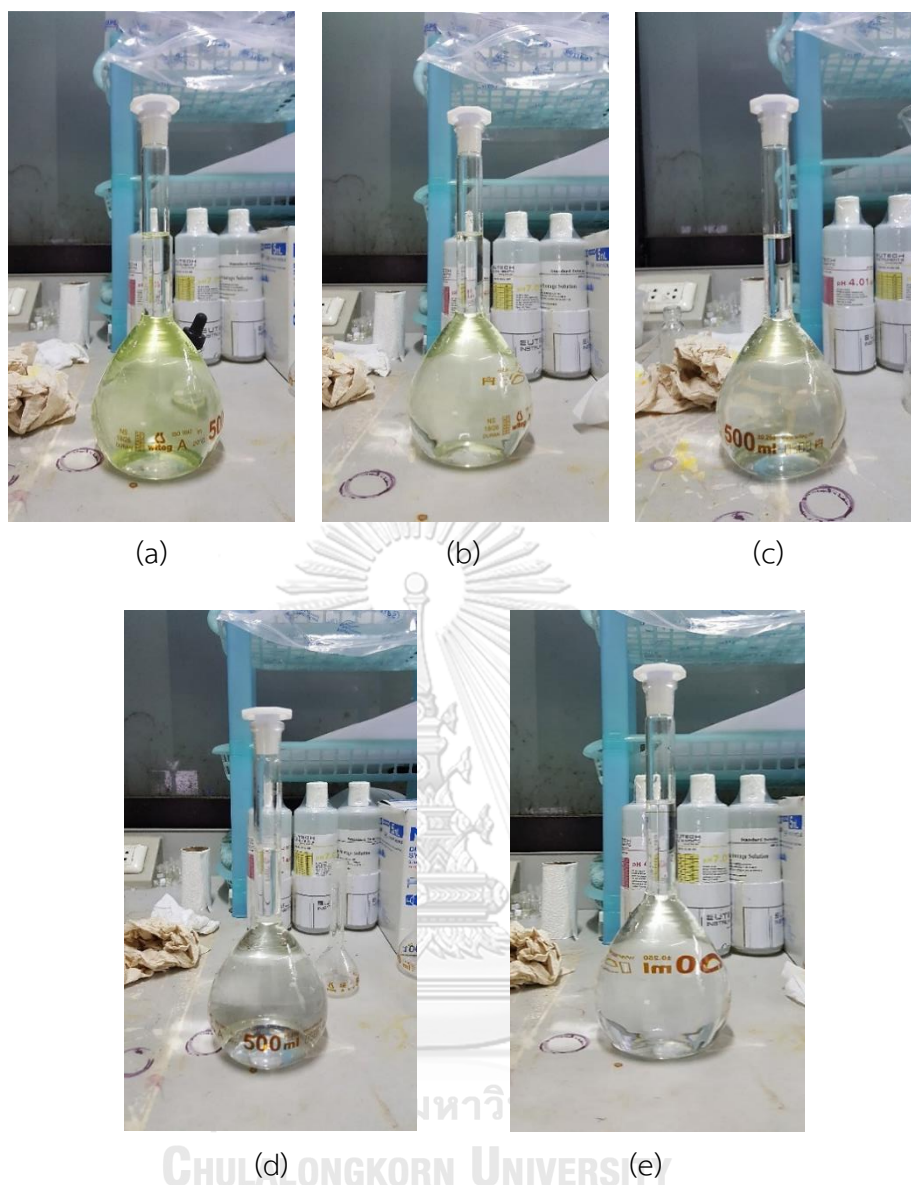**Figure 37.** *Physical appearances of fluorescein solutions with concentrations of (a) 200 ppb, (b) 100 ppb, (c) 50 ppb, (d) 10 ppb, and (e) 1 ppb.*

After, fluorescein solution was diluted down to 500 ppt, 100 ppt and 10 ppt. For these concentrations, only the spectrum of 500-ppt solution was still observed. The spectra of both 100-ptt and 10-ppt solutions could not be differentiated from the spectra of various pure waters including deionized water, tap water, and formation water as shown in figure 38. Therefore, detection limit of fluorescein solution using deionized water as solvent was determined to be at the concentration of 500 ppt.
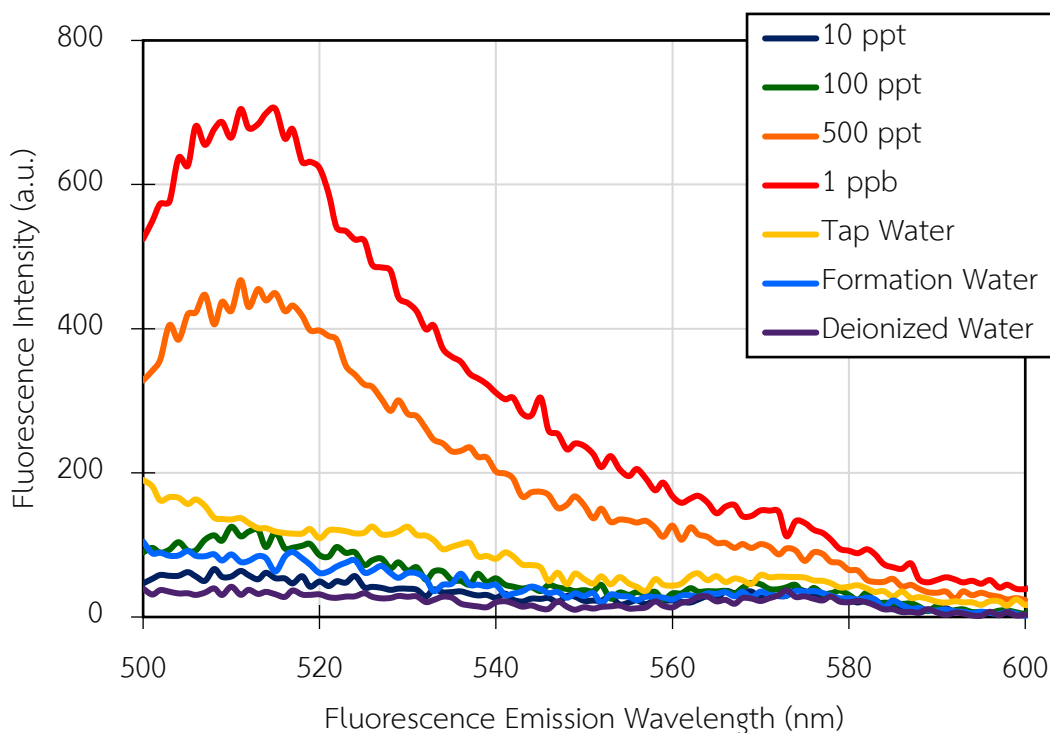
Figure 38. *Fluorescence spectra of fluorescein solutions of 1 ppb, 500 ppt, 100 ppt, 10 ppt and various types of water in determination of detection limit of fluorescein solution with PMT voltage of 800 V and slit size of 10 nm.*

In addition, fluorescein solution at 10 ppm was found to a concentration that reversed relationship between fluorescence intensity and fluorescein concentration. When the concentration was above 10 ppm, the intensity was inversely proportional to the concentration due to both self-quenching and self-absorption, whereas when the concentration was below 10 ppm, the intensity was directly proportional to the concentration due to having lower fluorescein molecules to emit fluorescence. Moreover, it was also found that fluorescence emission wavelength at maximum fluorescence intensity was a function of fluorescein concentration and stopped when the concentration was at 1 ppm at emission wavelength of 512 nm. The reason was that when the concentration is high, self-quenching and self-absorption caused a reduction in fluorescence energy, resulting in longer fluorescence emission wavelength at maximum fluorescence intensity. From these two results, self-quenching and self-adsorption was expected to stop at concentration between 1 – 10 ppm.

5.1.2. Investigation of Photosensitivity of Fluorescein Solution

In this subsection, appropriate storage for fluorescein solution was investigated and emphasized mainly on photosensitivity or effect of light exposure. Fluorescein solution at 100 ppm was placed into transparent glass bottles for all-time exposure to light, and amber-colored glass bottles for all-time concealment and normal exposure to light. Each samples form each set was collected within 1, 2, and 7 days, and characterized by using fluorescence spectrophotometer.

From the results, they showed that fluorescence of fluorescein solution could be photodegraded. As shown in figure 39, maximum fluorescence intensity of all-time exposure to light inside transparent glass bottle had significant lower than other conditions after 7 days. Also, fluorescence of the solution became darker with time as shown in figure 40. On the other hand, both all-time concealment and normal exposure to light inside amber-colored glass bottles showed very small difference in all results. Therefore, it could be concluded that amber-colored glass bottle was adequate to be an appropriate storage for fluorescein solution.

Figure 39. *Physical appearance of 100-ppm fluorescein solutions in all-time exposure to light including 1 day (left), 2 days (middle), and 7 days (right).*

Figure 40. *Fluorescence spectra of 100-ppm fluorescein solutions in evaluation of photosensitivity of fluorescein after 7 days with PMT voltage of 500 V and slit size of 5 nm.*

5.1.3. Investigation of pH-Sensitivity of Fluorescein Solution

In this subsection, appropriate pH value of fluorescein solution was investigated and emphasized on pH-sensitivity. Fluorescein solution at 100 ppm was prepared and equally divided into three beakers. Acetic acid and sodium carbonate were added into the first two beakers to make the solution acidic and basic, respectively and nothing was added into the last beaker to make the solution neutral. The pH value of each solution was measured by using pH universal indicator papers. All solutions were qualitatively observed and compared by pouring each solution into borosilicate glass measuring cylinders and characterized by fluorescence spectrophotometer.

From the results, pH values of fluorescein solutions were 3, 7, and 11 which represented acidic, neutral, and basic pH values, respectively and the measuring cylinders were utilized for qualitative observation and comparison as shown in figure 41. From the figure, the cylinder with acidic solution showed darker fluorescence compared to others which showed almost the same fluorescence due to presences

of hydrogen bonding between acetic acid and fluorescein molecules. Moreover, figure 42 apparently showed that acidic solution had lower intensity and shorter emission wavelength at maximum intensity than other pH values which was due to hydrogen bonding between acetic acid and fluorescein molecules. On the other hand, neutral and basic solutions showed nearly the same intensity and same fluorescence. Therefore, appropriate pH value for storage of fluorescein solution should be in neutral to alkaline range.
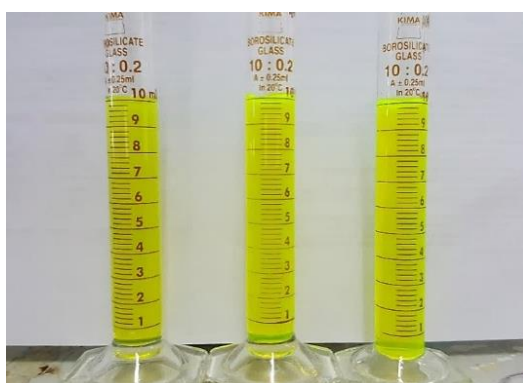
Figure 41. *Physical appearance of 100-ppm fluorescein solutions with different pH values in measuring cylinders including pH 3 (left), pH 7 (middle), and pH 11 (right).*
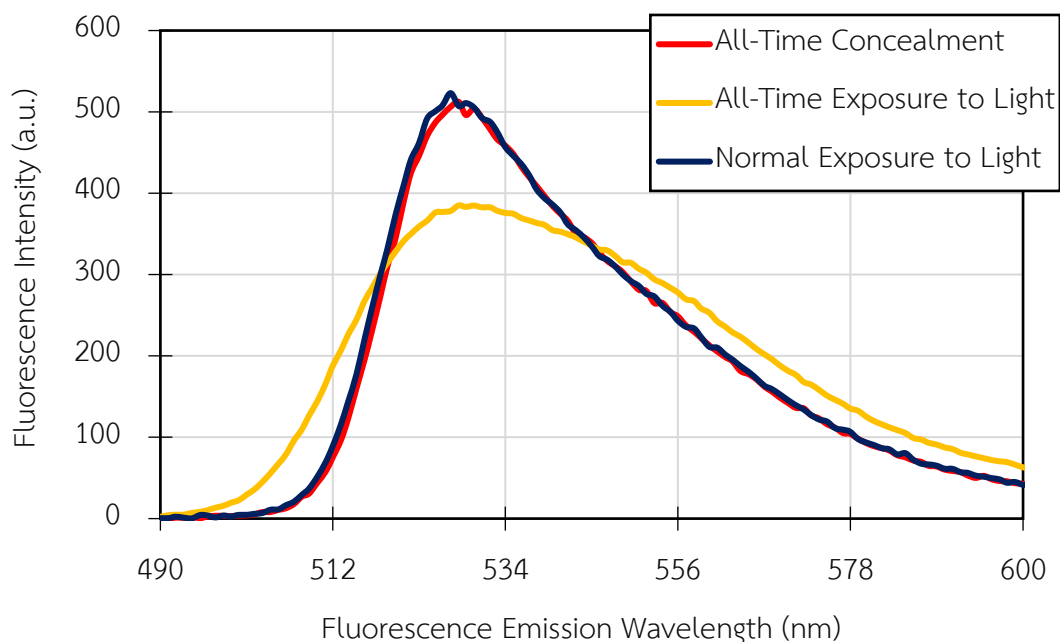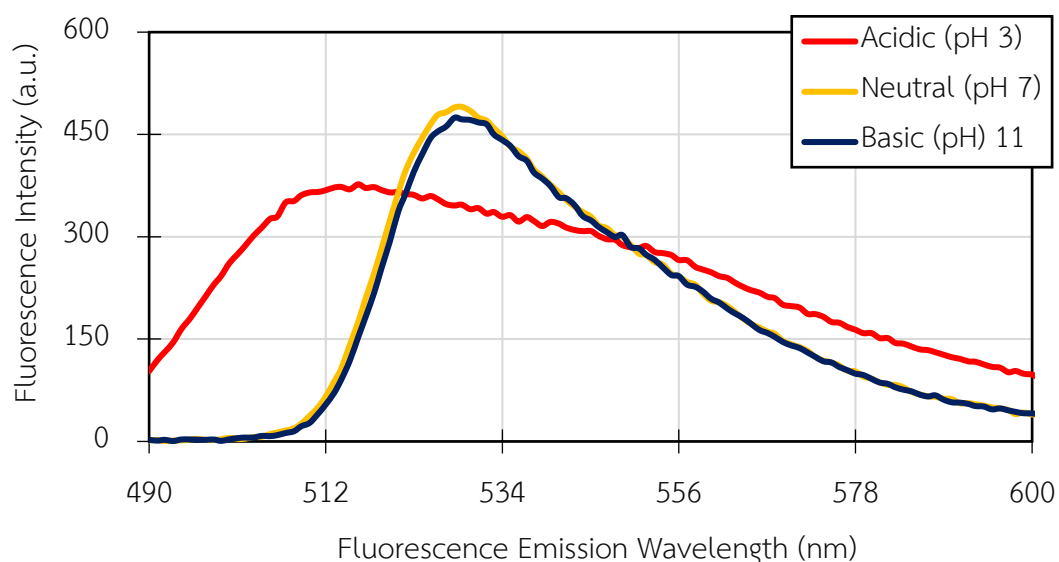

Figure 42. *Fluorescence spectra of 100-ppm fluorescein solutions in evaluation of pH-sensitivity of fluorescein solution with PMT voltage of 500 V and slit size of 5 nm.*

5.1.4. Determination of Thermal Stability of Fluorescein Solution

In this subsection, thermal stability of fluorescein solution at petroleum reservoir temperature was determined. Fluorescein solution at 100 pm was prepared and placed inside amber-colored glass bottles. The bottles were in plastic jar filled with water at 30 °C, and in BWS-20 water bath filled with water at 50 °C and 70 °C. Each sample from each temperature was collected and characterized by using fluorescence spectrophotometer.

From the results, fluorescence spectra of all temperatures showed almost the same trend as shown in figure 43. Moreover, a plot of maximum fluorescence intensity as a function of time at different temperatures as shown in figure 44 showed that there was no significant attenuation of maximum fluorescence intensity of 100-ppm fluorescein solution with time, meaning that fluorescein solution was unaffected by temperature up to 70 °C for 12 days. Therefore, fluorescein solution could be used in petroleum reservoirs under this temperature range without substantial thermal degradation.
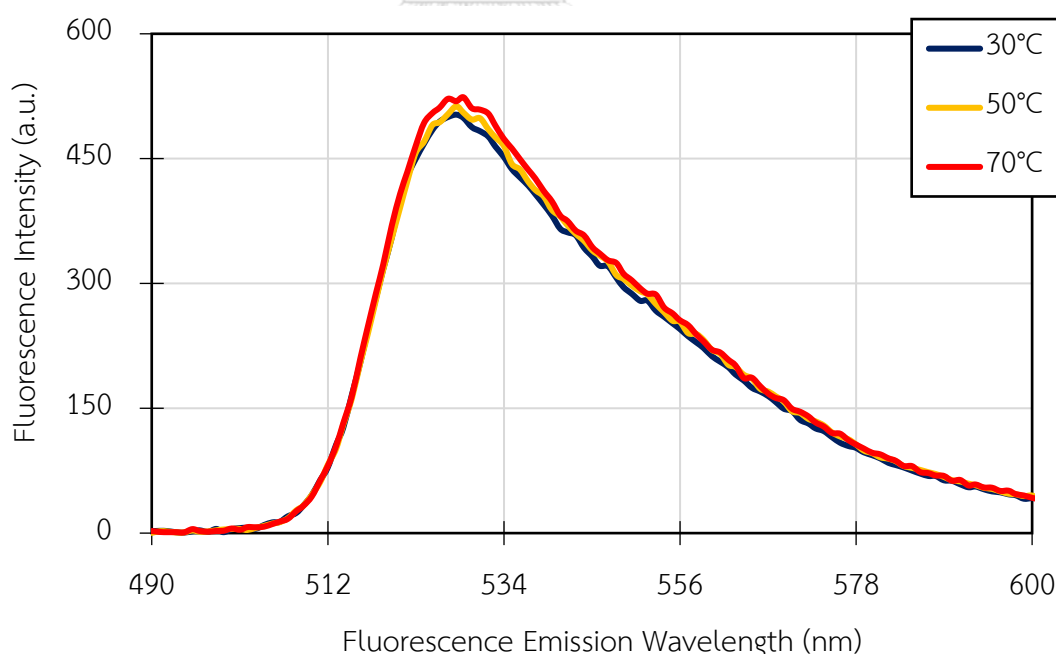
Figure 43. *Fluorescence spectra of 100-ppm fluorescein solution in evaluation of thermal stability of fluorescein solution after 12 days with PMT voltage of 500 V and slit size of 5 nm.*
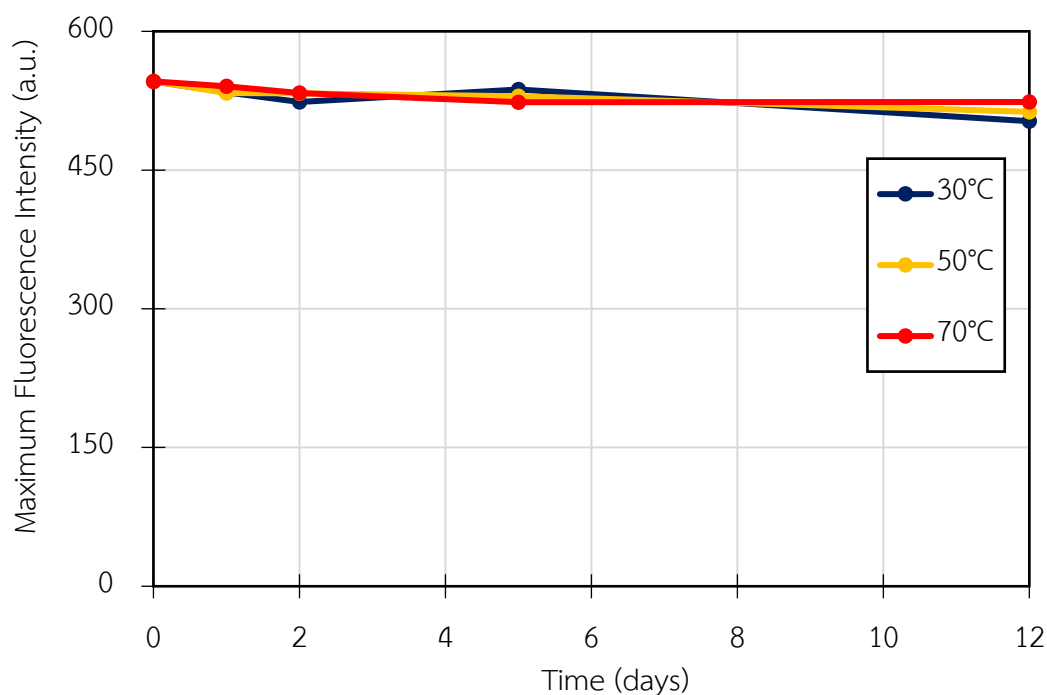
Figure 44. *Plot of maximum fluorescence intensity as a function of time of 100-ppm fluorescein solution at different temperatures in determination of thermal stability of fluorescein solution with PMT voltage of 500 V and slit size of 5 nm.*

5.2 Shaly-Sandstone Samples

5.2.1. Determination of Physical Properties of Shaly-Sandstone Core Samples

Physical properties of shaly-sandstone core sample as listed in table 7 was measured and calculated by using equations (5) to (8), and absolute permeability together with other parameters for calculation of the permeability were summarized in table 8.

Table 7. *Physical properties of shaly-sandstone core sample.*

Parameters	Value	Unit
Dried Weight	188.95	g
Saturated Weight	208.42	g
Saturation Liquid Density	1.005	g/cm^3
Length	8.15	cm
Diameter	3.80	cm
Cross-Sectional Area	11.34	cm^2
Bulk Volume	92.43	cm^3
Pore Volume	19.37	cm^3
Porosity	0.21	fraction

Table 8. *Absolute permeability of shaly-sandstone core sample and other parameters for calculation of the permeability.*

No.	Liquid Flow Rate (cm^3/s)	Liquid Viscosity (cP)	Pressure Gradient (atm)	Permeability (Darcy)
1	0.068333	0.85	0.250340	0.16673
2	0.051667	0.85	0.188435	0.16748
3	0.035000	0.85	0.125850	0.16988
			Average Permeability (Darcy)	0.16803
			Average Permeability (mD)	168.03

5.2.2. Characterization of Elemental Composition of Shaly‑Sandstone Samples

Elemental compositions of shaly-sandstone sample, characterized by X-ray fluorescence (XRF) analyzer, were revealed in table 9. From the table, major elemental compositions were silicon, followed by iron, potassium, aluminum, titanium, calcium and trace amounts of other compositions. Elemental composition of shaly-sandstone sample was important for fluorescein adsorption, and the effects of elemental composition on fluorescein solution would be discussed in the following sections.

Table 9. *Elemental compositions of shaly-sandstone sample characterized by X-ray fluoresence (XRF) analyzer.*

Element	Concentration	Element	Concentration
Silicon (Si)	49.647 %	Strontium (Sr)	0.104 %
Iron (Fe)	21.597 %	Vanadium (V)	913.4 ppm
Potassium (K)	12.294 %	Chromium (Cr)	890.6 ppm
Aluminum (Al)	8.031 %	Europium (Eu)	879.1 ppm
Titanium (Ti)	5.158 %	Nickel (Ni)	589.9 ppm
Calcium (Ca)	1.367 %	Copper (Cu)	411.5 ppm
Zirconium (Zr)	0.415 %	Niobium (Nb)	339.2 ppm
Tin (Sn)	0.248 %	Yttrium (Y)	325.3 ppm
Phosphorus (P)	0.154 %	Gallium (Ga)	214.1 ppm
Tellurium (Te)	0.136 %	Arsenic (As)	131.2 ppm
Rubidium (Rb)	0.134 %	Thorium (Th)	130.1 ppm
Manganese (Mn)	0.115 %	Germanium (Ge)	32.5 ppm
Zinc (Zn)	0.110 %	Ytterbium (Yb)	19.1 ppm

5.3. Static Investigation of Fluorescein Solution with Shaly-Sandstone

In this section, full interactions between fluorescein and shaly-sandstone powders were investigated by performing stirring tests. The powders were prepared in two ways including untreated and treated powders and were separately stirred with fluorescein solution at 1 ppb, 100 ppb, 1 ppm, 100 ppm, and 1,000 ppm using magnetic stirring bars cooperated with magnetic stirrer for 6 hours. After that, the powders were filtered from the mixtures by using 125-mm filter papers, and the filtrates were characterized by fluorescence spectrophotometer.

Figure 45 illustrated fluorescence spectra of deionized water, filtrates after stirred with untreated powder, and filtrates after stirred with treated powder. From the figure, it could be observed that fluorescence detection of deionized water was completely disturbed by the presences of shaly-sandstone, hydrocarbon, and/or drilling fluids. The sources of disturbance might come from the presence of shaly-sandstone. Figure 46 summarized fluorescence spectra of 1-ppb fluorescein solution, filtrate after stirred with untreated powder, and filtrate after stirred with treated powder. Similar results as occurred with deionized water appeared. Moreover, all spectra for filtrates in both figures showed peaks at 527 nm which might be due to presences of natural fluorescence in shaly-sandstone. This suggested that 500-ppt fluorescein solution stirred with shaly-sandstone powders was impractical as fluorescence detection might be disturbed by natural fluorochromes, shaly-sandstone, hydrocarbon and/or drilling fluids. Next, for 100-ppb fluorescein solution, the results showed that fluorescence spectra of stirred solutions could be clearly distinguished from that of 100-ppb pure fluorescein solution; however, fluorescence spectra of stirred solutions had higher maximum fluorescence intensity than that of the pure solution as shown in figure 47. This behavior was directly linked to the presence of shaly-sandstone, hydrocarbon, and/or drilling fluids.

Figure 45. *Fluorescence spectra of deionized water in static investigation of fluorescein solution with shaly-sandstone with PMT voltage of 600 V and slit size of 10 nm.*

Figure 46. *Fluorescence spectra of 1-ppb fluorescein solution in static investigation of fluorescein solution with shaly-sandstone with PMT voltage of 700 V and slit size of 5 nm.*
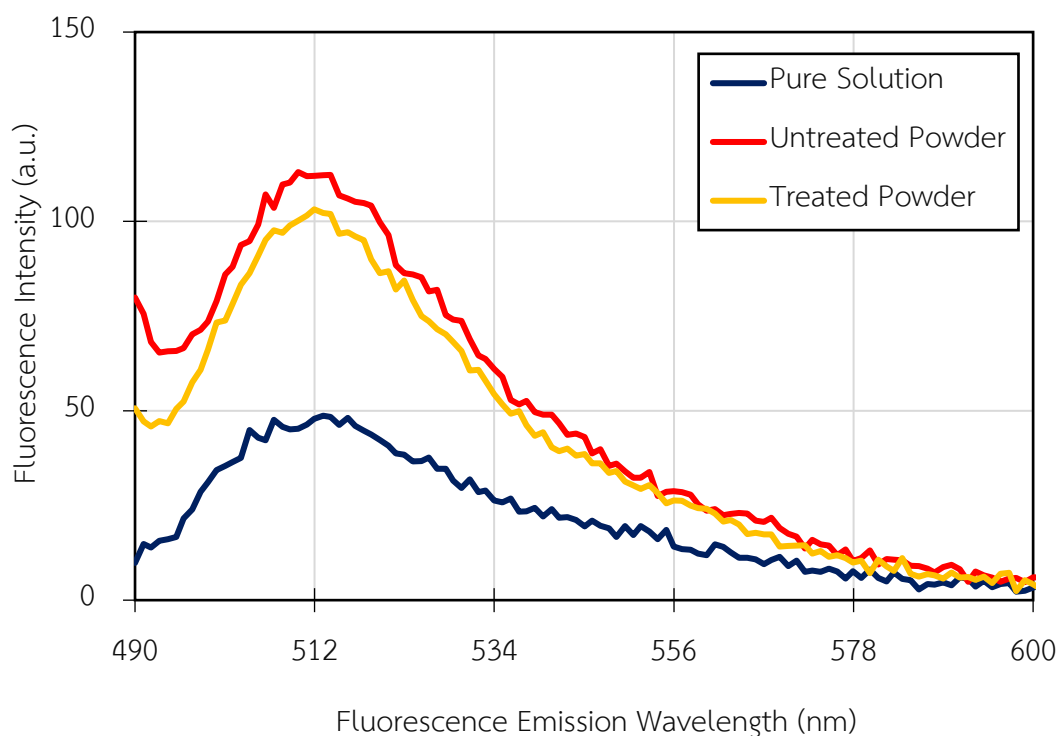
Figure 47. *Fluorescence spectra of 100-ppb fluorescein solution in static investigation of fluorescein solution with shaly-sandstone with PMT voltage of 500 V and slit size of 5 nm.*

From figures 45 to 47, the spectra obtained from filtrates after stirred with untreated powder showed higher intensity than that of treated powder, meaning that effects of shaly-sandstone, hydrocarbon, and/or drilling fluid were stronger than the effect of shaly-sandstone only.

Subsequently, as shown in figures 48 and 49, the spectra of 1-ppm and 100-ppm solutions stirred with untreated and treated powders were almost identical, meaning that the effects of shaly-sandstone, hydrocarbon, and/or drilling fluid were diminished by the presence of fluorescein in higher concentration. The spectra of 1-ppm stirred solutions still had higher maximum intensity than that of the 1-ppm pure solution, whereas 100-ppm stirred solutions had almost the same maximum intensity as the 100-ppm pure solution, meaning that effects of shaly-sandstone, hydrocarbon, and/or drilling fluid nearly stopped at this concentration.
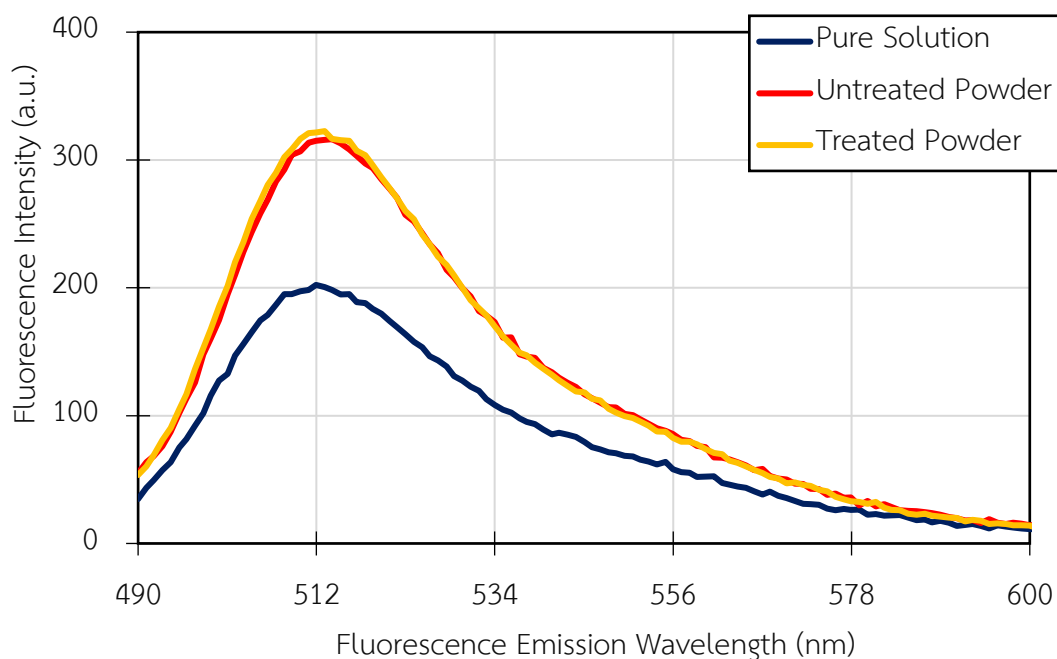
Figure 48. *Fluorescence spectra of 1-ppm fluorescein solution in static investigation of fluorescein solution with shaly-sandstone with PMT voltage of 450 V and slit size of 5 nm.*
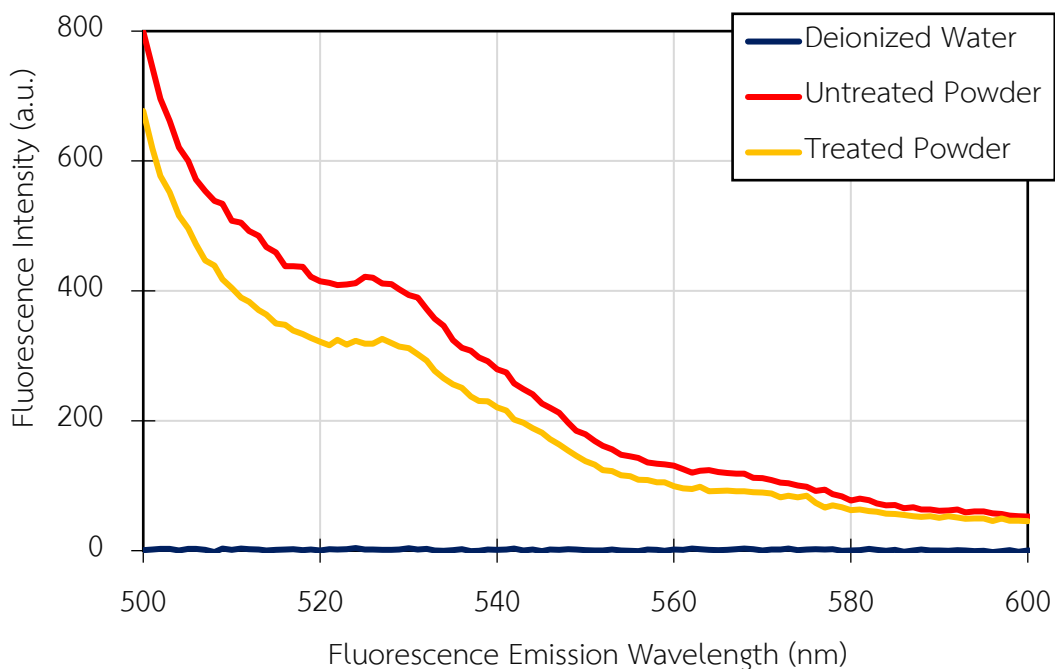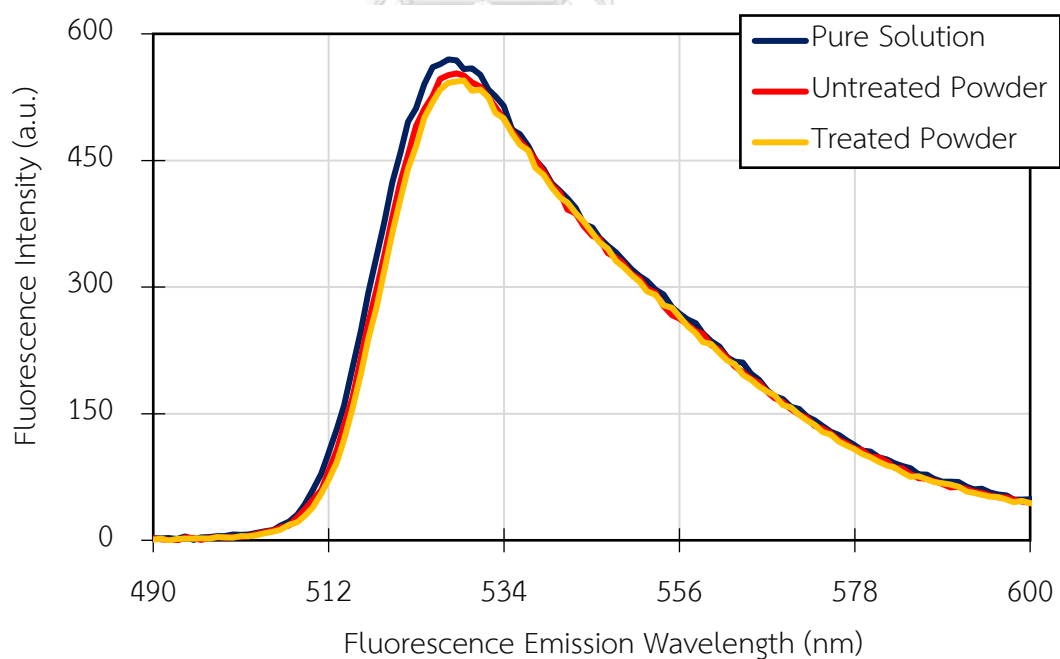

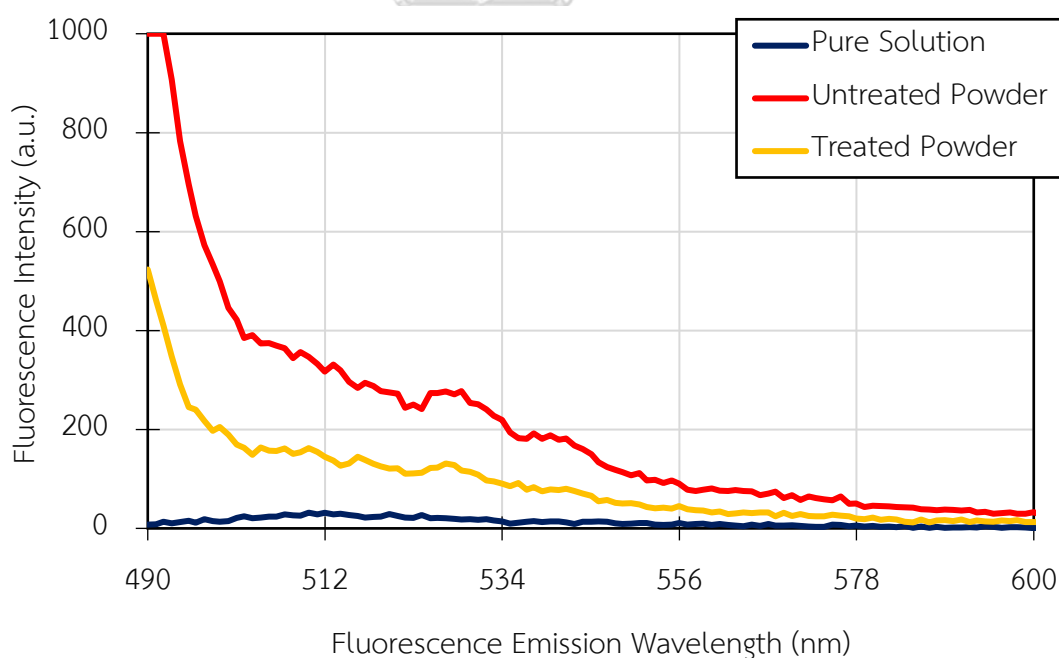**Figure 49.** *Fluorescence spectra of 100-ppm fluorescein solution in static investigation of fluorescein solution with shaly-sandstone with PMT voltage of 500 V and slit size of 5 nm.*

Once fluorescein concentration was higher than 10 ppm, fluorescence intensity was inversely proportional to fluorescein concentration. The increases in maximum intensity of stirred solutions over the pure solution of 1,000-ppm solution were shown in figure 50 which could be explained by fluorescein adsorption onto shaly-sandstone as at high fluorescein concentration, an increasing of maximum intensity indicated a reduction of fluorescein concentration. Additionally, the spectrum of the solution stirred with treated powder was higher than that of the solution stirred with untreated powder, implying that treated powder might have more surface area to adsorb fluorescein molecules, resulting in more reduction of fluorescein concentration.
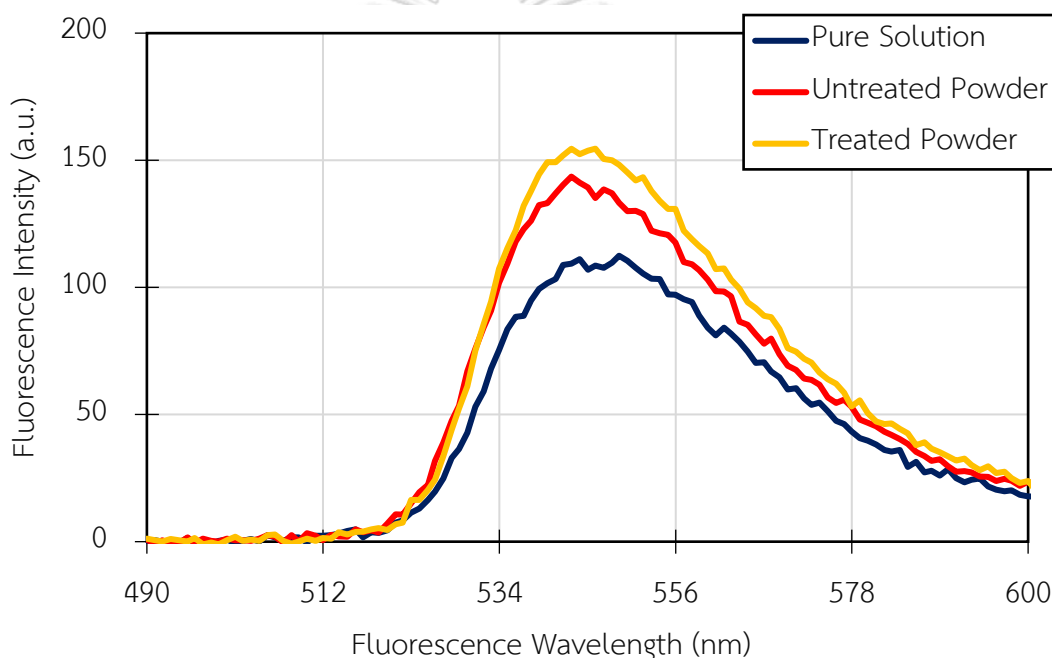
Figure 50. *Fluorescence spectra of 1,000-ppm fluorescein solution in static investigation of fluorescein solution with shaly-sandstone with PMT voltage of 500 V and slit size of 5 nm.*

By plotting semi-log plots of maximum fluorescence intensity as a function of fluorescein concentration (see in appendix A), equivalent fluorescein concentrations for filtrates stirred with untreated and treated powders could be determined and summarized in table 10 and table 11, respectively except for 1-ppb solution which could not be determined.

Table 10. *Equivalent fluorescein concentration of fluorescein solution stirred with untreated shaly-sandstone powder.*

Initial Concentration (ppm)	Equivalent Concentration (ppm)	Change in Concentration (ppm)	Percentage Change (%)
0.10	0.21	+0.11	+111.17
1.00	2.29	+1.29	+128.58
100	132.57	+32.57	+32.57
1,000	938.70	-61.30	-6.13

Table 11. *Equivalent fluorescein concentration of fluorescein solution stirred with treated shaly-sandstone powder.*

Initial Concentration (ppm)	Equivalent Concentration (ppm)	Change in Concentration (ppm)	Percentage Change (%)
0.10	0.19	+0.09	+94.16%
1.00	2.36	+1.36	+135.74%
100	148.77	+48.77	+48.77%
1,000	917.07	-82.93	-8.29%

Data from table 10 and table 11 were used to construct semi-log plot of percentage change in equivalent fluorescein concentration as a function of initial fluorescein concentration and the results were depicted in figure 50. From the figure, 1-ppm fluorescein solution had the highest percentage change due to the presence of shaly-sandstone, hydrocarbon, and/or drilling fluids, implying that the fluorescein concentration of the 1-ppm solution could be astonishingly amplified more than 100% of its initial concentration. The plot also showed that untreated and treated powders yielded almost the same results, meaning that the presences of hydrocarbon and/or drilling fluids diminutively affects fluorescein solution compared to shaly-sandstone itself. Therefore, shaly-sandstone core sample saturated with hydrocarbon would be

ignored in the next section. Since the 1-ppb solution stirred with shaly-sandstone could not be evaluated in this section, it would be then further evaluated in the next section. Finally, appropriate fluorescein concentrations for next section were selected to be 1 ppb, 100 ppb, and 1 ppm. Higher fluorescein concentrations were not selected as fluorescein adsorption was undesirable.
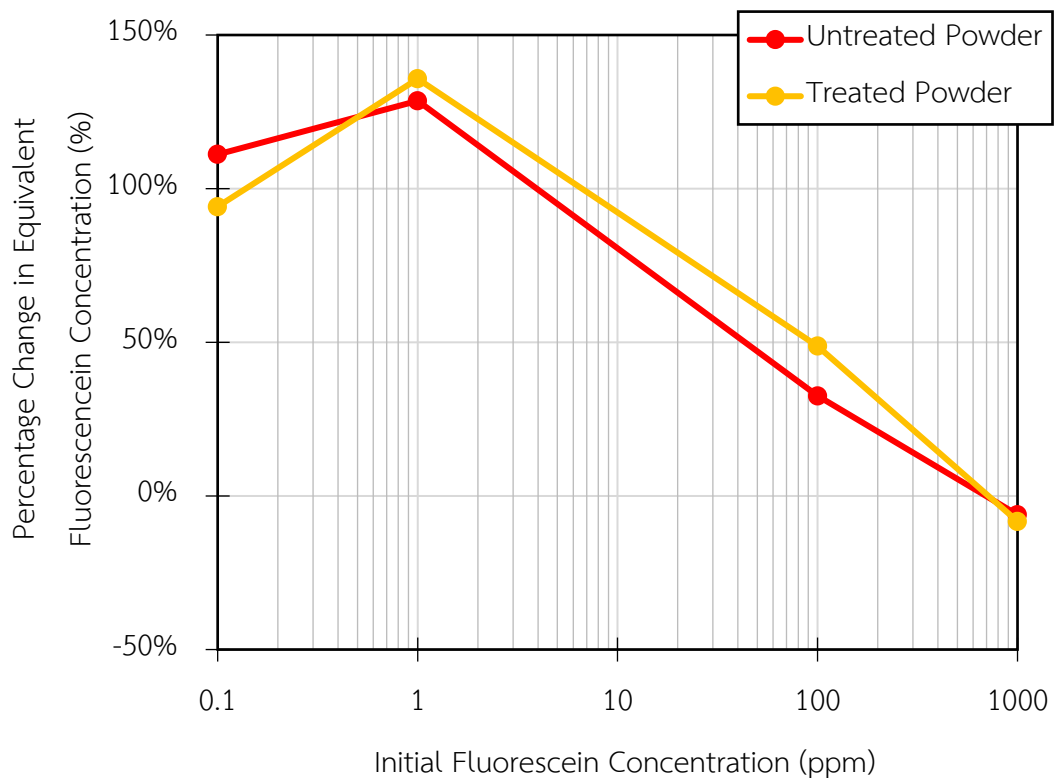
Figure 51. *Semi-log plot of percentage change in equivalent fluorescein concentration as a function of initial fluorescein concentration.*

5.4. Dynamic Investigation of Fluorescein Solution with Shaly-Sandstone

In this section, actual interactions between fluorescein and shaly-sandstone core sample were investigated by performing coreflooding tests. Shaly-sandstone core sample saturated with formation water was initially placed in coreflooding system. The same formation water was injected to fully saturate the system and after that fluorescein solution at concentration of 1 ppb was injected at an injection rate of 0.5 cm^3/min. Effluent samples were collected every 10 minutes for fluorescence

detection. Figure 52 summarized fluorescence spectra of 1-ppb fluorescein solution flowing through the core sample. From the figure, the effects from shaly-sandstone were not as obvious as in static investigation where maximum intensity of the 1-ppb solution at wavelength of 512 nm could be observed. However, the effects from shaly-sandstone had the highest intensity at 55 min and inverse trends at about 495 nm could be detected in all spectra.

Figure 52. *Fluorescence spectra of 1-ppb fluorescein solution in dynamic investigation of fluorescein solution with shaly-sandstone with PMT voltage of 700 V and slit size of 5 nm.*

By plotting histogram of maximum fluorescence intensity as a function of sample collecting time as shown in figure 53, fluorescein breakthrough time could be determined to be between 30 min and 40 min. The intensity sharply increased from 25 min to 35 min and increased to maximum intensity from 35 min to 45 min, and after 45 min, maximum intensity trended to lower down until 110 min which was

because the effects from shaly-sandstone might be alleviated with time for this concentration.

Figure 53. *Histogram of maximum fluorescence intensity of 1-ppb fluorescein solution as a function of sample collecting time in dynamic investigation of fluorescein solution with shaly-sandstone with PMT voltage of 700 V and slit size of 5 nm.*

From figure 53, it could be explained that fluorescein from the injection process might arrive at the production end in the period between 30 to 40 minutes. By the use of mathematical method shown in appendix B, approximated breakthrough time was about 32.16 minutes. However, since the system also contained dead pore volume of 4.32 cm^3, the production time required for this volume of 8.64 minutes must be subtracted from the calculated time. Hence, breakthrough time for 1-ppb solution was 23.52 minutes.

The same core sample was consecutively used for the next fluorescein solution at higher concentration which was 100 ppb. With an increment by 100 times of the concentration, the effect from previous lower concentration on fluorescence detection

was neglected. The spectra of 100-ppb solution were summarized in figure 54 and maximum intensity as a function of collecting time was plotted in figure 55, which illustrated that it took 45 minutes to reach maximum intensity. Similar to the previous case of the 1-ppb solution, the intensity sharply increased from 25 to 35 minutes and even more sharply increased from 35 to 45 minutes. Calculation of breakthrough time was also applied to this case and the breakthrough time was about 37.69 minutes. By the reduction of the time required for dead pore volume, actual breakthrough time was 29.05 minutes. Additionally, the effects from shaly-sandstone on inverse trends at about 495 nm could not be observed anymore compared to static investigation as shown in figure 47.
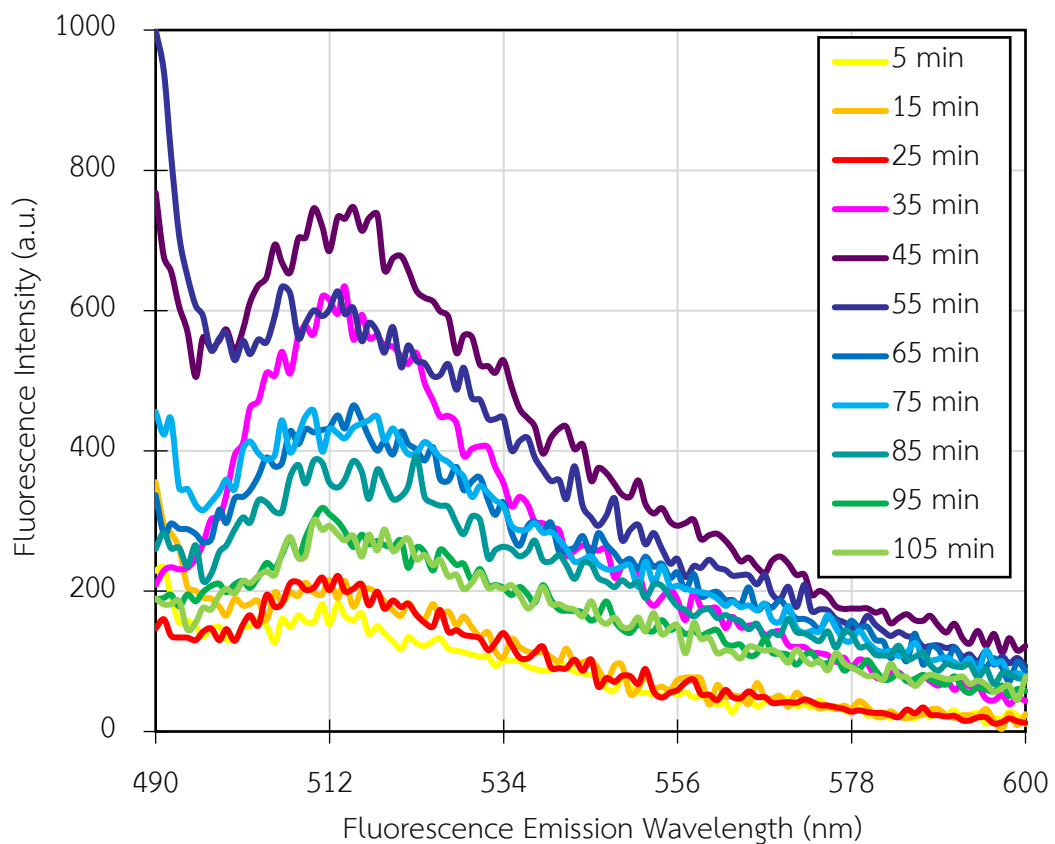

Figure 54. *Fluorescence spectra of 100-ppb fluorescein solution in dynamic investigation of fluorescein solution with shaly-sandstone with PMT voltage of 650 V and slit size of 5 nm.*
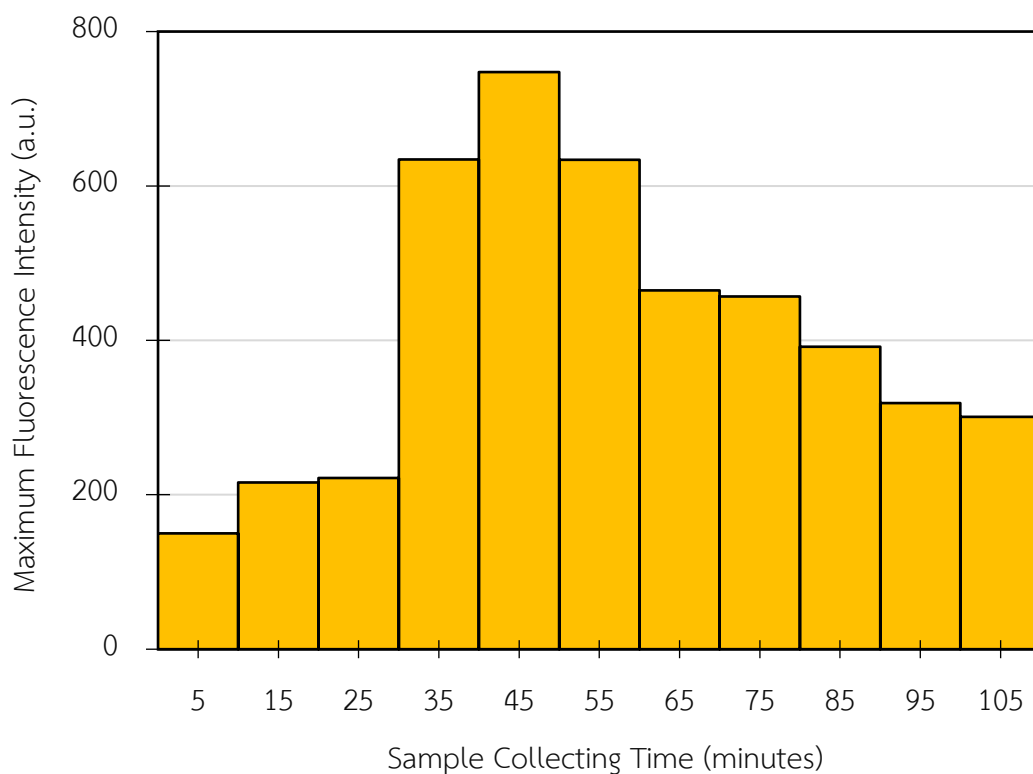
Figure 55. *Histogram of maximum fluorescence intensity of 100-ppb fluorescein solution as a function of sample collecting time in dynamic investigation of fluorescein solution with shaly-sandstone with PMT voltage of 650 V and slit size of 5 nm.*

Lastly, the 1-ppm solution was injected into the same core sample and due to much different on concentration, the effects of 100 ppb-solution on fluorescence detection of 1-ppm solution was minimized. The spectra of 1-ppm solution at different collecting time were illustrated in figure 56 and the maximum intensity as a function of collecting time was plotted in figure 57. The intensity sharply increased from 35 to 45 minutes, and then increased to maximum intensity at 80 minutes. Calculated breakthrough time for this case was 38.63 minutes and by subtracting the time required for dead pore volume, actual breakthrough time was 29.99 minutes.
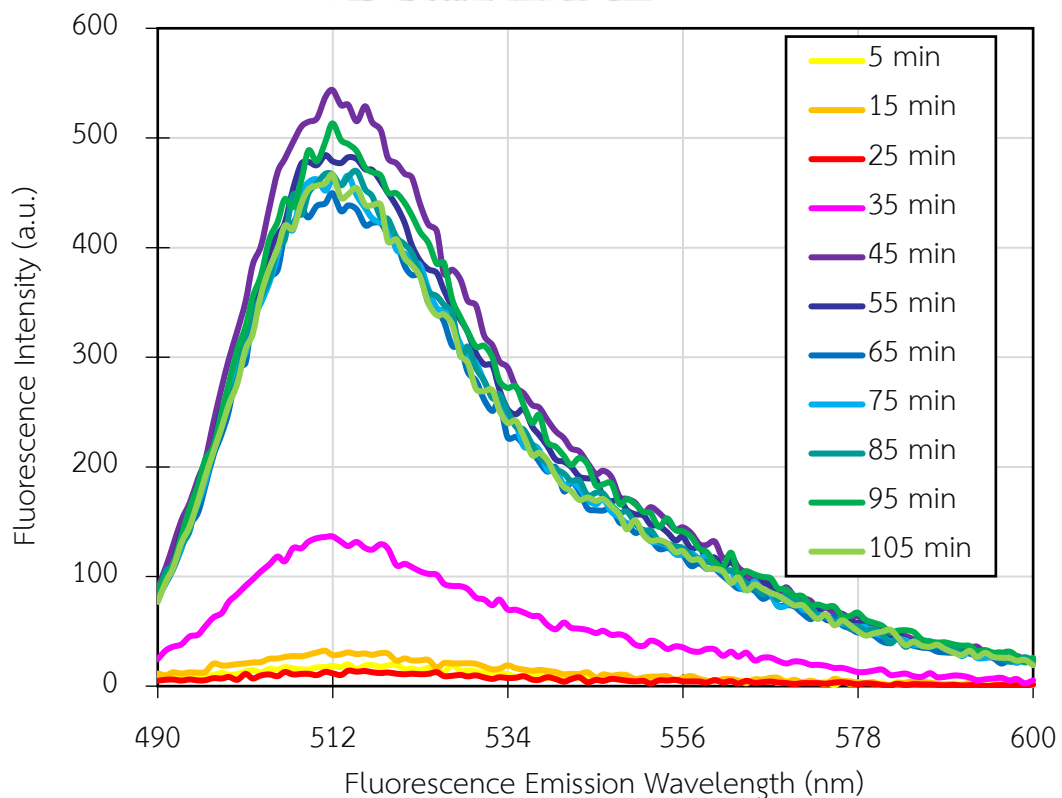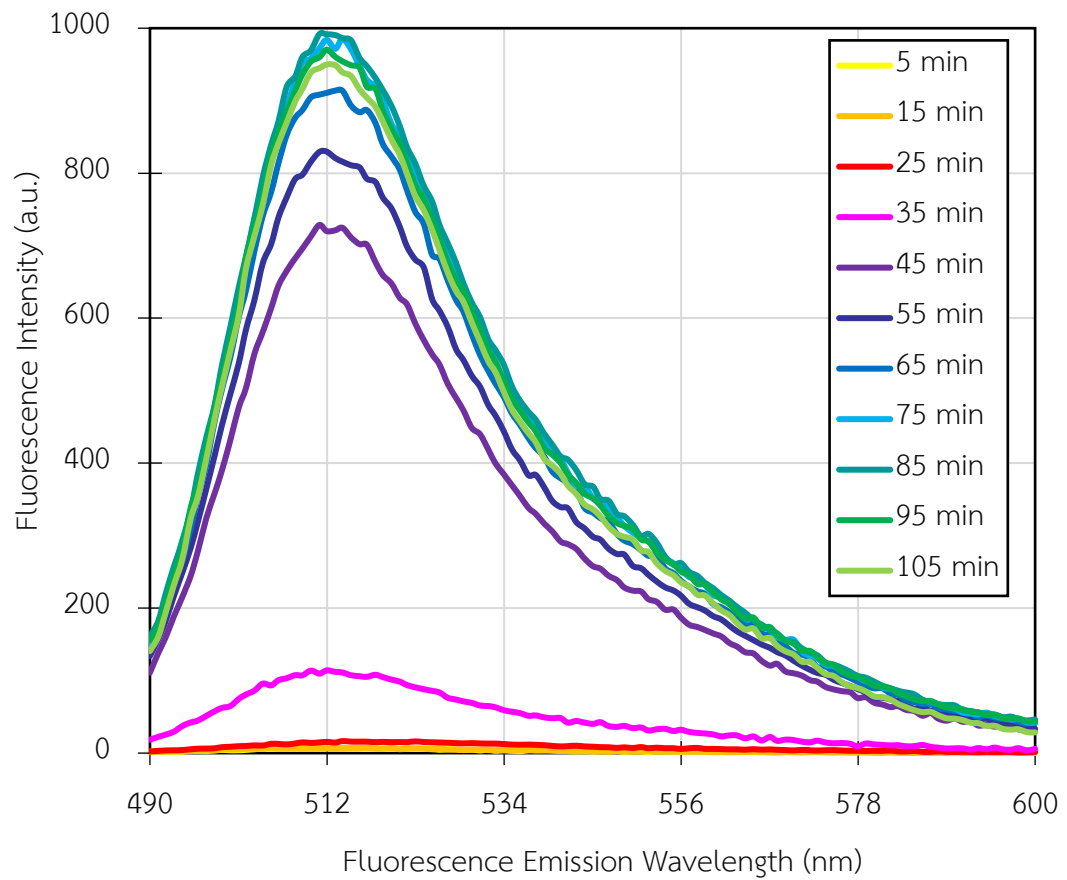
Figure 56. *Fluorescence spectra of 1-ppm fluorescein solution in dynamic investigation of fluorescein solution with shaly-sandstone with PMT voltage of 550 V and slit size of 5 nm.*
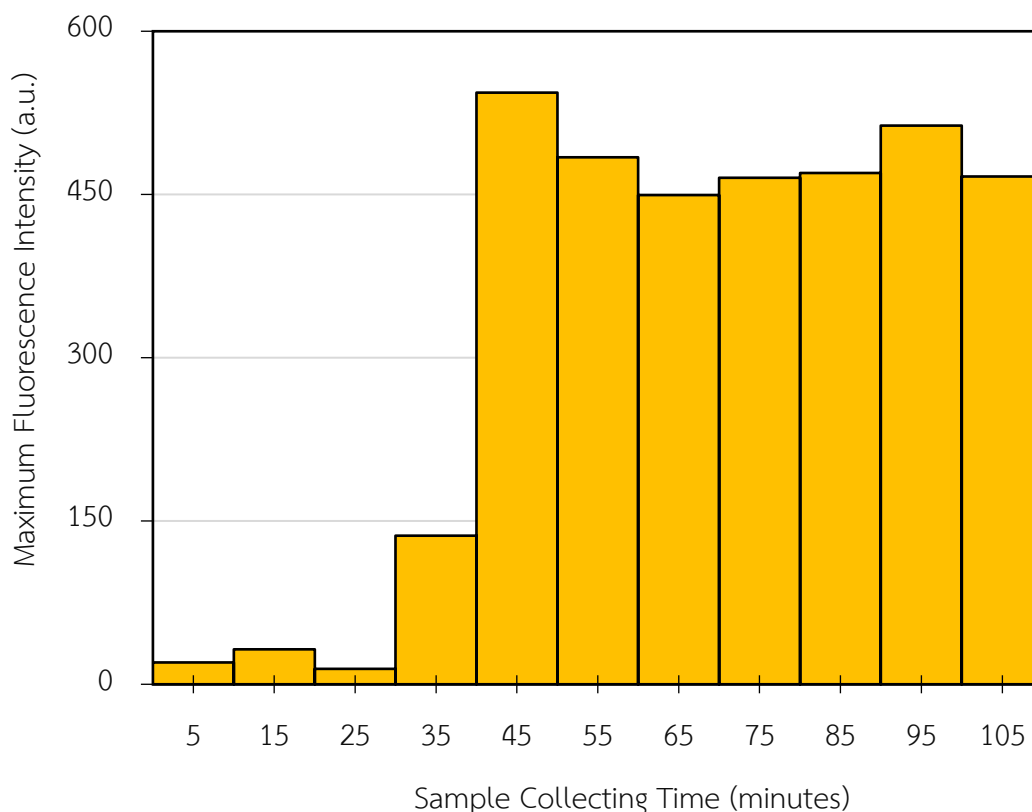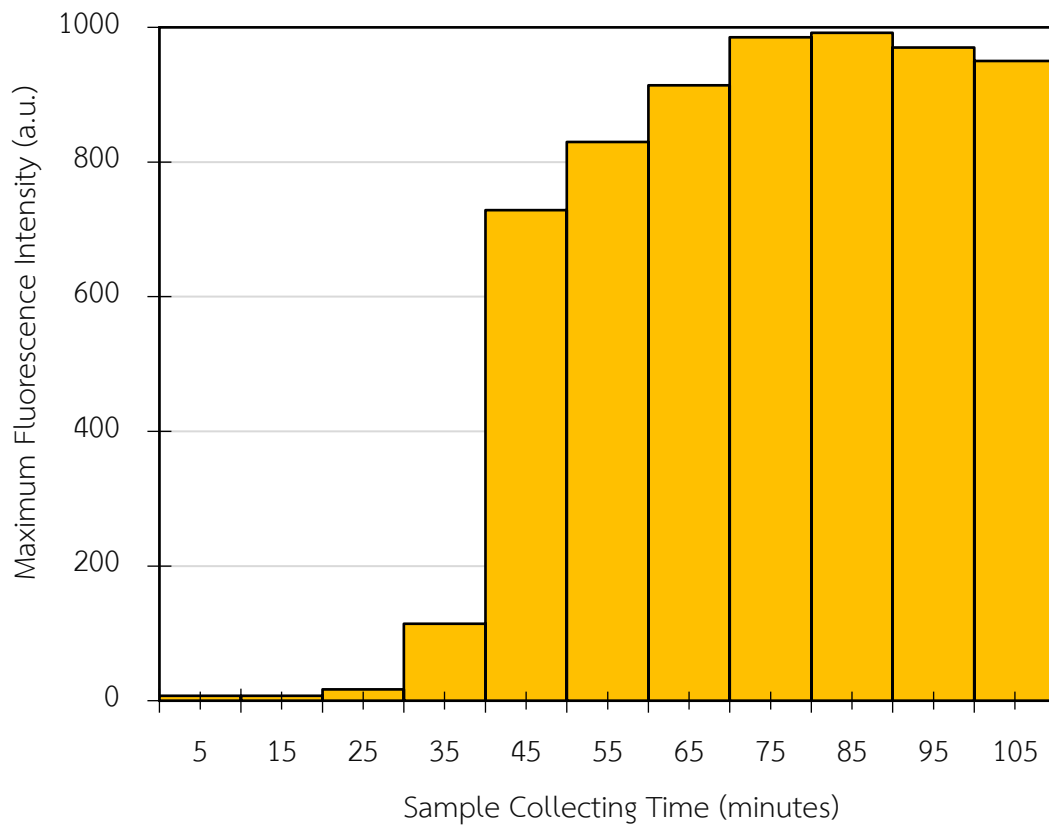
Figure 57. *Histogram of Maximum fluorescence intensity of 1-ppm fluorescein solution as a function of sample collecting time in dynamic investigation of fluorescein solution with shaly-sandstone with PMT voltage of 550 V and slit size of 5 nm.*

Calculated breakthrough times obtained from three solutions were then compared with pore volume of the core sample. From table 7, pore volume of this core sample was 19.37 cm^3. Since this core sample had been tested before and irreducible water saturation was found to be 0.45 [53], movable pore volume of this rock sample would be 10.65 cm^3. By using the injection rate of 0.5 cm^3/min, an ideal arrival time of fluorescein should be 21.31 minutes. From calculated breakthrough time, it could be observed that the 1-ppb solution with actual breakthrough time of 23.52 minutes was the nearest value with about 2 minutes difference. For 100-ppb and 1-ppm solutions, actual breakthrough times were 29.05 and 29.99 minutes, respectively which were about 9 minutes longer due to the diffusion of high fluorescein concentration into irreducible water. Even though this water did not move, fluorescein

could diffuse from movable pore with higher concentration to the dead-end pore, causing a retardation of fluorescein arrival. Together with the results obtained in section 5.3, the retardation of fluorescein breakthrough time could also be due to fluorescein adsorption on shaly-sandstone surface where both phenomena would likely occur at high fluorescein concentration.

5.5. Evaluation of Salt Effects on Fluorescein Solution

In this section, salt effects on fluorescein solution was evaluated. Fluorecein solution at 1 ppm was prepared and used to make formation water and individual salt solutions in the same content as in the formation. Then, pure 1-ppm solution was dilluted down to 1 ppb, 500 ppt, 100 ppt, and 10 ppt, and formation water using deionized water as solvent was added to each solution during solution dillution.

Although, in static and dynamic investigations of fluorescein solution with shaly-sandstone, fluorescein solution with shaly-sandstone had higher maximum intensity than pure fluorescein solution and it was concluded to be due to the effects from shaly-sandstone, presences of positively charged ions adsorbed on shaly-sandstone and elemental composition of shaly-sandstone were found to be an actual reason for this behavior. As shaly-sandstone contained several positively charged ions (table 9), these ions could desorb back to the surrounding water when the equilibrium was changed.

First, as shown in figure 58, the spectrum of 1-ppm fluorescein solution with formation water had higher maximum intensity than that of the solution using deionized water as solvent. Moreover, as shown in figure 59, the 1-ppm solution with individual salt in the same content as in formation water showed that $NaHCO_3$ had the major effect on fluorescence intensity amplification, following by $NaCl$, $CaCl_2$, and KCl, whereas $MgCl_2$ slightly lowered maximum intensity. This showed that bicarbonate ions (HCO_3^{2-}), which was small in quantity, had an obvious effect on fluorescence intensity amplification and this result also went in the same direction for storage of fluorescein solution to be more basic than acidic conditions. For the effect of individual cation, it

was difficult to directly conclude which cation had the strongest effect of fluorescence intensity amplification since their quantities were not controlled constantly. However, since sodium ions was a major cation in the formation water, fluorescence intensity amplification was mainly contributed by this ion. Later, as shown in figure 60, all solutions with salts had higher maximum intensity than the solutions without salts, even though 10-ppt and 100-ppt solutions with and without salts still had maximum intensity in ranges of formation water and deionized water. Furthermore, maximum intensity of 500-ppt solution with salt was almost the same as that of 1-ppb solution without salt. If 500-ppt solution were used in dynamic investigation, the results might still be possible to be detected. Thus, in dynamic investigation, appropriate fluorescein concentrations used for a tracer test in shaly-sandstone reservoir could be in a range of 500 ppt to 1 ppb depending to the type of injected water.

Figure 58. *Fluorescence spectra of 1-ppm fluorescein solution in a presence and an absence of salts with PMT voltage of 450 V and slit size of 5 nm.*
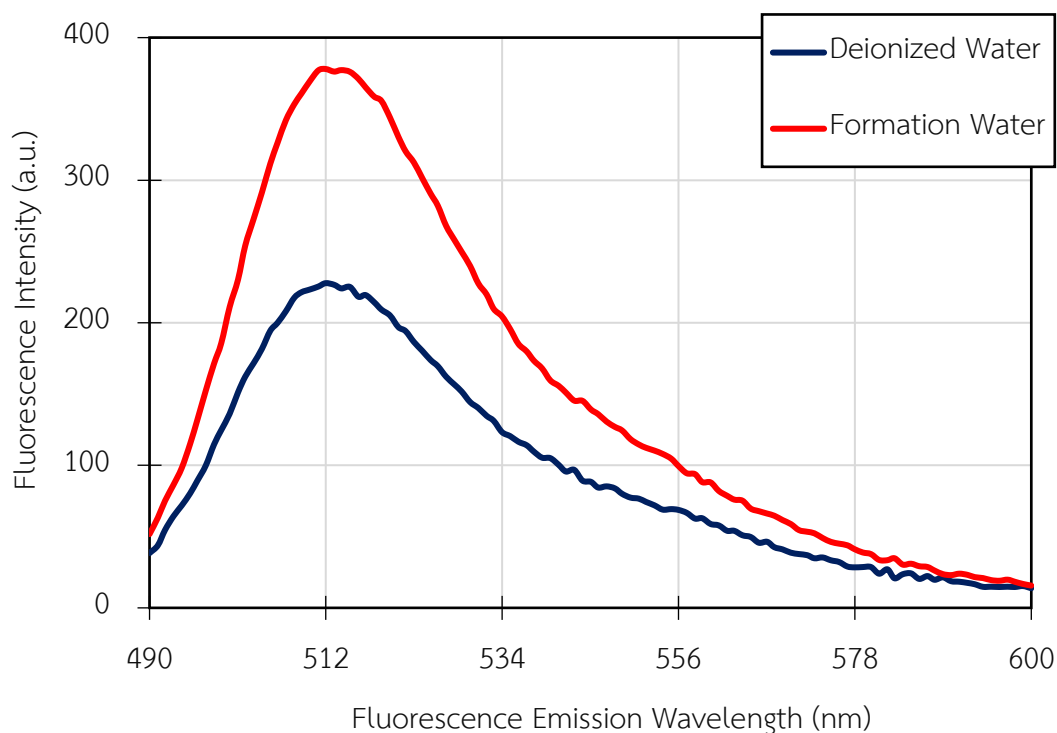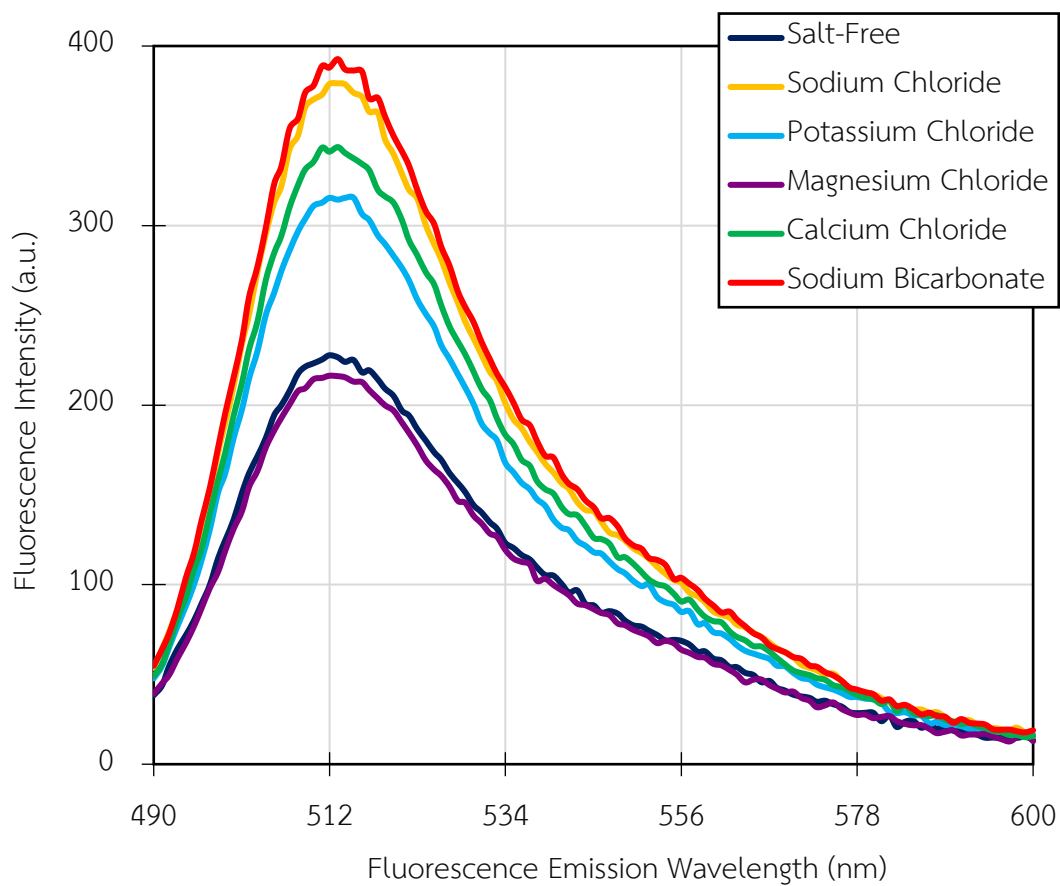
Figure 59. *Fluorescence spectra of 1-ppm fluorescein solution with various salts with PMT voltage of 450 V and slit size of 5 nm.*
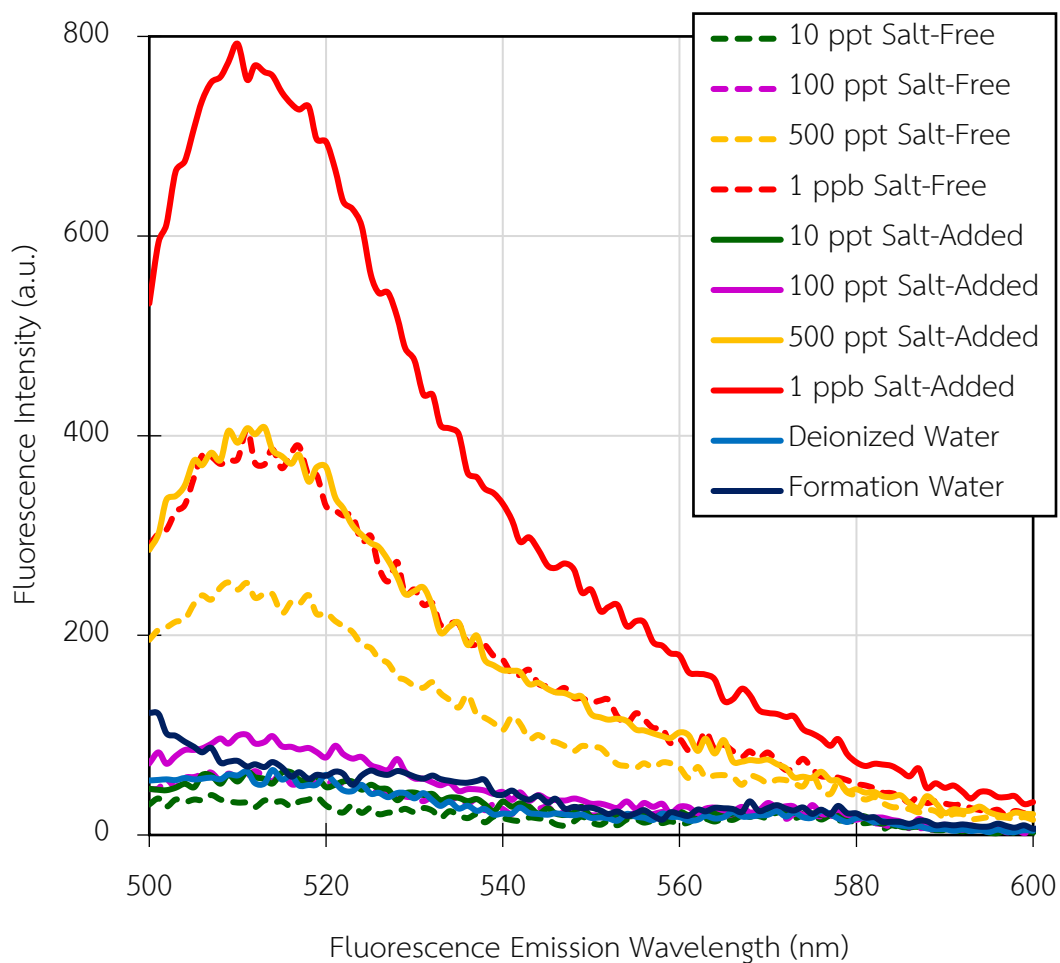
Figure 60. *Fluorescence spectra of fluorescein solutions at very low concentrations with various salts with PMT voltage of 750 V and slit size of 10 nm.*

CHAPTER 6: CONCLUSIONS AND RECOMMENDATIONS

6.1. Conclusions

In the first half of this study, characteristics of fluorescein solution using deionized water as solvent was evaluated. Detection limit of fluorescein solution characterized by fluorescence spectrophotometer using deionized water as solvent was determined to be at a concentration of 500 ppt. Fluorescein concentration at 10 ppm was critical concentration that reversed relationship between fluorescence intensity and fluorescein concentration; that is, at concentrations below 10 ppm, the intensity was directly proportional to the concentration, whereas at concentration above 10 ppm, the intensity was inversely proportional to the concentration. Fluorescence emission wavelength at maximum fluorescence intensity became a function of fluorescein concentration until emission wavelength of 512 nm at 1 ppm and there was no longer reduction of fluorescence emission wavelength beyond this value at lower concentrations. This was because self-quenching and self-absorption stopped at the concentration between 1 – 10 ppm, resulting in higher fluorescence energy and shortest fluorescence emission wavelength at maximum fluorescence intensity of 512 nm. Fluorescence of fluorescein solution could be photodegraded when stored inside transparent glass bottles in all-time exposure to light and the solution became darker with time. Maximum fluorescence intensity of the solution in all-time exposure to light was reduced compared to those of the solutions stored inside amber-colored glass bottles in both all-time concealment and normal exposure to light which were almost the same. Fluorescein solution at pH value of 3 was affected by hydrogen bonding between acetic acid and fluorescein molecules, resulting in less fluorescence emission, lower maximum fluorescein intensity and shorter fluorescence emission wavelength at maximum fluorescence intensity than the solutions at pH values of 7 and 11 which had almost identical results. Fluorescein solution was unaffected by petroleum reservoir temperatures in the range of 30-70℃ for 12 days. From this study, appropriate storage conditions for fluorescein solution were

recommended to be inside amber-colored glass bottle to prevent photodegradation at neutral or basic pH values. These results and recommendation could be further applied to petroleum, geothermal, medical, and pharmeutical applications. Table 12 summaried results of fluorescein solution in different storage conditions.

Table 12. *Summary of storage conditions for fluorescein solution.*

		Storages	
		Transparent Glass Bottle	Amber-Colored Glass Bottle
pH values	Basic	Lower fluorescence intensity by photodegradation	No effect from photodegradation and basic pH values
	Neutral	Lower fluorescence intensity by photodegradation	No effect from photodegradation and neutral pH values
	Acidic	Lower fluorescence intensity by both photodegradation and acidic pH value and shorter fluorescence emission wavelength at maximum fluorescence intensity by acidic pH value	Lower fluorescence intensity and shorter fluorescence emission wavelength at maximum fluorescence intensity by acidic pH value

In the second half of this study, the interactions between fluorescein and shaly-sandstone were investigated. In static investigation of fluorescein solution with untreated and treated shaly-sandstone powders, both types of the powder showed small difference in fluorescence detection, meaning that effects of shaly-sandstone itself dominated effects of hydrocarbon and/or drilling fluids. Furthermore, the presence of shaly-sandstone could completely overcome fluorescence detection of

deionized water and 1-ppb fluorescein solution stirred with the powders and could amplify maximum fluorescein intensity of the stirred solution compared to pure deionized water and pure fluorescein solutions. The presence of natural fluorescence in shaly-sandstone might occur at wavelength of 527 nm. The effects of shaly-sandstone were diminished as the concentration increased and disappeared at the concentration of 100 ppm. As the concentration increased above 100 ppm, fluorescein adsorption onto shaly-sandstone could be observed. Next, in dynamic investigation of fluorescein solution with shaly-sandstone core sample saturated with formation water, fluorescein breakthrough time of 1-ppb fluorescein solution flowing through the core sample was about 23.52 minutes which was the nearest to ideal breakthrough time for any liquid flowing through movable pore volume of the core sample of 21.31 minutes. At higher concentrations of 100 ppb and 1 ppm, the breakthrough times were 29.05 and 29.99 minutes, respectively. Retardation of the breakthrough times for higher concentrations compared to ideal breakthrough time illustrated that fluorescein molecules might diffuse into irreducible water portion of the core sample and fluorescein adsorption on shaly-sandstone surface could also occur at high concentration. Moreover, fluorescein solution with formation water had higher maximum intensity than the solution using deionized water as solvent, meaning that fluorescence intensity amplification on fluorescein solution in the presence of shaly-sandstone was due to the presences of positively charged ions adsorbed on shaly-sandstone and elemental composition of shaly-sandstone. Sodium ions also showed the highest contribution in the intensity amplification due to its abundance in the formation water. For very low fluorescein concentrations, the concentration of 500 ppt would still be possible for detection in the presence of shaly-sandstone. Therefore, appropriate fluorescein concentrations used for a tracer test in shaly-sandstone reservoir could be in a range of 500 ppt to 1 ppb depending to the type of injected water. Table 13 summaried the results from both static and dynamic investigation of fluorescein solution with shaly-sandstone.

Table 13. *Summary of static and dynamic investigation of fluorescein solution with shaly-sandstone.*

		Static Investigation (Stirring Tests)	Dynamic Investigation (Coreflooding Tests)
Fluorescein Concentration	1,000 ppm	Fluorescein adsorption	
	100 ppm	No effect observed	
	1 ppm	Fluorescence intensity amplification	Fluorescein diffusion and Fluorescein adsorption
	100 ppb	Fluorescence intensity amplification	Fluorescein diffusion and Fluorescein adsorption
	1 ppb	Disturbance on fluorescence detection	Almost no effects of shaly-sandstone on fluorescein flow
	500 ppt	Disturbance on fluorescence detection (Expected)	Almost no effects of shaly-sandstone on fluorescein flow (Expected)
	Deionized Water	Disturbance on fluorescence detection	

6.2. Recommendations

This study was an initial step of fluorescein investigation in applications of petroleum industry. Further investigations shall focus on the utilization of fluorescein solution in actual shaly-sandstone reservoir. Simultaneous utilization of fluorescein with other fluorescent tracers for multi-wells tracer tests, e.g. rhodamine and eosin, and practical field detection methods shall also be investigated.

Appendix

Appendix A: Maximum Fluorescence Intensity and Equivalent Fluorescein Concentration Conversion for Static Investigation of Fluorescein Solution with Shaly-Sandstone

Maximum fluorescence intensity of fluorescein solutions stirred with shaly-sandstone cutting powders could be converted into equivalent fluorescein concentrations by using semi-log plots of maximum fluorescence intensity as a function of fluorescein concentration as shown in figure 61 to figure 63. It was noted that PMT voltage and slit size of the stirred solutions must be the same as mentioned in each figure.

Figure 61. *Semi-log plots of maximum fluorescence intensity as a function of fluorescein concentration in a concentration range of 100 to 1,000 ppb with PMT voltage of 500 V and slit size of 5 nm.*

Figure 62. *Semi-log plots of maximum fluorescence intensity as a function of fluorescein concentration in a concentration range of 1 to 10 ppm with PMT voltage of 450 V and slit size of 5 nm.*
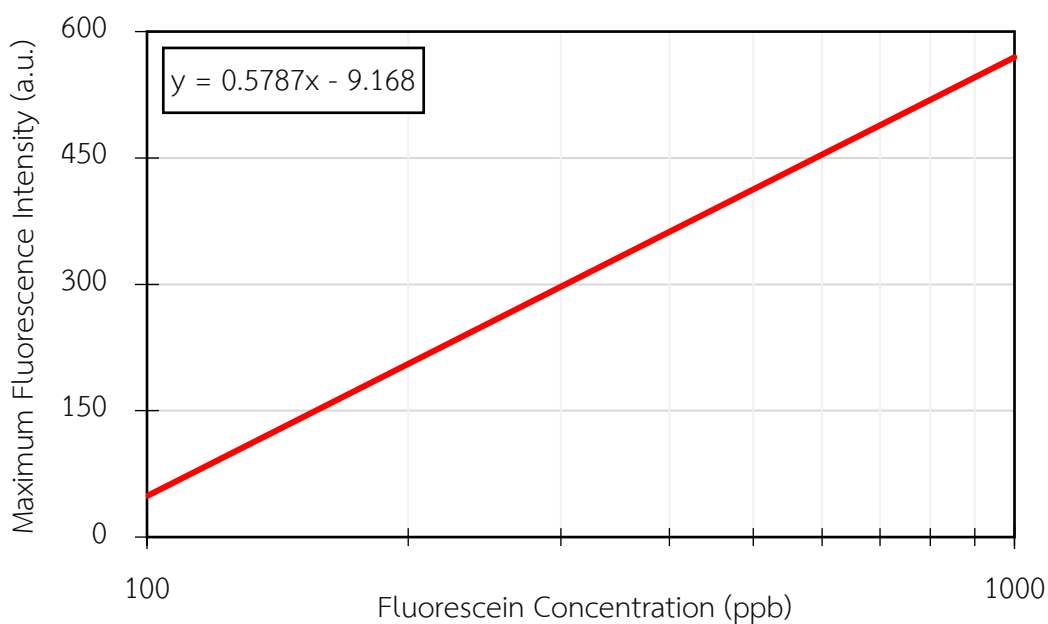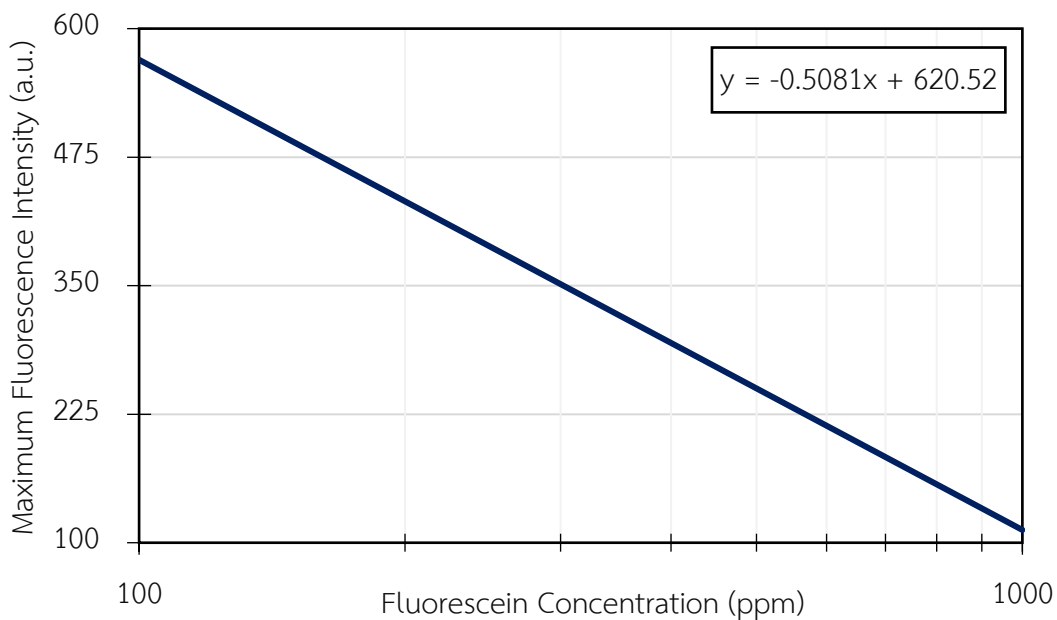

Figure 63. *Semi-log plots of maximum fluorescence intensity as a function of fluorescein concentration in a concentration range of 100 to 1,000 ppm with PMT voltage of 500 V and slit size of 5 nm.*
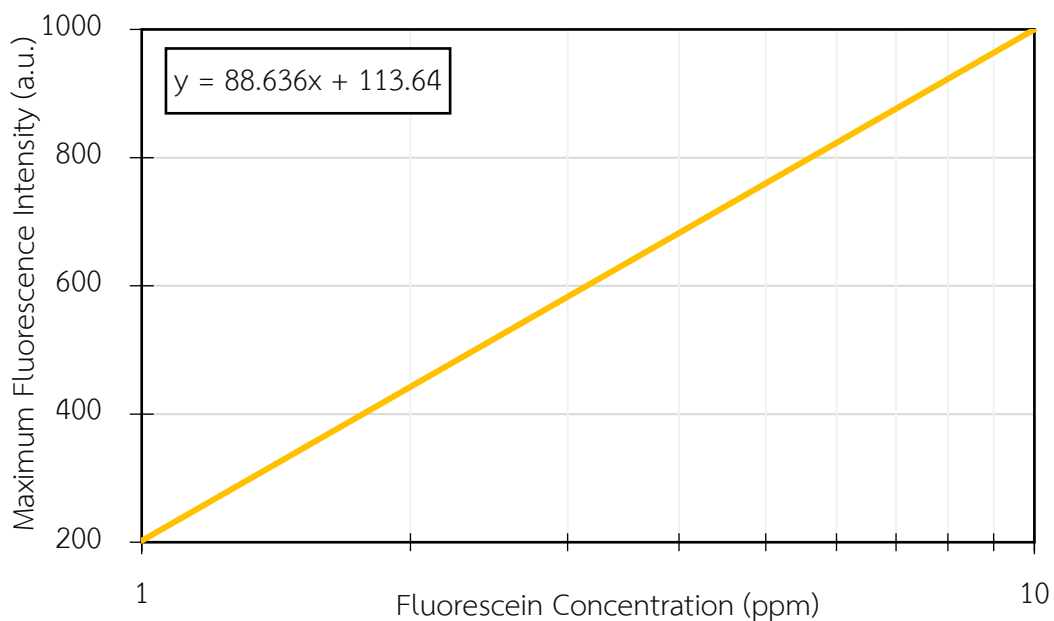
Appendix B: Fluorescein Breakthrough Time Calculation for Dynamic Investigation of Fluorescein Solution with Shaly-Sandstone

Fluorescein breakthrough time of fluorescein solution flowing through shaly-sandstone core sample could be calculated based on volume-weighted average calculation. Fluorescein breakthrough times of all solutions were expected to be between 30 and 40 minutes.

First, let X be time interval from 30 minutes to fluorescein breakthrough time for 1-ppb fluorescein solution. Based on figure 64, X could be calculated as follows:

$$(634.24)(10) = 221.93X + (747.64)(10-X)$$

$$X = 2.16 \text{ minutes}$$

Fluorescein breakthrough time for 1-ppb fluorescein solution was equal to:

$$30 + 2.16 = 32.16 \text{ minutes}$$

Figure 64. *Histogram of 1-ppb fluorescein solution in dynamic investigation of fluorescein solution with shaly-sandstone with PMT voltage of 700 V and slit size of 5 nm (time period from 20 to 50 minutes).*

Next, let *Y* be time interval from 30 min to fluorescin breakthrough time for 100-ppb fluorescein solution. Based on figure 65, *Y* could be calculated as follows:

$$(136.52)(10) = 14.10Y + (543.71)(10\text{-}Y)$$

$$Y = 7.69 \text{ minutes}$$

Fluorescein breakthrough time for 100-ppb fluorecein solution was equal to:

$$30 + 7.69 = 37.69 \text{ minutes}$$

Figure 65. *Histogram of 100-ppb fluorescein solution in dynamic investigation of fluorescein solution with shaly sandstone with PMT voltage of 650 V and slit size of 5 nm (time period from 20 to 50 minutes).*

Lastly, let *Z* be time interval from 30 min to fluorescein breakthrough time for 1-ppm fluorescein solution flowing through shaly-sandstone core sample. Based on figure 65, *Z* could be calculated as follows:

$$(114.14)(10) = 16.63Z + (728.60)(10\text{-}Z)$$

$$Z = 8.63 \text{ minutes}$$

Fluorescein breakthrough time for 1-ppm fluorescein solution was equal to:
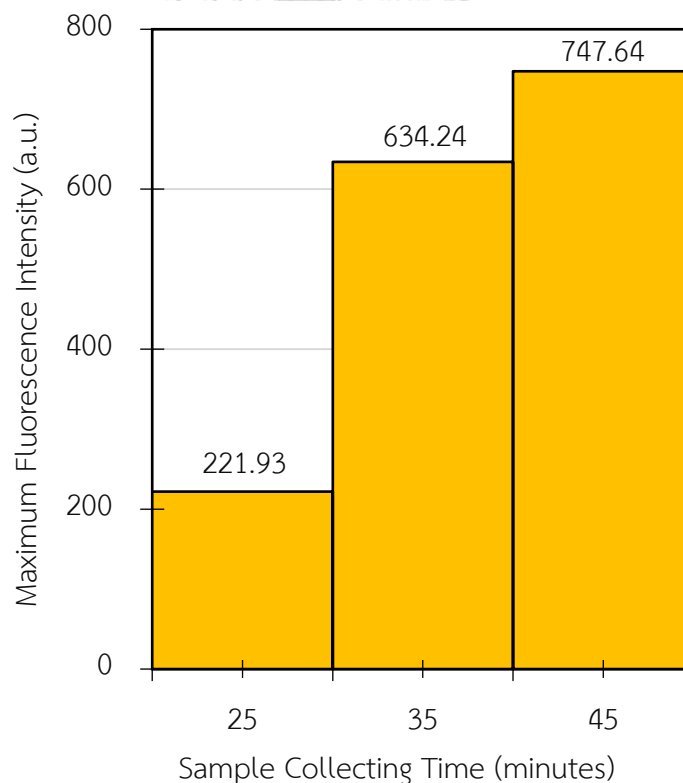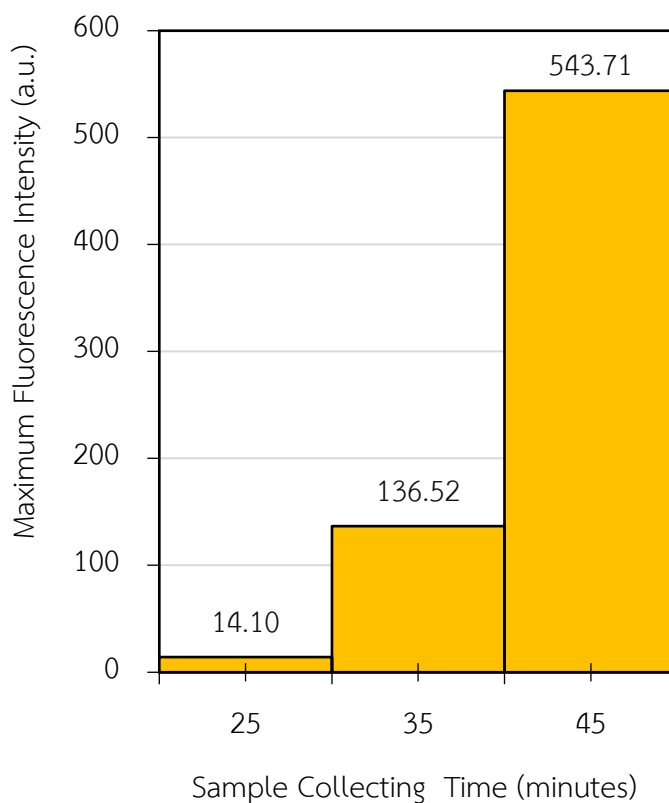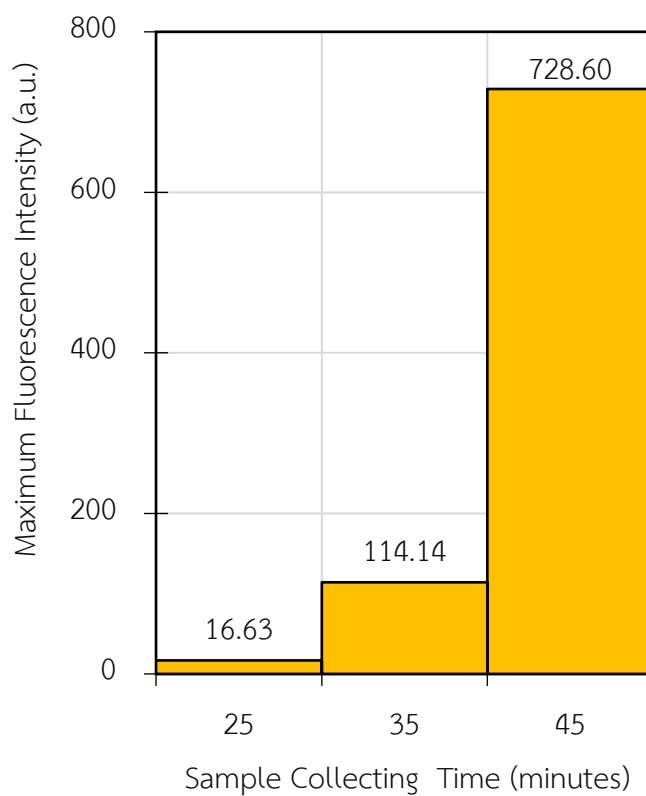
30 + 8.63 = 38.63 minutes

Figure 66. *Histogram of 1-ppm fluorescein solution in dynamic investigation of fluorescein solution with shaly sandstone with PMT voltage of 550 V and slit size of 5 nm (time period from 20 to 50 minutes).*

REFERENCES

[1]   M. Asadi and G. M. Shook, "Application of Chemical Tracers in IOR: A Case History," presented at the SPE North Africa Technical Conference and Exhibition, Cairo, Egypt, 14-17 February, 2010, SPE-126029-MS.

[2]   C. Serres-Piole, H. Preud'homme, N. Moradi-Tehrani, C. Allanic, H. Jullia, and R. Lobinski, "Water Tracers in Oilfield Applications: Guidelines," (in English), *Journal of Petroleum Science and Engineering,* vol. 98-99, pp. 22-39, 13 August 2012, doi: 10.1016/j.petrol.2012.08.009.

[3]   H. Födisch, J. Wegner, R. Hincapie, and L. Ganzer, "Impact of Connate Water Replacement on Chemical EOR Processes," presented at the SPE Latin American and Caribbean Petroleum Engineering Conference, Quito, Ecuador, 18-20 November, 2015, SPE-177196-MS.

[4]   E. J. Peters and D. L. Flock, "The Onset of Instability During Two-Phase Immiscible Displacement in Porous Media," (in English), *Society of Petroleum Engineers Journal,* vol. 21, no. 2, pp. 249-258, April 1981, Art no. SPE-8371-PA, doi: 10.2118/8371-PA.

[5]   R. S. Bryant, T. E. Burchfield, D. M. Dennis, and D. O. Hitzman, "Microbial-Enhanced Waterflooding: Mink Unit Project," (in English), *SPE Reservoir Engineering,* vol. 5, no. 1, pp. 9-13, February 1990, Art no. SPE-17341-PA, doi: 10.2118/17341-PA.

[6]   D. K. Olsen, M. D. Hicks, B. G. Hurd, A. A. Sinnokrot, and C. N. Sweigart, "Design of a Novel Flooding System for an Oil-Wet Central Texas Carbonate Reservoir," presented at the SPE/DOE Enhanced Oil Recovery Symposium, Tulsa, Oklahoma, United States of America, 22-25 April, 1990, SPE-20224-MS.

[7]   M. Aparecida de Melo, C. R. de Holleben, and A. R. Almeida, "Using Tracers to Characterize Petroleum Reservoirs: Application to Carmopolis Field, Brazil," presented at the SPE Latin American and Caribbean Petroleum Engineering Conference, Buenos Aires, Argentina, 25-28 March, 2001, SPE-69474-MS.

[8] R. A. Greenkorn, "Experimental Study of Waterflood Tracers," (in English), *Journal of Petroleum Technology,* vol. 14, no. 1, pp. 87-92, January 1962, Art no. SPE-169-PA, doi: 10.2118/169-PA.

[9] I. Durusu, "Laboratory Investigation of a Suitable Waterflood for the Bulgurdag Field and a Design of a Tracer Field," presented at the SPE European Spring Meeting, Amsterdam, Netherlands, 29-30 May, 1974, SPE-4826-MS.

[10] C. N. Khalil and M. C. K. Oliveira, "Organic Dye for Subsea Flowline Assessment," presented at the SPE International Symposium on Oilfield Chemistry, Houston, Texas, United States of America, 16-19 February, 1999, SPE-50768-MS.

[11] P. A. Doty, "Clear Brine Drilling Fluids: A Study of Penetration Rates, Formation Damage, and Wellbore Stability in Full-Scale Drilling Tests," (in English), *SPE Drilling Engineering,* vol. 1, no. 1, pp. 17-30, February 1986, Art no. SPE-13441-PA, doi: 10.2118/13441-PA.

[12] M. O. Metidji, M. Silva, A. Krivokapic, and T. Bjørnstad, "Synthesis and Characterization of a Reactive Fluorescent Tracer and Its Possible Use for Reservoir Temperature's Data Collection," in *IOR 2019 – 20th European Symposium on Improved Oil Recovery,* Pau, France, 8-11 April 2019: European Association of Geoscientists and Engineers, doi: 10.3997/2214-4609.201900062.

[13] B. M. Kennedy *et al.,* "A History of Geothermal Energy Research and Development in the United States: Reservoir Engineering (1976-2006)."

[14] J. P. Morris *et al.,* "Experimental Design for Hydrofracturing and Fluid Flow at the DOE EGS Collab Testbed," presented at the 52nd U.S. Rock Mechanics/Geomechanics Symposium, Seattle, Washington, United States of America, 17–20 June, 2018, ARMA-2018-007.

[15] D. L. Nielson, P. M. Wright, M. C. Adams, J. N. Moore, and A. C. Tripp, "Management of Geothermal Resources," in *National Energy Strategy - The Role of Geothermal Technology Development*, San Francisco, California, United States of America, 18-20 April 1990: U.S. Department of Energy Assistant Secretary for Conservation and Renewable Energy, Geothermal Division, pp. 69-74.

[16] J. W. Tester, R. L. Bivins, and R. M. Potter, "Interwell Tracer Analyses of a Hydraulically Fractured Granitic Geothermal Reservoir," (in English), *Society of Petroleum Engineers Journal,* vol. 22, no. 4, pp. 537-554, August 1982, Art no. SPE-8270-PA, doi: 10.2118/8270-PA.

[17] M. C. Adams and J. Davis, "Kinetics of Fluorescein Decay and Its Application as A Geothermal Tracer," (in English), *Geothermics,* vol. 20, no. 1/2, pp. 53-66, 1991, doi: 10.1016/0375-6505(91)90005-G.

[18] H. Sugita, I. Matsunaga, N. Yanagisawa, H. Tao, T. Yamaguchi, and K. Aoki, "Effects of pH and Dissolved Ions on Fluorescence Intensity of Sodium Fluorescein," (in Japanese), *Journal of the Geothermal Research Society of Japan,* vol. 25, no. 3, pp. 211-225, 2003, doi: 10.11367/grsj1979.25.211.

[19] R. Hiramoto, J. Bernecky, J. Jurand, and M. Hamlin, "The Effect of Hydrogen Ion Concentration on Fluorescent Labelled Antibodies," (in English), *Journal of Histochemistry and Cytochemistry,* vol. 12, no. 4, pp. 271-274, April 1st 1964, doi: 10.1177/12.4.271.

[20] M. J. Doughty, "pH Dependent Spectral Properties of Sodium Fluorescein Ophthalmic Solutions Revisited," (in English), *Ophthalmic and Physiological Optics,* vol. 30, no. 2, pp. 167-174, 2010, doi: 10.1111/j.1475-1313.2009.00703.x.

[21] J. Panchompoo, L. Aldous, M. Baker, M. I. Wallace, and R. G. Compton, "One-Step Synthesis of Fluorescein Modified Nano-Carbon for Pd(II) Detection via Fluorescence Quenching," (in English), *Analyst,* 10.1039/C2AN16261J vol. 137, no. 9, pp. 2054-2062, 2012, doi: 10.1039/C2AN16261J.

[22] R. Markuszewski and H. Diehl, "The Infrared Spectra and Structures of the Three Solid Forms of Fluorescein and Related Compounds," (in English), *Talanta,* vol. 27, no. 11, 2, pp. 937-946, November 1980, doi: 10.1016/0039-9140(80)80125-1.

[23] H. Diehl and R. Markuszewski, "Studies of Fluorescein-II The Solubility and Acid Dissociation Constants of Fluorescein in Water Solution," (in English), *Talanta,* vol. 32, no. 2, pp. 159-165, February 1985, doi: 10.1016/0039-9140(85)80049-7.

[24] N. Gs and B. G. Desai, "Selection and Identification of Interwell Tracers for Reservoir Characterization of Clastic Rock: A Case Study from Cretaceous

Himmatnagar Sandstones," *Petroleum & Petrochemical Engineering Journal,* vol. 2, no. 7, 2018.

[25]   D. Tayyib, A. Al-Qasim, S. Kokal, and O. Huseby, "Overview of Tracer Applications in Oil and Gas Industry," presented at the SPE Kuwait Oil & Gas Conference and Show, Mishref, Kuwait, 13-16 October, 2019, SPE-198157-MS.

[26]   S. Cheung, A. Edwards, and J. Howard, "A Novel Approach to Interwell Tracer Design and Field Case History," presented at the SPE Annual Technical Conference and Exhibition, Houston, Texas, United States of America, 3-6 October 1999, SPE-56610-MS.

[27]   J. Jacobs, "Fluorescein Sodium What is it?," *Journal of Ophthalmic Photography,* vol. 14, no. 2, p. 62, December 1992.

[28]   J. R. Lakowicz, *Principles of Fluorescence Spectroscopy*, 3rd ed. Singapore: Springer, 2006.

[29]   S. Y. Xiao *et al.*, "Application of Fluorescein Sodium in Breast Cancer Brain-Metastasis Surgery," *Cancer Management and Research,* vol. 10, pp. 4325–4331, 12 October 2018, doi: 10.2147/CMAR.S176504.

[30]   X. Zhao *et al.*, "Application of Fluorescein Fluorescence in Vascular Neurosurgery," *Frontiers in Surgery,* vol. 6, no. 52, 18 September 2019, doi: 10.3389/fsurg.2019.00052.

[31]   H. Wu *et al.*, "Stochastic Modeling of a Conservative Tracer Test for the Characterization of Fracture Flow Patterns in EGS Collab Experiment 1," presented at the 53rd U.S. Rock Mechanics/Geomechanics Symposium, New York, United States of America, 23-26 June, 2019, ARMA-2019-1807.

[32]   J. W. Tester, H. D. Murphy, C. O. Grigsby, R. M. Potter, and B. A. Robinson, "Fractured Geothermal Reservoir Growth Induced by Heat Extraction," (in English), *SPE Reservoir Engineering,* vol. 4, no. 01, pp. 97-104, February 1989, Art no. SPE-15124-PA, doi: 10.2118/15124-PA.

[33]   V. S. Agarwala, K. S. Rajan, M. G. Durrett, R. E. Johnson, and A. Singh, "Fluorescent Materials Utilized as Early Warning Sensors for Corrosion of Aluminum Alloy Surfaces," presented at the NACE - International Corrosion

Conference Series, San Antonio, Texas, United States of America, 25-30 April, 1999, NACE-99505.

[34]   C. Areejitranusorn, "Fluorometer," in *Scientific Instruments*, 3rd ed. Khon Kaen: Klungnana Witthaya Press, 2001, ch. 13.

[35]   P. Hamm and J. Helbing, "Fluorescence Quenching," *Physikalisch-Chemisches Praktikum I.*

[36]   P. Pramotethana, "Photoluminescence Extraction from Scales of Seabass Lates calcarifer Bloch, 1790," Master of Science in Chemical Technology, Deparament of Chemical Technology, Faculty of Science, Chulalongkorn University, Bangkok, Thailand, 2002.

[37]   S. Sahasithiwat. (2015, September) Emerging of Life! A Memo of Light Producer by Using Fluorescent Diode of Organic Substance. *Journal of Materials Technology*. 33-40.

[38]   P. T. So and C. Y. Dong, "Fluorescence Spectrophotometry," (in English), *Encyclopedia of Life Science,* 20 June 2001, doi: 10.1038/npg.els.0002978.

[39]   J. H. Gutow, "Halide (Cl⁻) Quenching of Quinine Sulfate Fluorescence: A Time-Resolved Fluorescence Experiment for Physical Chemistry," (in English), *Journal of Chemical Education,* vol. 82, no. 2, p. 302, 1 February 2005, doi: 10.1021/ed082p302.

[40]   World Health Organization, "Fluorescence Spectrophotometry," in *The International Pharmacopoeia*, 9th ed.: WHO, 2019, ch. 1.

[41]   S. R. Phillips, L. J. Wilson, and R. F. Borkman, "Acrylamide and Iodide Fluorescence Quenching as a Structural Probe of Tryptophan Microenvironment in Bovine Lens Crystallins," (in English), *Current Eye Research,* vol. 5, no. 8, pp. 611-619, 1986, doi: 10.3109/02713688609015126.

[42]   H. D. Burrows, M. E. Azenha, and C. J. P. Monteiro, "Homogeneous Photocatalysis," in *Catalysis from Theory to Application. An Integrated Course*, J. L. Figueiredo, M. M. Pereira, and J. Faria Eds., 1st ed. Coimbra, Portugal: Coimbra University Press, 2008, ch. 2.

[43]   Perkin Elmer, "An Introduction to Fluorescence Spectroscopy."

[44]   R. A. and D. Dileep, "Spectrophotometry and Spectrometry - Concept and Applications," (in English), *International Journal of Advance Research and Innovative Ideas in Education,* vol. 2, no. 4, pp. 96-100, 2017.

[45]   S. Sangsrichan, "Spectroscopy," Maejo University.

[46]   S. Abbott, "Transgressive-Regressive Cycles: Pebbley Beach Formation, Sydney-Bowen Basin."

[47]   K. F. Fozao, A. E. Djieto-Lordon, E. A. A. Ali, C. M. Agying, D. M. Ndeh, and M. K. Zebaze Djuka, "Analysis of Shaly Sand Reservoir Rocks in the Eastern Niger Delta Basin Using Geophysical Well logs," (in English), *Journal of Petroleum and Gas Engineering,* vol. 10, no. 1, pp. 1-13, January 2019, Art no. D049C7059749, doi: 10.5897/JPGE2018.0300.

[48]   A. Abdullatif, I. A. Al-Hulail, and E. Al-Mutawa, "Robust Clay Stabilizer to Control Swelling in a Rich Swellable Clay Formation: A Laboratory Study," presented at the International Petroleum Technology Conference, Dhahran, Saudi Arabia, 13-15 January, 2020, IPTC-20305-MS.

[49]   K. K. Spilker, V. Dwarakanath, T. Malik, E. B. Tao, and Z. Mirkovic, "Characterizing Tracer Applicability in Different Mineralogy," presented at the SPE Improved Oil Recovery Conference, Tulsa, Oklahoma, United States of America, 11-13 April, 2016, SPE-179656-MS.

[50]   N. Rohilla, R. Ravikiran, C. T. Carlisle, N. Jones, M. B. Davis, and K. B. H. Finch, "Design of a Robust ASP Formulation for Clay Rich and Moderate Permeability Sandstone Reservoir: From Laboratory to Single Well Chemical Tracer Test in the Field," presented at the SPE Improved Oil Recovery Conference, Tulsa, Oklahoma, United States of America, 11-13 April, 2016, SPE-179678-MS.

[51]   C. D. Barton and A. D. Karathanasis, "Clay Minerals," in *Encyclopedia of Soil Science*, R. Lal, Ed., 3rd ed. Boca Raton, Florida, United States of America: CRC Press, 2016, pp. 187-192.

[52]   K. K. Mohan, R. N. Vaidyab, M. G. Reed, and H. S. Fogler, "Water Sensitivity of Sandstones Containing Swelling and Non-Swelling Clays," (in English), *Colloids and Surfaces A: Physicochemical and Engineering Aspects,* vol. 73, pp. 237-254, 29 June 1993, doi: 10.1016/0927-7757(93)80019-B.

[53]   H. V. Quoc, "Effectiveness of Ammonium Ion in Low Salinity Waterflooding in Shaly-Sandstone Reservoir," Master Degree of Engineering in Georesources and Petroleum Engineering, Department of Mining and Petroleum Engineering, Faculty of Engineering, Chulalongkorn University, Bangkok, Thailand, 2019.

VITA

NAME	Harid Pataveepaisit
DATE OF BIRTH	2 May 1996
PLACE OF BIRTH	Hua Chiew Hospital, Bangkok, Thailand
INSTITUTIONS ATTENDED	- Master's Degree: Department of Mining and Petroleum Engineering, Faculty of Engineering, Chulalongkorn University - Bachelor's Degree: School of Bio-Chemical Engineering and Technology, Sirindhorn International Institute of Technology (SIIT), Thammasat University - High School: Saint Gabriel's College
HOME ADDRESS	63 Ratchaphruek 25, Laddarom Ratchaphruek-Pinklao, Taling Chan Sub District, Taling Chan District, Bangkok 10170, Thailand
PUBLICATION	1) "Effectiveness Evaluation of Fluorescein Sodium as Fluorescent Tracer in Shaly-Sandstone Reservoir" published in ICIET2020 Proceedings 2) "Characteristics Evaluation of Fluorescein Sodium as Fluorescent Tracer for Petroleum Wells" published in Journal IOP: Earth & Environmental Sciences and WMESS2020 Proceedings 3) "Preservation of Nicotine by Nanoencapsulation Technique using Beta-Cyclodextrin" published in PACCON2018 Proceedings
AWARD RECEIVED	2020: Research Scholarship from The King Prajadhipok and Queen Rambhai Barni Memorial Foundation 2019: Teaching Assistant Scholarship from Graduation School, Chulalongkorn University 2018: First-Class Honor in Bachelor of Engineering in Chemical Engineering (International Program) from Thammasat University 2016-2018: Good Academic Performance and Good Conduct Scholarships from SIIT cooperated with Keidanren